University of Alberta

Architecture of Tidally Influenced Point Bars

by

Barton Jeremy Blakney

A thesis submitted to the Faculty of Graduate Studies and Research
in partial fulfillment of the requirements for the degree of

Master of Science

Department of Earth and Atmospheric Sciences

Edmonton, Alberta
Fall, 2006

Library and Archives Canada

Published Heritage Branch

395 Wellington Street
Ottawa ON K1A 0N4
Canada

Bibliothèque et Archives Canada

Direction du Patrimoine de l'édition

395, rue Wellington
Ottawa ON K1A 0N4
Canada

Your file Votre référence
ISBN: 978-0-494-22229-4
Our file Notre référence
ISBN: 978-0-494-22229-4

NOTICE:
The author has granted a non-exclusive license allowing Library and Archives Canada to reproduce, publish, archive, preserve, conserve, communicate to the public by telecommunication or on the Internet, loan, distribute and sell theses worldwide, for commercial or non-commercial purposes, in microform, paper, electronic and/or any other formats.

The author retains copyright ownership and moral rights in this thesis. Neither the thesis nor substantial extracts from it may be printed or otherwise reproduced without the author's permission.

AVIS:
L'auteur a accordé une licence non exclusive permettant à la Bibliothèque et Archives Canada de reproduire, publier, archiver, sauvegarder, conserver, transmettre au public par télécommunication ou par l'Internet, prêter, distribuer et vendre des thèses partout dans le monde, à des fins commerciales ou autres, sur support microforme, papier, électronique et/ou autres formats.

L'auteur conserve la propriété du droit d'auteur et des droits moraux qui protège cette thèse. Ni la thèse ni des extraits substantiels de celle-ci ne doivent être imprimés ou autrement reproduits sans son autorisation.

In compliance with the Canadian Privacy Act some supporting forms may have been removed from this thesis.

While these forms may be included in the document page count, their removal does not represent any loss of content from the thesis.

Conformément à la loi canadienne sur la protection de la vie privée, quelques formulaires secondaires ont été enlevés de cette thèse.

Bien que ces formulaires aient inclus dans la pagination, il n'y aura aucun contenu manquant.

Canada

ABSTRACT

Successions of inclined heterolithic stratification (IHS) within the McMurray Formation, northeastern Alberta, comprise stacked, genetic units averaging 6 to 10 m in thickness. Within the McMurray Type Section, these units are interpreted to represent the growth stages of a large, meandering channel deposited within the middle estuary.

Characterization of several modern, tidally-influenced depositional systems yielded the following generalizations: 1) a tripartite zonation of tidally-influenced systems is identifiable: 2) channel abandonments are rare within tide-dominated channel reaches; 3) large meander scroll bars form in systems with comparatively high fluvial input; and 4) tidally-influenced channels maintain lower sinuosity values than their fluvial counterparts.

ACKNOWLEMENTS

I would like to thank my supervisor Dr. Murray Gingras for his guidance, friendship, and unwavering patience. I am very fortunate to have the love and support of a beautiful family, including parents Amy and George, brother Devere, and sister Shima. Special thanks I extend to JP Zonneveld who has provided endless support and many opportunities for a young geologist. Lastly, I thank my wife Janetlee for her love and support and for the painstaking editing provided without hesitation.

This work was generously funded by Imperial Oil Limited and NSERC granted to Dr. Murray Gingras.

TABLE OF CONTENTS

CHAPTER 1.
INTRODUCTION

INTRODUCTORY REMARKS 1
STEAM-ASSISITED GRAVITY DRAINAGE (SAGD) 1
CRETACEOUS STRATIGRAPHY OF NORTHERN ALBERTA 3
PALEOTOPOGRAPHY OF THE MCMURRAY SUBBASIN 3
PREVIOUS WORK 6
The McMurray Formation 6
Inclined Heterolithic Stratification 7
STUDY AREA AND RESEARCH RATIONALE 9
THESIS LAYOUT 11
REFERENCES 11

CHAPTER 2.
FACIES DESCRIPTIONS AND INTERPRETATIONS

OBJECTIVES 15
BACKGROUND ON THE TURBIDITY MAXIMUM AND THE SALT WATER WEDGE 15
METHODOLOGY 17
OVERVIEW OF OUTCROPS 17
SEDIMENTARY FACIES 18
Facies Association 1 18
Facies A- 20
Facies B- 22
Facies C- 25
Facies D- 28
Facies E- 30
Facies F- 34
Facies Association 2 37
Facies G- 37
Facies H- 41
FACIES ASSOCIATION AND FACIES SUCCESSION 43
Facies Association 1 43
Facies Association 2 53

DISCUSSION 53
REFERENCES 55

CHAPTER 3.
THE MORPHOLOGICAL SIGNATURE OF ESTUARINE POINT BARS
INTRODUCTION 58
METHODOLOGY 58
CHARACTERIZATION OF CHANNEL MORPHOLOGY
THROUGH THE ESTUARY: PREVIOUS WORK 59
OVERVIEW OF THE DATA SET 61
South Alligator River, northern Australia 66
Ord River, northern Australia 68
King River, northern Australia 70
Fly River, Papua New Guinea 72
Rio Tuira, Panama 74
Salmon River, Nova Scotia, Canada 76
Digul River, Indonesia 76
Willapa River, Washington, U.S.A 79
Tillamook River, Oregon, U.S.A. 81
DISCUSSION 83
Estuarine Processes 83
Channel Morphology 84
Channel Width Variation 85
Underlying Sediment Composition 86
Stratigraphic Implications 87
McMurray Formation Paleochannels 87
SUMMARY 90
REFERENCES 91

CHAPTER 4.
SUMMARY AND CONCLUSIONS 93

APPENDIX 1. 94
APPENDIX 2. 100

LIST OF TABLES

Chapter 2.

Table 2-1. Summary of sedimentary facies in the McMurray Formation within the Fort MacKay and Fort McMurray areas, northeastern Alberta. 19

LIST OF FIGURES

Chapter 1.

Figure 1-1.	Location map of the major oils sands accumulations in northeastern Alberta.	2
Figure 1-2.	Lower Cretaceous Statigraphy of northeast Alberta.	4
Figure 1-3.	Isopach map of the Lower Cretaceous Mannville Group.	5
Figure 1-4.	Scematic depositional model for the Lower Cretaceous Mannville Group.	8
Figure 1-5.	Location map of the two outcrops incorporated into the study. a) Athabasca outcrop, Fort McMurray. b) Amphitheatre outcrop, Fort MacKay.	10

Chapter 2.

Figure 2-1.	Relative position of the turbidity maximum within the estuary during periods of low fluvial discharge and periods of high fluvial discharge.	16
Figure 2-2.	Outcrop photographs of Facies A.	21
Figure 2-3.	Outcrop photographs of Facies B.	23
Figure 2-4.	Outcrop photographs of Facies C.	26
Figure 2-5.	Outcrop photographs of Facies D.	29
Figure 2-6.	Outcrop photographs of Facies E.	32
Figure 2-7.	Outcrop photograph of Facies E.	33
Figure 2-8.	Outcrop photographs of Facies F.	35
Figure 2-9.	Outcrop photographs of Facies F.	36
Figure 2-10.	Outcrop photographs of Facies G.	39
Figure 2-11.	Outcrop photographs of Facies G.	40

Figure 2-12. Outcrop photographs of Facies H. 42

Figure 2-13. Outcrop photographs showing common facies relationships within Facies Association 1. 44

Figure 2-14. Type Section outcrop photograph showing the up-dip transition from sandy and muddy IHS (Facies C and D) to the muddy IHS of Facies D and E. 46

Figure 2-15. Cross-sectional view through the Athabasca outcrop section showing the stratigraphic boundaries between genetic IHS units. 47

Figure 2-16. Christina River outcrop section showing the stratigraphic boundaries between genetic IHS units. 48

Figure 2-17. Syncrude Northmine exposure showing the stratigraphic boundaries between genetic IHS units. 49

Figure 2-18. Overview of the Amphitheatre outcrop, Fort MacKay area. 52

Chapter 3.

Figure 3-1. Schematic showing the measurements collected from Landsat images of the estuaries within the study. 60

Figure 3-2. Schematic showing the proposed development of estuarine meanders. 60

Figure3-3. Schematic tripartite zonation within a typical tide-dominated estuary. 62

Figure 3-4. Sinuosity profiles for the nine estuaries examined in the study. 63

Figure 3-5. Wavelength-to-amplitude profiles for the nine estuaries examined in the study. 64

Figure 3-6. Channel width profiles for the nine estuaries examined in the study. 65

Figure 3-7. South Alligator River, northern Australia. a) location map and measured channel segments. b) and c) characteristic channel forms. d) schematic depicting the three channel zones. 67

Figure 3-8. Ord River, northern Australia. a) location map and measured channel segments. b) characteristic channel forms. c) schematic depicting the three morphological channel zones. 69

Figure 3-9. King River, northern Australia. a) location map and measured channel segments. b) schematic identifying the location of the three morphological zones. c) schematic depicting the three morphological channel zones. 71

Figure 3-10. Fly River, Papua New Guinea. a) location map and measured channel segments. b) and c) characteristic channel forms. d) schematic depicting the three morphological channel zones. 73

Figure 3-11. Rio Tuira, Panama. a) location map and measured channel segments. b) characteristic channel forms and deposits. c) schematic depicting the three morphological channel zones. 75

Figure 3-12. Salmon River, eastern Canada. a) location map and measured channel segments. b) characteristic channel forms and deposits. c) schematic depicting the three morphological channel zones. 77

Figure 3-13. Digul River, Indonesia. a) location map and measured channel segments. b) characteristic channel forms and deposits. c) schematic depicting the three morphological channel zones. 78

Figure 3-14. Willapa River, Washington, U.S.A. a) location map and measured channel segments. b) characteristic channel forms and deposits. c) schematic depicting the three morphological channel zones. 80

Figure 3-15. Tillamook River, Oregon, U.S.A. a) location map and measured channel segments. b) schematic depicting the three morphological channel zones. 82

Figure 3-16. Schematic representation of the development of variable stacked channels during progradation. 89

Figure 3-17. Schematic illustration showing how a dip angle profile can increase upwards during lateral accretion or decrease upwards within a vertical accretion fill.

CHAPTER 1.
INTRODUCTION

INTRODUCTORY REMARKS

Maximizing the efficiency of in-situ bitumen recovery of the valley-fill deposits of the McMurray Formation hinges on the ability to predict the subsurface architecture of the dominant reservoir units, a significant proportion of which comprise successions of inclined heterolithic stratification (IHS). Outcrop sections of the McMurray Formation in the Fort McMurray and Fort MacKay areas were studied to further the understanding of the architecture of IHS-dominated media. From detailed lithological mapping of outcrop sections, 2-dimensional lithological outcrop models were constructed. In addition, the geomorphology of modern estuarine environments was assessed to provide a range of characteristic channel forms in various tidally-influenced environments.

STEAM-ASSISITED GRAVITY DRAINAGE (SAGD)

The greatest accumulations of oil sands in the world amount to approximately 250-billion m^3 in-place and are situated in the northern portion of Alberta, Canada (Figure 1-1). These comprise four main oil sands areas: the Peace River, Athabasca, Wabasca, and Cold Lake deposits. The Athabasca deposits host the bulk of these reserves and the majority of these deposits are contained within the McMurray Formation. Only approximately 7% of the reserves in the Athabasca area are surface mineable and include areas buried by less than 75 m of overburden. The amount of overburden increases towards the south, forcing the exploitation of the remainder of bitumen into the subsurface. The most prominent subsurface method of extraction is SAGD, a method developed at the Alberta Oil Sands Technology and Research Authority (AOSTRA) underground test facility. This method utilizes a pair of wells drilled horizontally into the producing unit/s. The upper well acts as the injector well, emitting steam into the overlying reservoir. The steam helps to separate the bitumen from the sand thus mobilizing the bitumen. This results in the drainage of the bitumen downwards to the lower producing well.

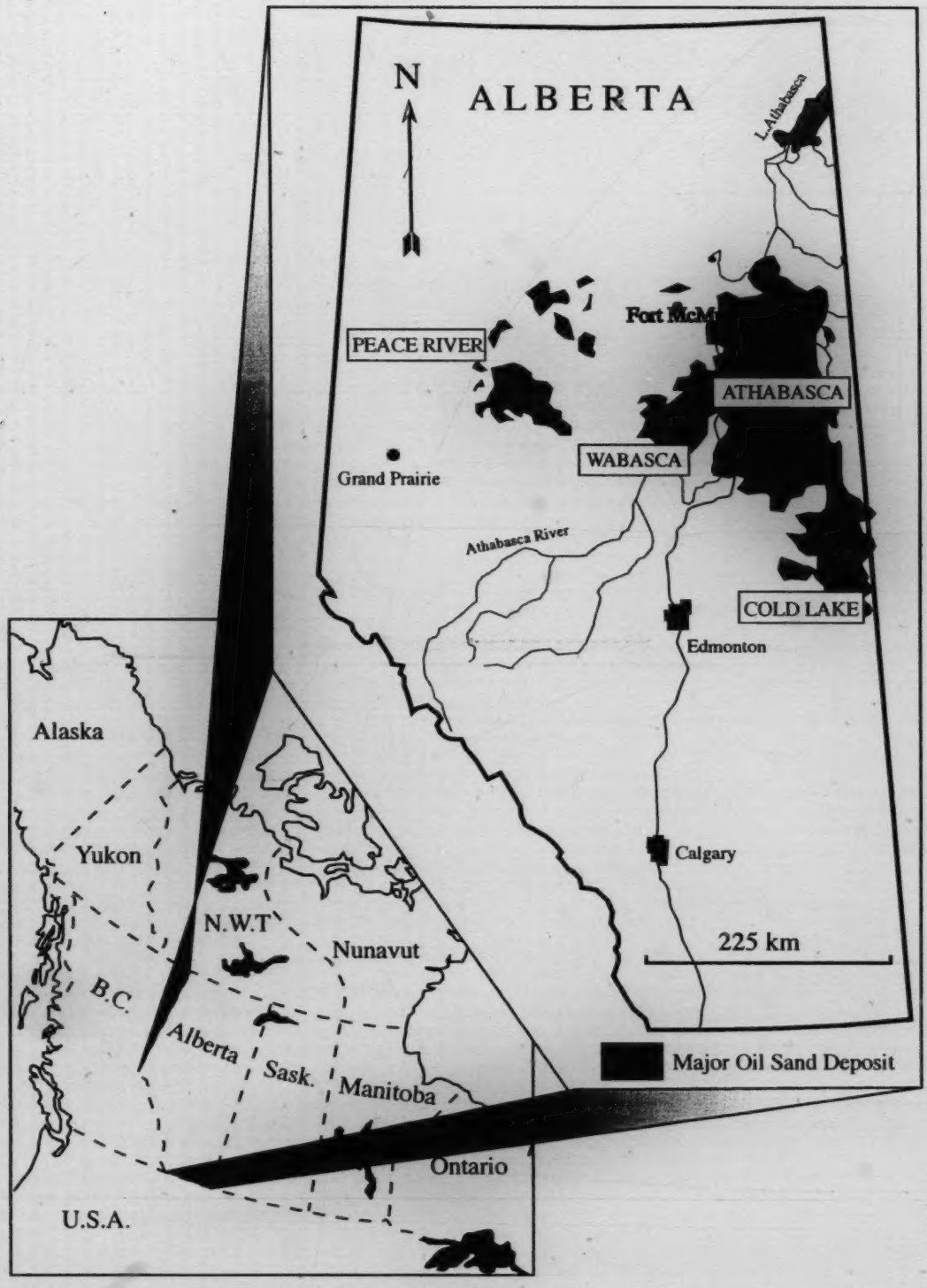

Figure 1-1. Location map of the major oil sands accumulations in northeastern Alberta including the Athabasca, Cold Lake, Peace River, and Wabasca deposits.

CRETACEOUS STRATIGRAPHY OF NORTHERN ALBERTA

The McMurray Formation is an early Cretaceous, Lower Mannville succession of Neocomian/Aptian-age siliciclastics (Figure 1-2). The average thickness of the McMurray Formation is 40 m and comprises uncemented, very fine to medium-grained quartz sand, interbedded with shales in complex channel systems. It fills the topographic lows of the McMurray Subbasin and is age equivalent to the Gething Formation within the Peace River Subbasin and other McMurray sediments within the Wabasca Subbasin. The McMurray Formation rests unconformably on Middle to Upper Devonian carbonates of the Beaverhill Lake Group and the Upper Devonian carbonates of the Woodbend Group. Overlying the McMurray sediments are shallow marine deposits of the Clearwater Formation, which are overlain by fully marine deposits of the Clearwater Formation.

PALEOTOPOGRAPHY OF THE MCMURRAY SUBBASIN

Mapping the Sub-Cretaceous unconformity upon which the McMurray sediments were deposited within the central and northern parts of Alberta reveals a northwest/ southeast trending axial ridge that separates sediments within the McMurray Subbasin from those within the Wabasca Subbasin. The valley within which these sediments were deposited was bounded to the east by the highlands of the Canadian Shield and to the West by the axial ridge system, composed of the Wainright Ridge in central Alberta and the Grosmont High in northeastern Alberta. Localization of the paleotopographic low of the McMurray valley axis was controlled largely by dissolution of the Middle Devonian Prairie evaporite as well as Lower Devonian Cold Lake and Lotsberg Formations (Ranger and Pemberton, 1997). This structural control persisted prior to and during deposition of the McMurray sediments as well as the overlying Wabiskaw Member.

Aside from the main axial ridge system, subordinate spurs obliquely attached to the Grosmont High constrained sedimentation patterns of the Athabasca deposits (Figure 1-3). The main trunk system is separated into two between townships 9 and 10 and ranges 77 to 70 by a large ridge that extends northward from the Wainright Ridge in the south. In addition, a spur attached to the Grosmont high in townships 16 and 17 extends northward from ranges 80 and 81 to range 94 causing a large bifurcation of the main valley system in the north (Ranger and Pemberton, 1997). Collectively, these tributaries converge around the Bitumount Basin and significantly impact the regional accumulation patterns of the Athabasca deposits.

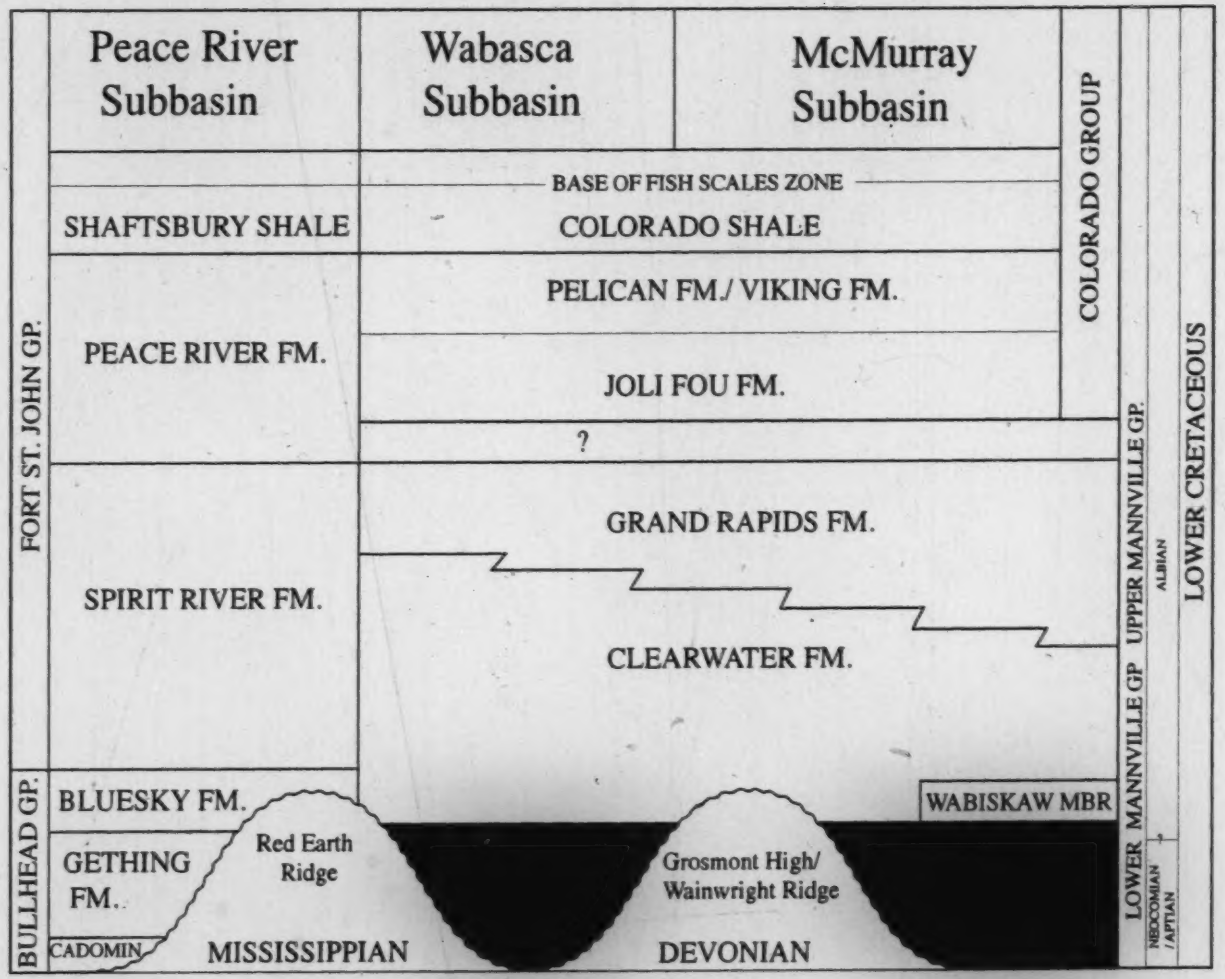

Figure 1-2. Lower Cretaceous stratigraphy of northeast Alberta. (after Ranger and Gingras, 2005).

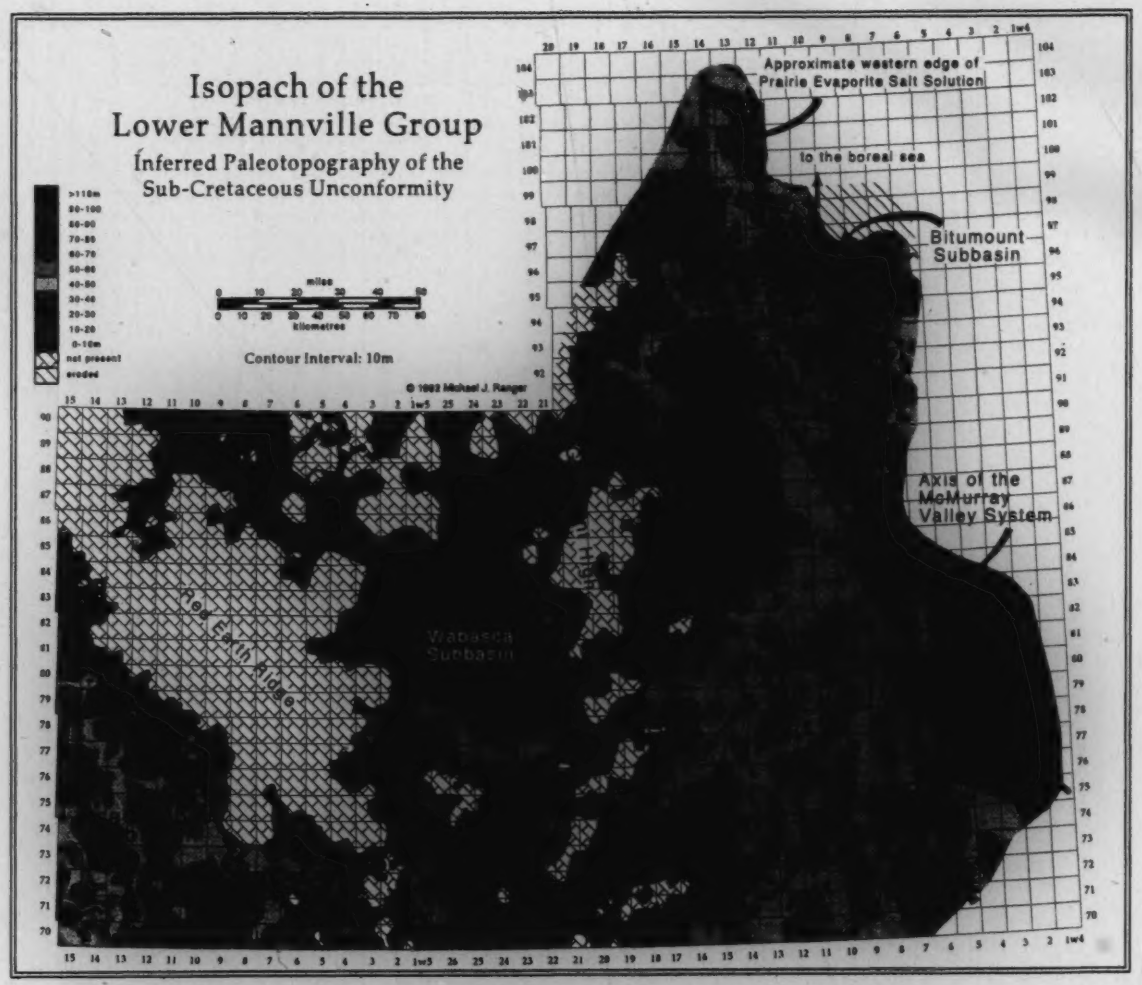

Figure 1-3. Isopach map of the Lower Cretaceous Mannville Group showing the Grosmont High, the McMurray Subbasin, and secondary spurs within this subbasin. (after Ranger and Pemberton, 1997).

The McMurray valley axis, initiated by dissolution of underlying evaporite units, developed during regression of the coastline of the Boreal Sea, an interior seaway occupying northeastern Alberta during the lower Cretaceous. Transgression of this coastline resulted in the filling of a drowned fluvial valley system, one stage of which represents estuarine valley-fill complexes of the McMurray Formation. Further transgression shifted sedimentation within the drowned valley complexes to shallow marine. These deposits of the upper McMurray and Wabiskaw Member are overlain by deep marine deposits of the Clearwater, deposited during the final stages of transgression.

PREVIOUS WORK

The McMurray Formation

The economic potential of the heavy oil deposits in northern Alberta near the town of Fort McMurray was noted by Bell (1885). This observation initiated attempts by the Geological Survey of Canada in the 1920's to quantify the volume of bitumen-saturated sand present (Ells, 1926; Clark and Blair, 1927). Strata enveloping the oil sands were given the name McMurray in 1917 (McLearn, 1917). A considerable number of textural studies on the McMurray Formation and the geologic controls to which these sedimentary fabrics ascribe were completed in the 1960's and 1970's (Carrigy, 1962, 1963a, 1963b, 1963c, 1966, 1967, 1973; Flach, 1977 (unpublished thesis); Stewart, 1963, 1981; Stewart and MacCallum, 1978). Carrigy (1963a) created the three-fold classification of the McMurray Formation that remains in use today: the lower, middle, and upper, which are referred to informally as members.

The geologic succession of the McMurray Formation was first interpreted by Carrigy (1967, 1973) to encompass sediments of fluvial floodplain origin at the base, marine-influenced deltaic foresets and deltaic-lagoonal sediments in the middle, and open-shelf marine sediments within the upper portion. Stewart (1963), and Stewart and MacCallum (1978) later postulated that the lower member was composed of fluvial-derived sands, the middle McMurray Formation sediments comprised estuarine deposits, and open marine sands characterized the upper McMurray. Debate regarding the degree of marine influence on the middle McMurray sediments lasted through the late 1970's to late 1980's. Some authors interpreted the epsilon cross-stratification comprising a large portion of the middle McMurray Formation to be the result of deep channel fills in a fluvial setting (Mossop, 1978; Flach and Mossop, 1985; and Mossop and Flach, 1983). These authors remissibly interpreted the middle McMurray sediments amidst

seminal research on the ichnology of the McMurray sediments (Pemberton *et al.*, 1982; Pemberton and Wightman, 1987).

These studies recognized the presence of low-diversity and individual high-density suites of trace fossils within the middle McMurray Formation suggesting that brackish-water conditions existed, at least in part, during middle McMurray deposition (Pemberton and Wightman, 1987). Additionally, marine forms of spores and pollen were absent throughout most of the McMurray Formation (Singh, 1964) negating the possibility of deposition through marine-influenced deltaic environments proposed by Carrigy (1973). Comparative sedimentologic studies by Smith (1988a, 1988b) between modern estuarine deposits in Willapa Bay, Washington and the McMurray Formation also suggested that marine influence was present during McMurray deposition. More specifically, the similarities between the epsilon cross-stratification, formalized to 'inclined heterolithic stratification' (henceforth, IHS) (Thomas *et al.*, 1987), in modern tidal-fluvial channels and the McMurrray Formation were uncanny. This suggested that the middle member was characterized by lateral accretion deposits in an estuarine setting (Smith, 1987, 1988a, 1988b), an interpretation widely accepted today (Bechtel *et al.*, 1994; Ranger and Pemberton, 1992; Ranger and Pemberton, 1997).

The stratigraphic relationships within the McMurray Formation remain somewhat elusive, in part because recent studies encompass areas of limited extent (Strobl *et al.*, 1997, Bechtel *et al.*, 1994), but also because stratal relationships have proved difficult to correlate appreciable distances (Flach, 1984). Additionally, there exists an overwhelming amount of subsurface data to analyze and interpret, including geophysical well logs and cores. Regional studies on the McMurray Formation (Ranger and Pemberton, 1997) are limited and suggest a far more complex distribution of facies and stratigraphic units than the generalized three-component model referred to by previous authors. Currently, the model best describing the stratigraphy of the McMurray Formation recognizes correlatable genetic units, 8 to 12 m thick that are separated by regionally persistent shale markers (Nelson and Glaister, 1978) (Figure 1-4). These time-stratigraphic units are overshadowed by the persistence of lowstand systems tracts comprising complex channel fills that incise the shoreface units (Ranger and Pemberton, 1997). These channel fills are composed largely of inclined heterolithic stratification and are generally associated with the middle member of the McMurray Formation.

Inclined Heterolithic Stratification

Thomas *et al.* (1987) formalized the term 'inclined heteroloithic stratification' to replace pre-existing terms used to define the parallel to sub-parallel strata wherein the

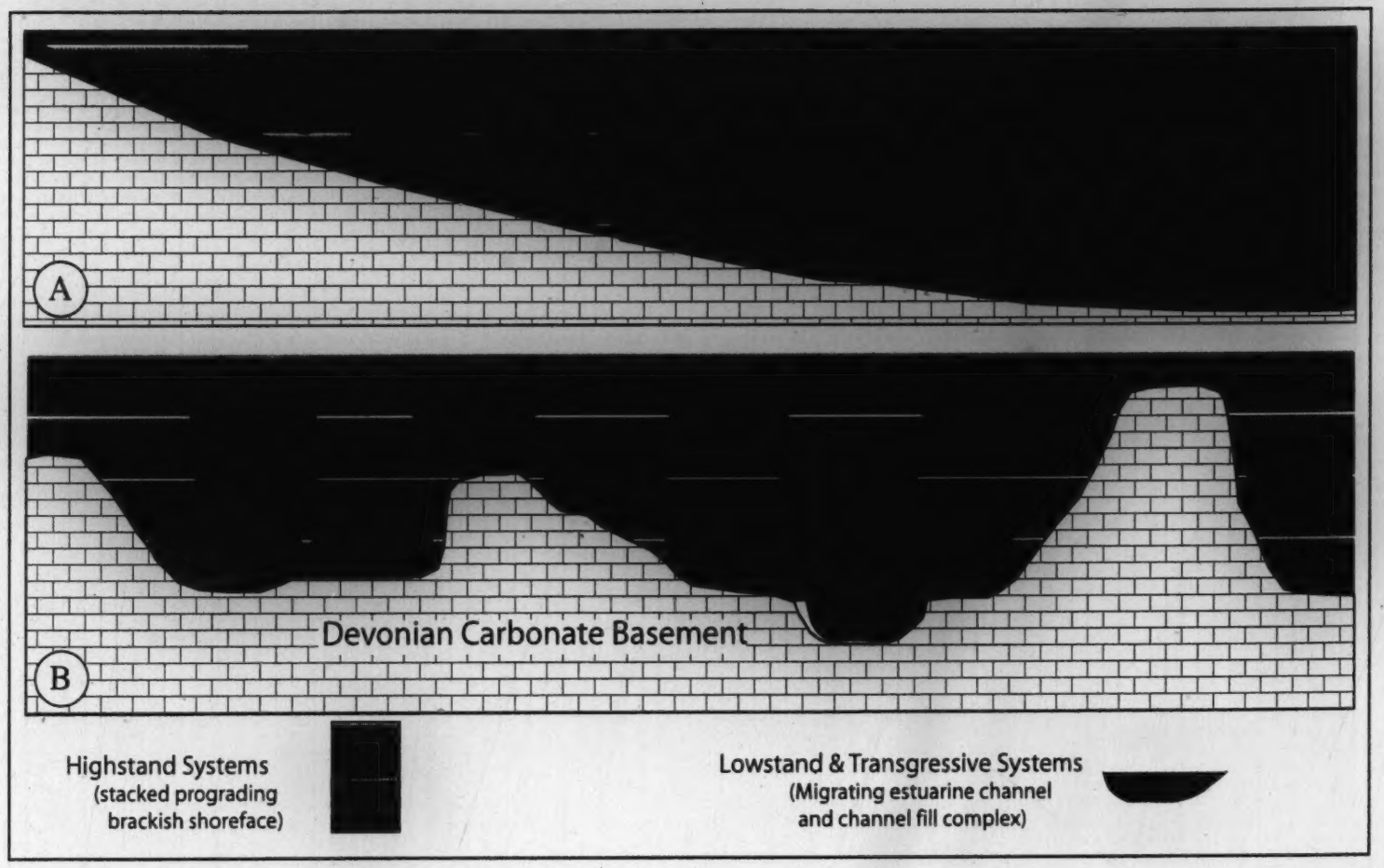

Figure 1-4. Schematic depositional model for the Lower Cretaceous Mannville Group (after Ranger and Pemberton, 1997). A. Schematic model parallel to the McMurray paleovalley. B. Schematic model perpendicular to the McMurray paleovalley axis.

dip reveals original architectural elements. Numerous ancient sedimentary examples of IHS have been documented and associated with a variety of sedimentary environments ranging from submarine, deltaic, estuarine, and wholly fluvial (Thomas *et al.*, 1987 and references therein). The affiliation of IHS with tidally influenced, marginal marine environments has become increasingly common (Smith, 1988b; Ranger and Pemberton, 1992; Rasanen et al., 1995; Gingras *et al.*, 1999). This trend may have been imparted by the enhanced understanding of the hydrodynamic processes necessary to form IHS, but more noteworthy is the study of brackish-water assemblages of ichnofossils within IHS-bearing successions. Many studies have focused on the ichnology of the McMurray Formation, colonization events of infaunal burrowers, and the depositional factors influencing successions of IHS (Bechtel *et al.*, 1994; Yuill *et al.*, 1994; Ranger and Pemberton, 1997; and Gingras *et al.*, 2002).

STUDY AREA AND RESEARCH RATIONALE

The study area comprises two outcrop localities (Figure 1-5): the first is located along the banks of the Athabasca River approximately 2 km downstream of the town of Fort McMurray within the McMurray Formation Type Section (Twp 89, R9W4); the second is located on the MacKay River, approximately 3 km northeast of the town of Fort MacKay. This outcrop is referred to in previous studies as the Amphitheatre Outcrop.

Outcrop work was conducted during the summer of 2002. Three sections from the Athabasca River outcrop and two from the MacKay River section were measured in detail to the cm scale, logged, sampled, and photographed.

Observations made from outcrop in the study area and within other areas of the outcrop belt initiated a study focusing on qualifying the accretion deposit types and channel morphologies within variable modern estuarine settings. These data were used to help conceptualize the 3-dimensional architecture of accretion deposits within the study area. This study relied heavily on satellite imagery available to the public from NASA and assisted greatly in the development of relevant geological models.

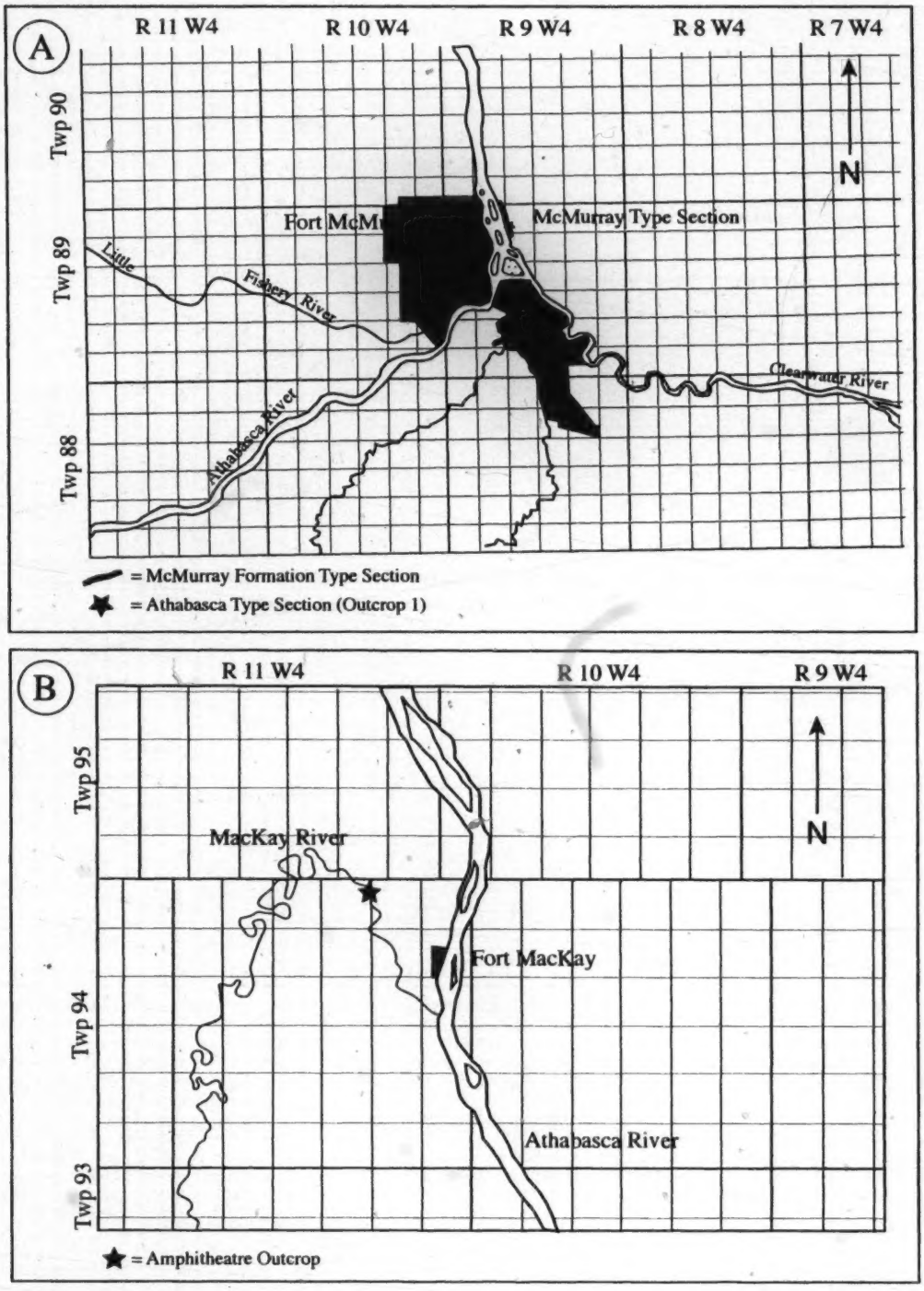

Figure 1-5. Location map of the two outcrops incorporated into the study. A. Athabasca outcrop located 2 km north of the town of Fort McMurray, Alberta, Canada. B. Amphitheatre outcrop located west of Fort MacKay, Alberta, Canada.

THESIS LAYOUT

This thesis is organized in the following manner: Chapter 1 discusses background information on the McMurray Formation and introduces the study areas; Chapter 2 comprises outcrop descriptions and interpretations from the study area; and Chapter 3 focuses the characterization of the morphological elements within nine modern estuaries.

REFERENCES

Bechtel, D.J., Yuill, C.N., Ranger, M.J. and Pemberton, S.G. 1994. Ichnology of inclined heterolithic stratification of the McMurray Formation, northeastern Alberta. *In*: S.G. Pemberton, D.P. James, and D.M. Wightman (eds.), Canadian Society of Petroleum Geologists Mannville Core Conference, Canadian Society of Petroleum Geologists, Exploration Update 1994, p. 351-368.

Bell, R. 1885. Report on the part of the basin of the Athabasca River, North-west Territory. Geological Survey of Canada, Report on Progress, 1882-83-84, part CC, V 37 pp.

Carrigy, M.A. 1962. Effect of texture on the distribution of oil in the Athabasca Oil Sands, Alberta, Canada. Journal of Sedimentary Petrology, v. 32, p. 312-325.

Carrigy, M.A. 1963a. Criteria for differentiating the McMurray and Clearwater formations in the Athabasca Oil Sands. Research Council of Alberta, Bulletin 14, 32 pp.

Carrigy, M.A. 1963b. Paleocurrent directions from the McMurray Formation. Bulletin of Canadian Petroleum Geology, v. 11, p. 389-395.

Carrigy, M.A. 1963c. Petrology of coarse-grained sands in the lower part of the McMurray Formation. *In*: M.A. Carrigy (ed.), The K.A. Clark Volume, Research Council of Alberta, Information Series, no. 45, p. 43-54.

Carrigy, M.A. 1966. Lithology of the Athabasca Oil Sands. Research Council of Alberta, Bulletin18, 48 pp.

Carrigy, M.A. 1967. Some sedimentary features of the Athabasca Oil Sands. Sedimentary Geology, v. 1, p. 327-352.

Carrigy, M.A. 1973. Mesozoic geology of the Fort McMurray area. *In*: M.A. Carrigy and J.W. Kramers (eds.), Guide to the Athabasca Oil Sands Area, Alberta Research Council, Information Series, no. 65, p. 77-101.

Clark, K.A. and Blair, S.M. 1927. The bituminous sands of Alberta. Part I-Occurrence. Scientific and Industrial Research Council of Alberta, Report no. 18, 74 pp.

Ells, S.C. 1926. Bituminous sands of northern Alberta. Report on investigations to the end of 1924, Canada Department of Mines, Mines Branch, no. 632, 244 pp.

Flach, P.D. 1977. A lithofacies analysis of the McMurray Formation, Lower Steepbank River, Alberta. Unpublished MSc. Thesis, University of Alberta, Edmonton. 139 pp.

Flach, P.D. 1984. Oil sands geology- Athabasca deposit north. Alberta Research Council, Bulletin 46, 3 pp.

Flach, P.D. and Mossop, G.D. 1985. Depositional environments of Lower Cretaceous McMurray Formation, Athabasca oil sands, Alberta. American Association of Petroleum Geologists Bulletin, v. 69, no. 8, p. 1195-1207.

Gingras, M.K., Rasanen, M. and Ranzi, A. 1999. The significance of bioturbated inclined heterolithic stratification in the southern part of the Miocene Solimoes Formation, Rio Acre, Amazonia Brazil. Palaios, v. 17, p. 591-601.

Gingras, M.K., Pemberton, S.G. and Sauders, T. 2002. The ichnology of modern and Pleistocene brackish-water deposits at Willipa Bay, Washington: Variability in estuarine settings. Palaios, v. 14, p. 352-374.

McLearn, F.H. 1917. Athabasca River section, Alberta. Geological Survey of Canada, Summary Report 1916, p. 145-151.

Mossop, G.D. 1978. Epsilon cross-strata in the Athabasca oil sands (abs.) *In*: A.D. Miall (ed.), Fluvial Sedimentology, Canadian Society of Petroleum Geologists, Memoir 5, p. 854-855.

Mossop, G.D. and Flach, P.D. 1983. Deep sedimentation in the Lower Cretaceous McMurray Formation, Athabasca Oil Sands, Alberta. Sedimentology, v. 30, p. 493-509.

Nelson, H.W. and Glaister, R.P. 1978. Subsurface environmental facies and reservoir relationships of the McMurray oil sands, northeastern Alberta. Bulletin of Canadian Petroleum Geology, v. 26, no. 2, p. 177-207.

Pemberton, S.G., Flach, P.D. and Mossop, G.D. 1982. Trace fossils from the Athabasca oil sands, Alberta, Canada. Science, v. 217, p. 825-827.

Pemberton, S.G. and Wightman, D.M. 1987. Brackish water trace fossil suites: examples from the Lower Cretaceous Mannville Group. *In*: P.J. Currie and E.H. Koster (eds.), Mesozoic terrestrial ecosystems, Occasional Paper of the Tyrrell Museum of Palaeontology, 3, p. 183-190.

Ranger, M.J. and Gingras, M.K. 2005. Geology of the Athabasca Oil Sands: Field Guide and Overview, Canadian Society of Petroleum Geology Annual Convention. 132 pp.

Ranger, M.J. and Pemberton, S.G. 1992. The sedimentology and ichnology of estuarine point bars in the McMurray Formation of the Athabasca oil sands deposit, northeastern Alberta, Canada. *In*: S. G. Pemberton (ed.), Applications of Ichnology to Petroleum Exploration, Society of Economic Paleontologists and Mineralogists, Core Workshop No. 17, p. 401-421.

Ranger, M.J. and Pemberton, S.G. 1997. Elements of a stratigraphic framework for the McMurray Formation in South Athabasca. *In*: S.G. Pemberton and D.P. James (eds.), Petroleum Geology of the Cretaceous Mannville Group, Western Canada, Canadian Society of Petroleum Geologists, Memoir 18, Calgary, p. 263-291.

Rasanen, M.E., Linna, A.M. and Santos, C.R. 1995. Late Miocene Tidal Deposits in the Amazonian Foreland Basin. Science, v. 269, p. 386-390.

Singh, C. 1964. Microflora of the Lower Cretaceous Mannville Group, east-central Alberta. Alberta Research Council, Bulletin 15, 239 p.

Smith, D.G. 1987. Meandering river point bar lithofacies models: modern and ancient examples compared. *In*: F.G. Ethridge, R.M. Flores, M.D. Harvey, and J.N. Weaver (eds.), Recent developments in fluvial sedimentology, Society of Economic Paleontologists and Mineralogists, Special Publication 39, p. 83-91.

Smith, D.G. 1988a. Modern point bar deposits analogous to the Athabasca oil sands, Alberta, Canada. *In:* P.L. de Boer, A. van Gelder, and S.D. Nio (eds.), Tide-influenced sedimentary environments and facies, D. Reidel Publishing Co., The Netherlands, p. 417-432.

Smith, D.G. 1988b. Tidal bundles and mud couplets in the McMurray Formation, northeastern Alberta, Canada. Bulletin of Canadian Petroleum Geology, v. 36, p. 216-219.

Stewart, G.A. 1963. Geological Controls on the distribution of Athabasca Oil Sand reserves. *In*: M.A. Carrigy (ed.), The K.A. Clark Volume, Research Council of Alberta, Information Series, no. 45, p. 15-26.

Stewart, G.A. 1981. Athabasca Oil Sands. *In*: R.F. Meyer, C.T. Steele and J.C. Olson (eds.), The Future of Heavy Crude Oils and Tar Sands, United Nations Institute for Training and Research, McGraw-Hill, New York, p. 208-222.

Stewart, G.A. and MacCallum, G.T. 1978. Athabasca Oil Sands guide book. Canadian Society of Petroleum Geologists international conference: Facts about principles of world petroleum oil occurrence, Canadian Society of Petroleum Geologists, 33 p.

Strobl, R.S., Muwais, W.K., Wightman, D.M., Cotterill, D.K. and Yuan, L. 1997. Geological Modeling of McMurray Formation reservoirs based on outcrop and subsurface analogues. *In*: S.G. Pemberton and D.P. James (eds.), Petroleum Geology of the Cretaceous Mannville Group, Western Canada, Canadian Society of Petroleum Geologists, Memoir 18, Calgary, p. 292-311.

Thomas, R.G., Smith, D.G., Wood, J.M., Visser, J., Calverly-Range, E.A. and Koster, E.H. 1987. Inclined heterolithic stratification- terminology, description, interpretation, and significance. Sedimentary Geology, v. 53, p. 123-179.

Yuill, C.N., Bechtel, D.J. and Pemberton, S.G. 1994. Sedimentology and Ichnology of the McMurray Formation at the OSLO and Steepbank areas, northeastern Alberta. *In*: S.G. Pemberton, D.P. James (eds.), Canadian Society of Petroleum Geologists, Mannville Core Conference, Society of Economic Paleontologists and Mineralogists, Special Publication No. 51, p. 45-60.

CHAPTER 2.
FACIES DESCRIPTIONS AND INTERPRETATIONS

OBJECTIVES

The primary objectives of this chapter are to: 1) present the findings from this study including the descriptions and interpretations of the facies and the facies associations within the field area; 2) place the outcrops in a regional paleoenvironmental context; and 3) review the previous work and the accepted depositional model of the McMurray Formation.

BACKGROUND ON THE TURBIDITY MAXIMUM AND THE SALT WATER WEDGE

The turbidity maximum, defined by Postma (1967), is the area where suspended sediment concentrations reach their highest values in an estuarine setting. It is within this area that mud particles flocculate, the process by which mud particles adhere to one another. Several conditions must be met for salt induced flocculation to take place: 1) suspended sediment must have surface electrochemical properties that make them conducive to flocculation; 2) a significant concentration of suspended matter must be present, preferably several grams per litre; and 3) the velocity of the water must be low enough to allow flocculated material to settle out of suspension (Meade, 1972). A simplified synopsis of this procedure outlines two steps: first, small positive ionic charge such as Na^+ are present to act as nuclei for the slightly negatively charged mud particles; second, these flocculates grow in size to the point where they can no longer remain in the water column, at which point they settle out as clumped grains. An appreciation of the hydraulic behavior of mud should be engraved from this procedure. Although mud can be deposited from suspension in stagnant water, deposition of mud within the turbidity maximum is more analogous to deposition of sand-sized particles, a well-documented observation (Meade, 1972; Johnson, 1983; Stone and Droppo, 1994; Thill *et al.*, 2001).

The turbidity maximum is generally located near the interface where marine derived salt water intrudes landward to meet the influx of fresh water (Meade, 1972). Inherent to this system is a migratory effect of the turbidity maximum coincident with diurnal, spring, and neap tidal fluctuations, as well as storms and fluctuating fluvial discharge (Thomas *et al.*, 1987). In short, this zone will be located furthest downstream

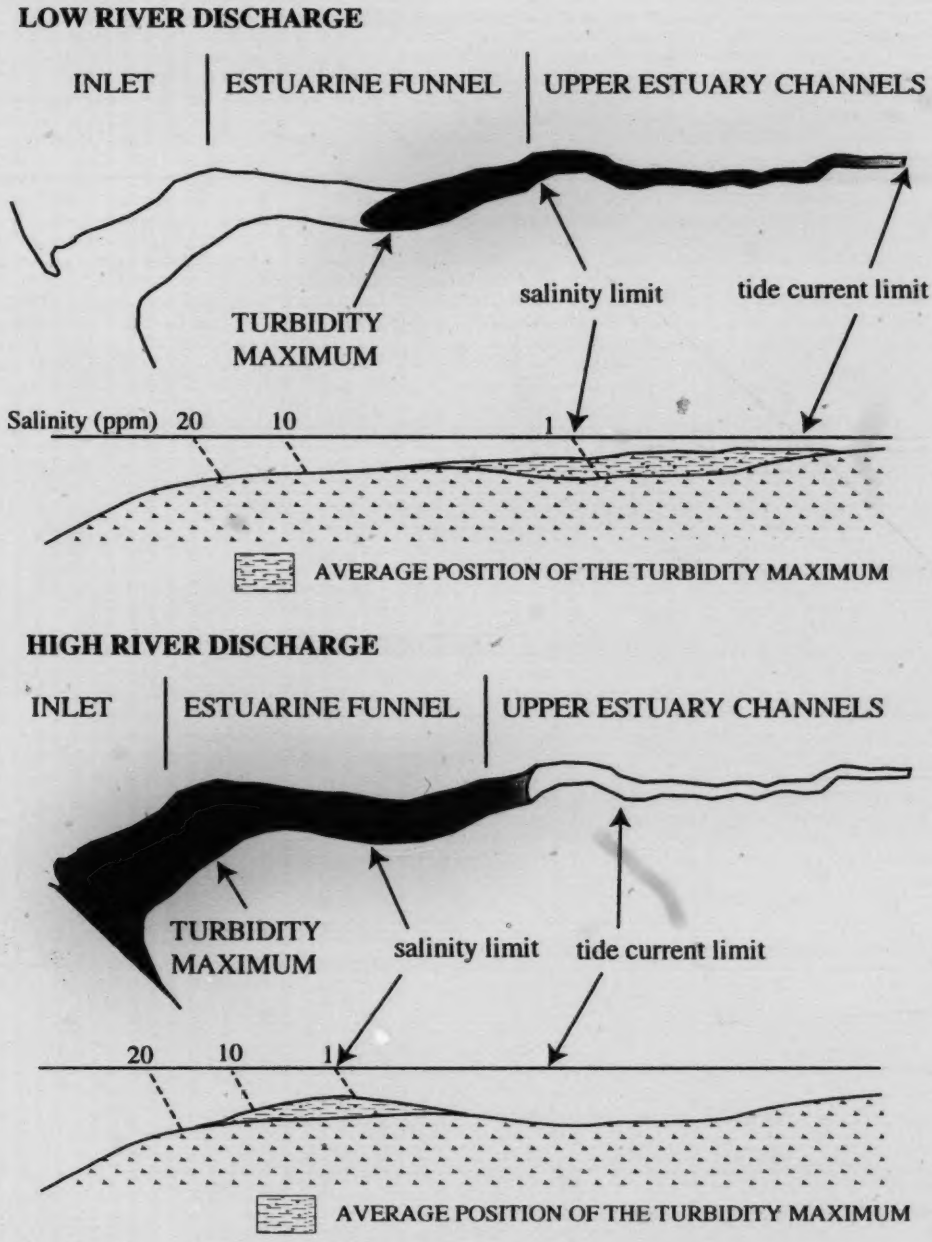

Figure 2-1. Relative position of the turdidity maximum within the estuary during periods of low fluvial discharge and during periods of high fluvial discharge (modified from Allen, 1991).

when high fluvial discharge rates are coincident with neap tides, and furthest upstream when low fluvial discharge rates are countered by spring tides (Figure 2-1).

METHODOLOGY

Two outcrops were examined in this study (Figure 1-5). The first is located on the banks of the Athabasca River approximately 2 km downstream of Fort McMurray along the McMurray Formation Type Section. The second is situated in the Fort MacKay area, near the banks of the MacKay River, also known as the Amphitheatre outcrop. A zodiac boat was used to access the base of the first outcrop. Due to the height and steepness of the outcrop, it was necessary to use repelling equipment to facilitate sedimentological and ichnological observations.

Three vertical sections from the Athabasca River outcrop and two from the Amphitheatre outcrop were measured and described to the cm scale. Strip logs were constructed documenting the grain size, bed thickness and bedding contacts, sedimentary structures, and biogenic sedimentary structures (Appendix 1). Mud beds that were too thin and discontinuous to incorporate into the strip logs were noted in an appropriate column of the strip log. Numerous photos were taken of noteworthy structures and ample photos were collected of small-scale components of the outcrop for laboratory reconstruction of the lateral distribution of mud-beds. Three-dimensional numerical flow models of facies samples were generated to assess the bulk horizontal and vertical permeabilities of facies units. These models were based on samples, approximately 20 cm^3 in size, collected at the outcrop. Sample locations were chosen to reflect the spectra of facies found within the outcrop and do not necessarily comply with a regular stratigraphic interval. In general, six or seven samples were collected from each vertical transect. The methodology of permeability analyses is discussed in Chapter 4.

To accurately depict the original dip of each outcrop and to correlate facies between the outcrop sections, it was necessary to generate a horizontal datum. This was achieved using a water balance, capable of generating a structural elevation line with minimal vertical error (2 cm vertical error for every 10 m laterally) (Harris, 2003, unpublished thesis).

OVERVIEW OF OUTCROPS

Striking similarities exist between the two outcrops examined within this study, including the presence of two facies associations and a similar stacking of those

associations. In general, these include a medium-to coarse-grained, high-angled cross-bedded unit and variably interbedded successions of inclined heterolithic stratification (IHS). The base of both units is invariably erosional. The base of the Amphitheatre outcrop is marked by a thin succession of IHS abruptly overlain by a coarse-grained to pebbly sand. This sand grades upwards into the medium-grained sand unit. The section is capped by another thin succession of IHS. Within the Type Section outcrop, it is the high-to medium-grained sand unit that is located at the base of the succession. This unit is erosionally truncated by granular lag, which grades upwards into a succession of massive-appearing, fine-grained sand. This sandy unit grades upwards into variably bedded IHS. The medium-grained, high-angled sand unit erosionally truncates the top of the IHS succession.

The bioturbation index (B.I.) referred to below is a measure of the relative degree of bioturbation within each bed or bed set (Appendix 1). This index ranges from 0, or completely devoid of any biogenic structures to V, representing the most intense degree of burrowing observed. In this case, the original bedding has been completely destroyed by biogenic reworking.

SEDIMENTARY FACIES

Eight facies were identified from the outcrops of the McMurray Formation (Facies A through H; Table 2-1). Based on distinct sedimentological or ichnological characters, these facies were futher subdivided into Facies Associations 1 and 2. A number of facies within Facies Association 1 comprise IHS of variable thickness and character. The terms describing these facies are consistent with those outlined by Thomas *et al.* (1987). The characterization of the following facies is based largely on the relative proportions of sand and mud. This is done for the sole purpose of numerical modeling, a subject that is discussed at length in Chapter 4. A distinction is made between thinly bedded, thickly bedded, and interlaminated sand/mud because it is hypothesized that the differences in bed thickness and relative mud content significantly affect horizontal and vertical bulk permeability within these strata. Bulk permeability is discussed in later sections.

FACIES ASSOCIATION 1

Facies Association 1 consists of variably bedded IHS deposited within tidally influenced channels in an estuarine environment. A normal succession includes repeated stacking of coarse-grained sands (Facies A), rippled sand and sandy-IHS (Facies B and

Facies	Dominant grain-size and lithology	Sedimentary Structures	Biogenic Structures/ Accessories	Interpretation
A	Moderately to poorly sorted coarse- to medium-grained sand containing basal rip-up clasts of semi-consolidated mud.	Low-angle cross-stratification and normally-graded bedding.	Coal fragments found on basal surface.	Upper estuarine channel-lag deposit.
B	Fine-grained micaceous, quartz-rich sand with abundant carbonaceous debris.	Ripple- to climbing-ripple bedding, carbonaceous flasers.	Rare to absent (0-I) *Cylindrichnus (Cy), Skolithos (Sk)* Carbonaceous debris common.	Accretion deposits in estuarine channels and tidally influenced fluvial channel.
C	Thickly bedded (>10cm) fine-grained micaceous sand and mud or interlaminated silty sand and mud (>50% sand within each couplet, commonly >95%).	Sand: normally graded current- to climbing-current ripple bedding, massive. Mud: planar, wavy and lenticular laminations, rare double-mud drapes.	Predominantly monospecific assemblages of *Cy; Sk; Gyrolithes (Gy)* commonly observed.	Middle to inner estuarine channels.
D	Medium bedded (2 to 10 cm) fine-grained sand or silt and mud. Mud proportion between 10% and 50% of couplet.	Sand: current and climbing-current ripple bedding, commonly massive. Mud: rare planar and wavy laminations preserved.	Monospecific assemblages of *Cy or Gy*, local assemblages of *Gy* and *Cy*, bioturbation index commonly II-III, rarely IV-V.	Quiescent conditions, with small fluctuations in energy; upper intertidal point bar, upper estuarine point bar.
E	Thinly bedded homogeneous mud or interlaminated fine-grained sand or silt and mud. Mud proportion exceeds 50% of the couplet, often >90%.	Sand: very rare climbing and current ripple bedding, massive appearance. Mud: rare planar and wavy laminations, original structure often destroyed by biogenic reworking.	Monospecific assemblages of *Cy or Gy*, local assemblages of *Gy* and *Cy*, bioturbation index commonly III-V.	Quiescent conditions, with small fluctuations in energy; intertidal proper to upper intertidal point bar and upper estuarine point bar.
F	Fine- to medium-grained sand with rounded- to sub-angular clasts of mud, locally burrow rip-ups.	High-angle to low-angle cross-stratification defined largely by imbrication of mud clasts along bedding contacts.	Clasts locally composed of ripped up *Cy?*	Reworked cut-bank collapse or storm-generated flooding inducing erosion of upper point bar surface.
G	Coarse- to medium-grained and medium- to fine-grained micaceous sand with abundant carbonaceous debris.	High-angle cross-stratified sands with reactivation surfaces, grain striping, discernable spring/neap bundles.	Rare *Co*, escape structures, and *Cy* common near tops of bedsets. Organic detritus common.	Outer estuarine subaqueous 2-and 3-dimensional dunes.
H	Coarse- to medium-grained sand that is moderately to poorly sorted containing basal rip-clasts of semi-consolidated mud.	Low-angle cross-stratification and normally graded beds.	Coal fragments found on basal surface.	Transgressive lag deposit.

Table 2-1. Summary table showing the sedimentary and ichnological characteristics, and evironmental interpretations of the facies observed within the study areas.

C), capped by muddy-IHS (Facies D and E). The channel deposits of facies association 1 are characterized by sedimentary structures indicative of current and tidal processes, moderate quantities of organic detritus, evidence of basal erosion, and ichnologic structures indicative of stressed salinity conditions. This physical evidence indicates that facies association 1 was deposited during lateral migration of tidally influenced point bars.

Facies A- Coarse-grain to pebbly sand

Description

Facies A is characterized by poorly sorted, fine-to pebbly-sand exhibiting low-angle cross-stratification (Table 2-1, Figure 2-2). Grains are composed of a quartz (60%), feldspar (20%), and lithic fragments (20%). At the Type Section outcrop, Facies A displays a sharp, erosive contact with underlying strata, and is devoid of trace fossils. Typically, this facies grades upward into ripple-laminated fine-to medium-grained sand (Facies B) or thickly bedded IHS (Facies C). Coal fragments ranging from 1 mm to 30 cm in length are observed at the Amphitheatre outcrop at the base of the upper IHS succession (Figure 2-2b).

Interpretation

Facies A is interpreted to be deposited as a channel lag deposit at the base of fluvial or estuarine channel deposits, and is coeval with initial channel incision into underlying strata. Low-angle cross bedding of medium- to coarse-grained sand is the result of migration of subaqueous dunes generated by unidirectional currents within the upper flow regime. Allen (1980) describes an upward transition from cross-bedded sands to cross-laminated sands within fluvial environments. The change in bedding scale from the dunes of Facies A to the ripple-lamination of Facies B or C is coincident with the migration of a channel thalweg and a shift from deposition under upper to lower flow regime conditions. Walker (1992), summarizing Walther's Law, states that, "in a vertical sequence, a gradational transition from one facies to another implies that the two facies represent environments that were once adjacent laterally". The presence of an erosional base, moderate sorting, and upward transition of Facies A into Facies B or C then supports the interpretation of channel incision into underlying strata and lateral migration of a channel thalweg. In addition, migration of the thalweg results in the preservation of bedforms that thin upwards and resided within the channel.

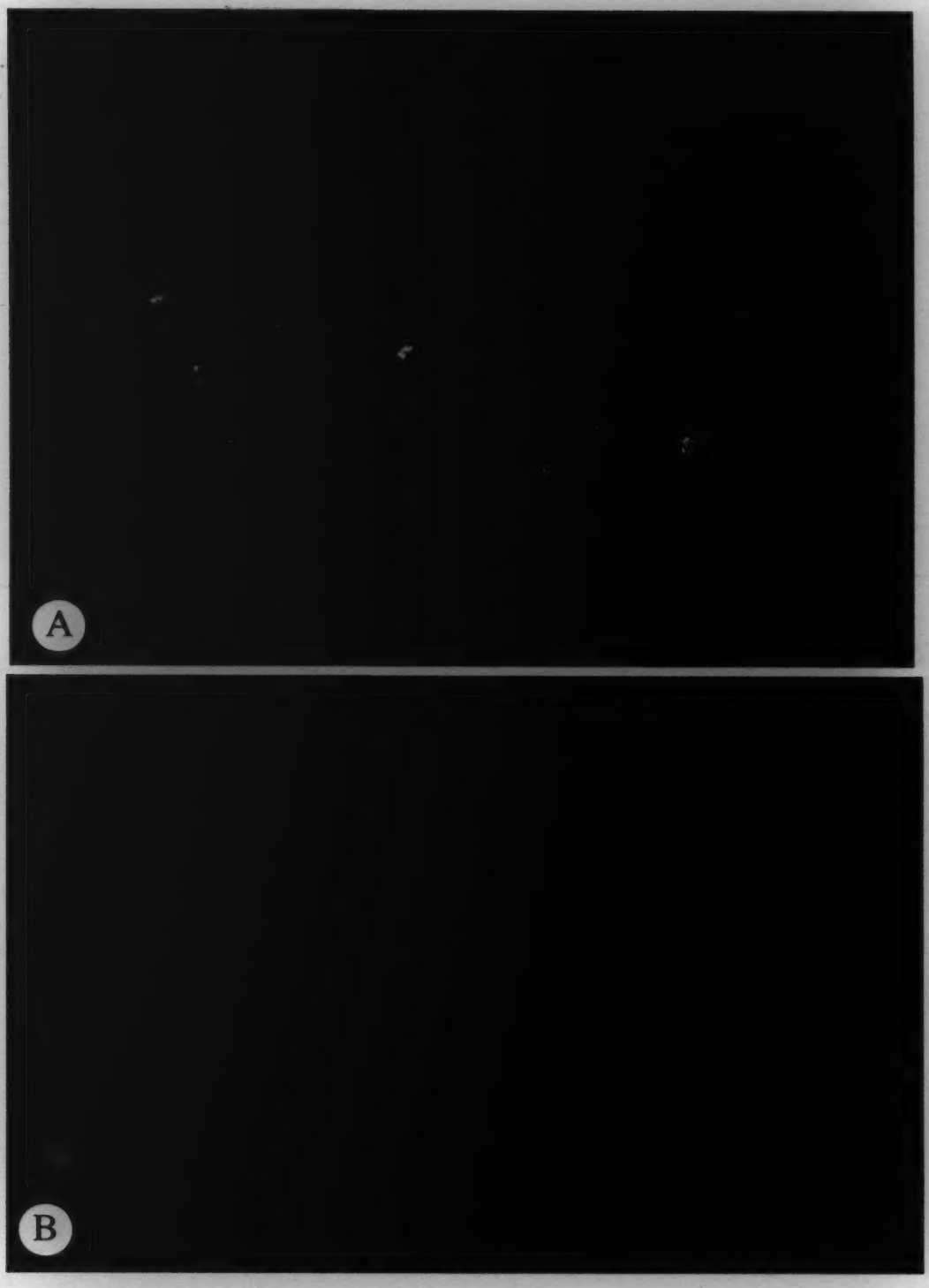

Figure 2-2. Facies A showing pebbly sand (A), and large coal fragment (B), designated by arrow.

Facies B- Ripple-laminated fine-grained sand

Description

Facies B (Table 2-1) is characterized by very fine-to fine-grained, well-sorted, rounded micaceous sand. Carbonaceous debris is very common and is observed as flasers that consist of a few sub-mm thick flakes of organic material. These flasers exhibit minimal lateral continuity (generally less than 2 cm). These laminations are restricted to low-relief areas between bedding surfaces, coincident with the troughs and the toesets of ripples.

The sedimentary structures observed within this facies are dominantly ripple-lamination, or small-scale trough cross-beds, and climbing current ripples (Figure 2-3a). Bed sets, as defined by McKee and Weir (1953), are typically less than 5 cm thick and average 2 to 3 cm in thickness. The current-rippled bed sets exhibit sharp bases and usually truncate bed sets of underlying current ripples. Bedding contacts are planar parallel to planar sub-parallel. Bed sets reach thicknesses in excess of 70 cm.

Bioturbation is very rare within this facies and manifests as mud-lined burrows comprising *Cylindrichnus (Cy)*, *Skolithos (Sk)*, and fugichnia (Fu) (Figure 2-3). These burrows make up a minute proportion of the sedimentary fabric of this facies (B.I. of I-II). Locally, several *Cylindrichnus* are observed extending downward from a singular bedding contact, but more commonly these burrows appear as discrete elements. The size of these burrows ranges from 1.5 cm to 5 cm in vertical length and approximately 0.3 to 1 cm in diameter. Although burrows themselves are mud-lined, no mud laminations are observed above the burrows along the bedding contact.

This facies is commonly overlain by Facies C or Facies D (i.e. IHS) and is locally observed overlying Facies A, E, and G (i.e. other sand-dominated units).

Interpretation

Facies B is interpreted to be deposited within estuarine and fluvial channels. Small-scale trough cross-beds and climbing ripples are indicative of sediment deposition under unidirectional flow conditions in the lower flow regime. Climbing ripples develop as a result of non-equilibrium, unidirectional migration of ripples during a state of net-deposition (Allen, 1970). Up-dip of the underlying dunes of Facies A, away from the thalweg, there is decline in mean flow velocity and stream power. This results in the deposition of finer-grained sand compared to what accumulates closer to the thalweg.

The presence of mud-lined burrows at discrete horizons within relatively thick bed sets of sand in Facies B indicates that brackish conditions sporadically persisted

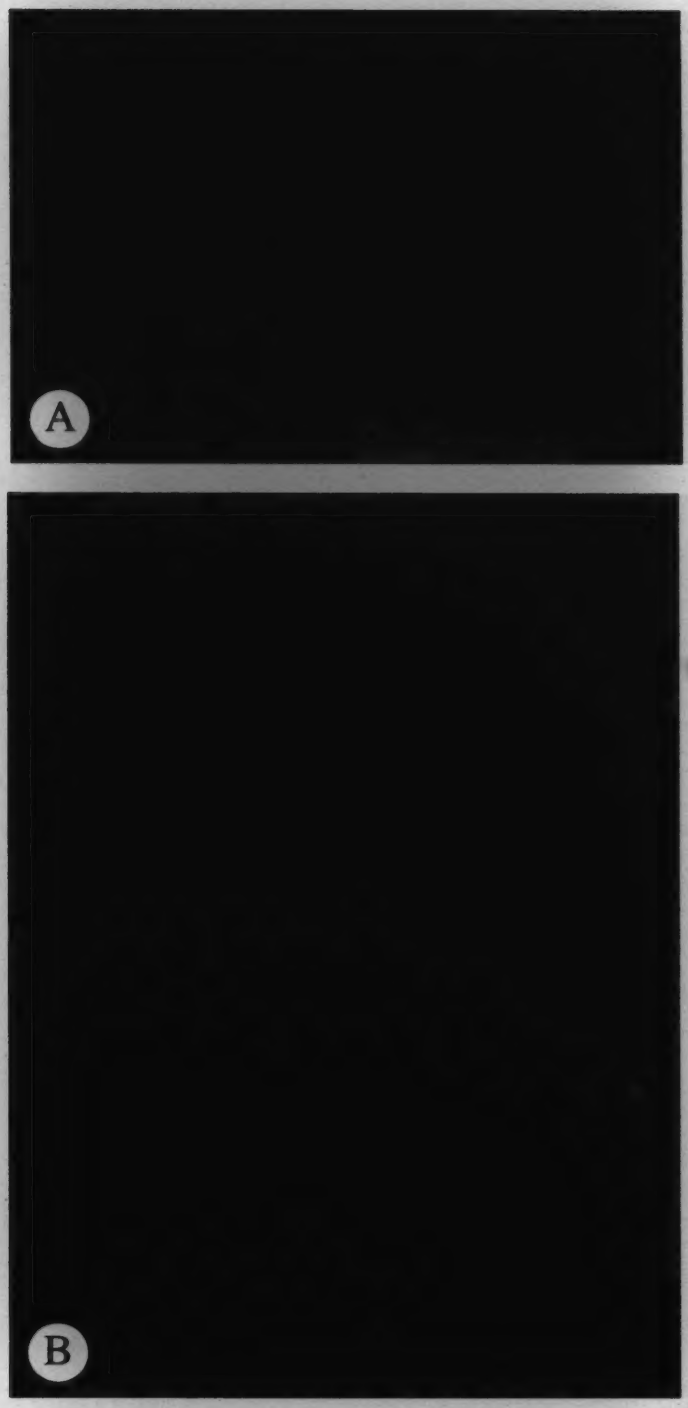

Figure 2-3. A. Facies B showing climbing ripples. Angle of climb is denoted by a dashed line. B. Facies B showing fugichnia (Fu) and *Cylindrichnus* (*Cy*), the most common ichnofossils found within Facies B.

long enough to allow colonization by the *Cylindrichnus* burrow-makers. The absence of mud laminations above these burrowed horizons can be interpreted in two ways: 1) mud was deposited and subsequently removed by an increase in hydraulic energy, or 2) colonization of the point bar surface occurred in an area that experienced mud by-pass. In both scenarios, mud must be present within the water column as part of the suspended load, but in the latter need not be deposited in order for the construction of *Cylindrichnus*. It is interpreted that these burrows were constructed in the absence of mud deposition because if mud were deposited and subsequently eroded, sand would also likely be eroded thus reducing the chance of burrow preservation. In any case, it is evident that these burrow-makers were capable of extracting mud from suspension to line the walls of their burrows.

Since mud, or at least thick deposits of mud, are thought to accumulate within the turbidity maximum, then deposition of this facies occurs on point bars in one of two areas within the estuary: a) in the middle estuary downstream of the turbidity maximum, or b) in the upper reaches of the inner estuary upstream of the turbidity maximum. Both locations, at some time throughout the season, offer a potential source of mud and provide adequate salinity conditions. Colonization downstream is statistically more likely however.

Colonization of point bars in the middle estuary entails the deposition of sand seaward of the turbidity maximum followed by a seasonal influx in fluvial hydraulic energy. This flooding event pushes the turbidity maximum downstream and delivers a higher concentration of mud than normal conditions offer. As conditions return to normal, the burrow-maker or its larvae can be directed upstream following the source of higher mud concentrations. Alternatively, high rates of sand deposition in these reaches of estuarine point bars may force organisms to abandon their burrows.

Colonization of point bars in the upper reaches of the inner estuary, upstream of the turbidity maximum, requires high spring tides during low fluvial influx. This delivers stratified salt water and mud within the water column to the upper reaches of the estuary that otherwise remain fresh and sandy. Burrowing is restricted to zones downstream of the salt-wedge intrusion. Only discrete horizons are burrowed and so periodic brackish conditions need only exist long enough to allow organisms to construct burrows. This minimum time frame is suggested to be one season (Gingras *et al.*, 2002). Upstream of the turbidity maximum may not offer sufficient time for construction of burrows by infaunal organisms. It is more likely that Facies B is deposited downstream of the turbidity maximum within the middle estuary. This is evidenced by the presence

of mud-clast breccia within Facies B where, locally, mud clasts comprise ripped-up *Cylindrichnus*.

Facies C- Thickly-bedded sand-dominated inclined heterolithic stratification

Description

Facies C (Table 2-1) consists of thickly interbedded couplets of fine-grained sand and mud or interlaminated silt and fine sand. Couplets range in thickness between 10 cm and 50 cm (Figure 2-4a). The dominant constituent of the couplet is the sand member; composed of fine-grained, micaceous sand; it comprises approximately 90% of the total thickness of the couple. These sand/mud couplets maintain a stratigraphic dip between 7° and 12° in outcrop. The mud member consists of homogeneous mud or finely interlaminated fine sand or silt and mud.

The bases of sand beds are sharp and locally erosive. Sedimentary structures are difficult to discern on freshly exposed outcrop surfaces, but, where surfaces are weathered, bedding structures are recognizable. Sand members host bed sets of climbing-ripples, ripple-lamination, and sigmoidal bedding. Locally, decimeter scale cross-stratified beds characterize the sand member (Figure 2-4b). Carbonaceous debris is locally observed draping the toesets of current ripples. The transition from sand to mud is abrupt but non-erosive. Planar, lenticular and wavy laminations are observed within the mud member, as well as rare double mud drapes. The laminations are discontinuous, generally extending for only a few meters laterally before pinching out.

In general, mud beds maintaining an appreciable lateral continuity (> 10 m) often amalgamate and bifurcate repetitively up-dip whereas sand beds tend to diminish in thickness up-dip. The net result is an interdigitation of sand and mud.

The ichnofossil assemblage comprises *Cylindrichnus*, *Skolithos*, *Gyrolithes*, and *Planolites*. A monospecific assemblage of *Cylindrichnus*, characterized by a series of mud-lined burrows that extend downward from the base of the mud member, is the most common biogenic fabric within this facies. Less commonly, *Skolithos, Gyrolithes,* and *Cylindrichnus* can be located within the lower portions of the sand member, having no obvious relationship with the overlying mud beds.

Interpretation

Facies C is interpreted to be deposited within laterally accreting point bars in a tidally-influenced fluvial environment in the upper estuary. This is evidenced by several

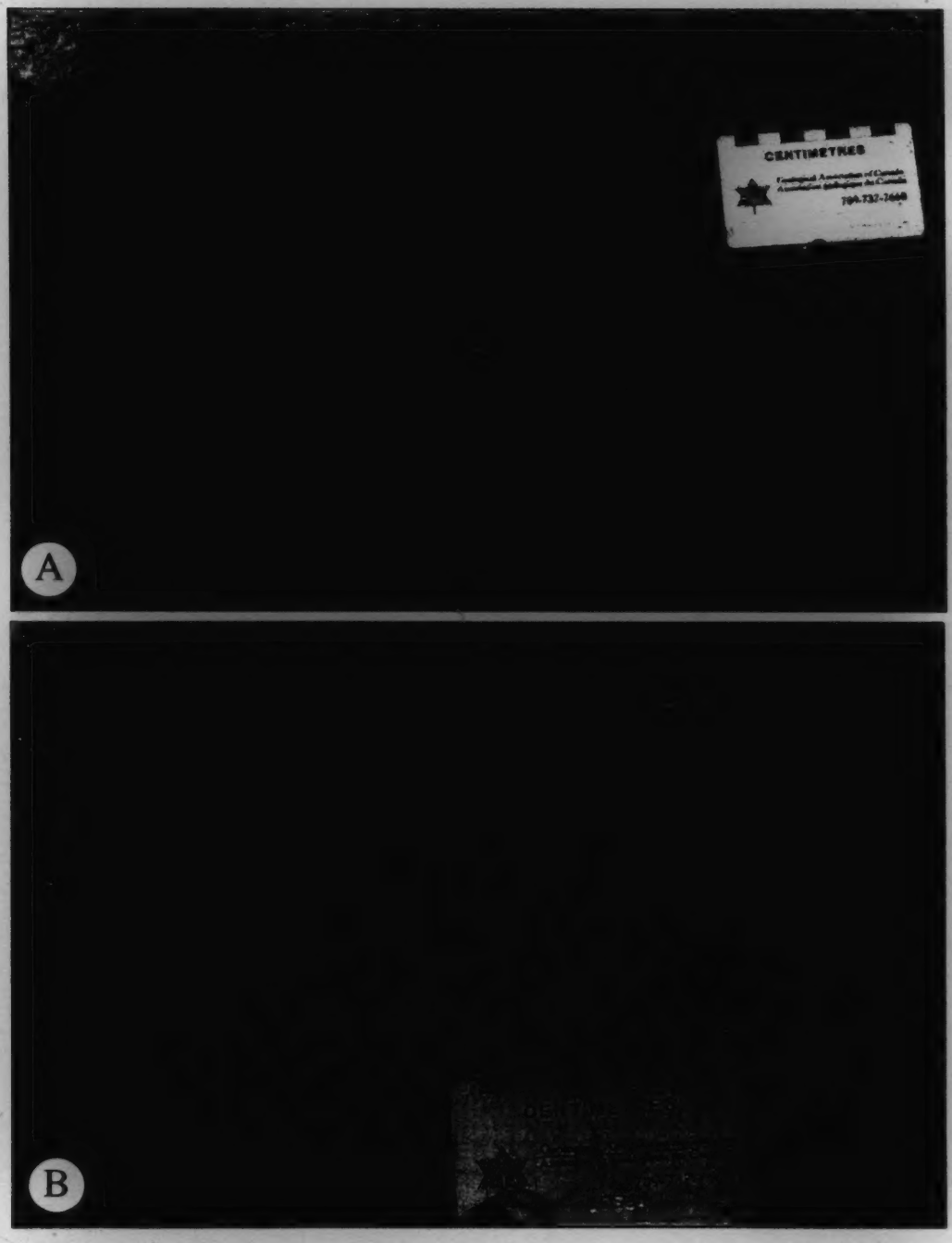

Figure 2-4. A. Facies C characterized by couplets ~15 cm thick. Abundant *Skolithos* (*Sk*) and *Cylindrichnus* (*Cy*) extend downward from the mud member. B. Facies C in which the sand member is characterized by a 10 cm thick cross-bedded unit with abundant *Skolithos* (*Sk*).

observations: 1) the preponderance of climbing and current-ripple bedding, 2) the cyclicity in deposits, 3) the presence of a brackish-water trace fossil assemblage, and 4) the accumulation of mud on the upper point bar surfaces.

The origin of the ripple-lamination and cross-bedding in Facies C is identical to those structures in Facies B. The fine-grained sands within the sand member are deposited under unidirectional flow conditions in the lower flow regime. Local occurances of thin, high-angle cross-stratified sand beds within this facies are interpreted to result from the migration of small subaqueous 2-and 3-dimensional dunes under more energetic hydrodynamic conditions. Storms entering the bay may cause fluctuating energy levels, but increased fluvial discharge energy may also be responsible.

It has been suggested that it is the cyclical nature of tidal deposits that permit them from being distinguished from fluvial or other IHS deposits (Thomas *et al.*, 1987). This is because there is a multitude of processes at work within the system including semidiurnal, diurnal, and seasonal shifts in tidal energy (i.e. neap and spring tides), seasonal fluctuations in the fluvial discharge, and storm activity. Sedimentary structures observed within this facies reflect shorter temporal, cyclical fluctuations in the hydrodynamics of the system. These include pinstriped laminations, interlaminated fine sand and silt or mud within the mud member of couplets, and the repetitive nature of the couplets.

The trace fossil assemblage within this facies is consistent with the brackish-water ichnological model presented by Pemberton *et al.* (1982). The trace fossil assemblage in this model is characterized by several criteria, including: 1) diminutive sizes of individual traces, 2) a low diversity of species, often consisting of monospecific assemblages, and 3) a high abundance of traces. These criteria are met within successions of IHS within this study of the McMurray Formation, an observation also noted by several previous authors (Pemberton *et al.*, 1982; Ranger and Pemberton, 1992; Bechtel *et al.*, 1994; Wightman and Pemberton, 1997). The combination of channel bedforms with brackish-water trace fossil assemblages, and indicators of bi-directional currents indicate deposition on point bars within a tidally influenced setting in the upper estuary.

The temporal significance of the IHS couplet remains poorly understood. Tidal fluctuations and changes in fluvial discharge have both been identified as potential processes responsible for sand deposition superimposed by mud deposition (Thomas *et al.*, 1987; Smith, 1987; Bechtel *et al.*, 1994; Rasanen *et al.*, 1995). Burrow fabrics within deposits of IHS in the Amazonia Basin reveal that a single tidal cycle is not a sufficient period of time to allow the colonization of these point bars surfaces. Based on larval

growth rates of infaunal animals colonizing the point-bar substrate, the minimum amount of time to facilitate the accumulation of one sand/mud couplet is approximately one season (Gingras *et al.*, 2002).

It is clear that two different mechanisms of sand delivery to the aggrading, laterally accreting point bar are possible. The mud member likely corresponds to higher fluvial inflow in tidal estuarine settings (Clifton and Gingras, 1999). In tidal delta settings, the sand is deposited during higher fluvial discharge. Smith (1988a) proposed that the mud member is deposited during fluvial flood periods and that sedimentation for the duration of the season is dominated by tidal fluctuations delivering mud and fine sand or silt to the point bar surface. Burrows emanating from the sand member suggest that there was some marine influence present during deposition (Gingras *et al.*, 2002). The deposition of the mud member is facilitated by basinward displacement of the turbidity maximum during a high fluvial discharge event. This is evidenced locally in sand beds that host discrete horizons of *Cylindrichnus*. When flood conditions wane, the turbidity maximum moves back upstream and sand deposition on the point bar can recommence thus allowing opportunistic organisms to colonize the newly deposited muddy substrate.

Facies D- Medium-bedded sand-dominated inclined heterolithic stratification

Description

This facies consists of thinly interbedded fine-grained sand and mud, or interlaminated silt and fine sand and mud (Table 2-1). Couplet thicknesses range from 2 to 10 cm and display a wider range of sand/mud proportions within the couplet than Facies C. In general however, mud comprises between 10% and 50% of the total couplet (Figure 2-5).

Sand beds are similar to those described in Facies C but thinner current-to climbing-current ripple bedding is observed within the sand member. More commonly the sand member is massive appearing. Planar laminations are common within the mud member. Rare starved ripple laminations, double mud-drapes, and wavy to lenticular laminations are preserved. Locally, carbonaceous debris is observed draping the toesets of ripples. Mud beds commonly amalgamate and bifurcate up-dip, where individual beds can be traced laterally anywhere from 10's of meters to only a few meters.

The trace fossil assemblage has a similar diversity to that in Facies B and C but there are more occurances of *Skolithos* and *Gyrolithes*. Monospecific assemblages of *Cylindrichnus* are most common within the sand member, and assemblages of

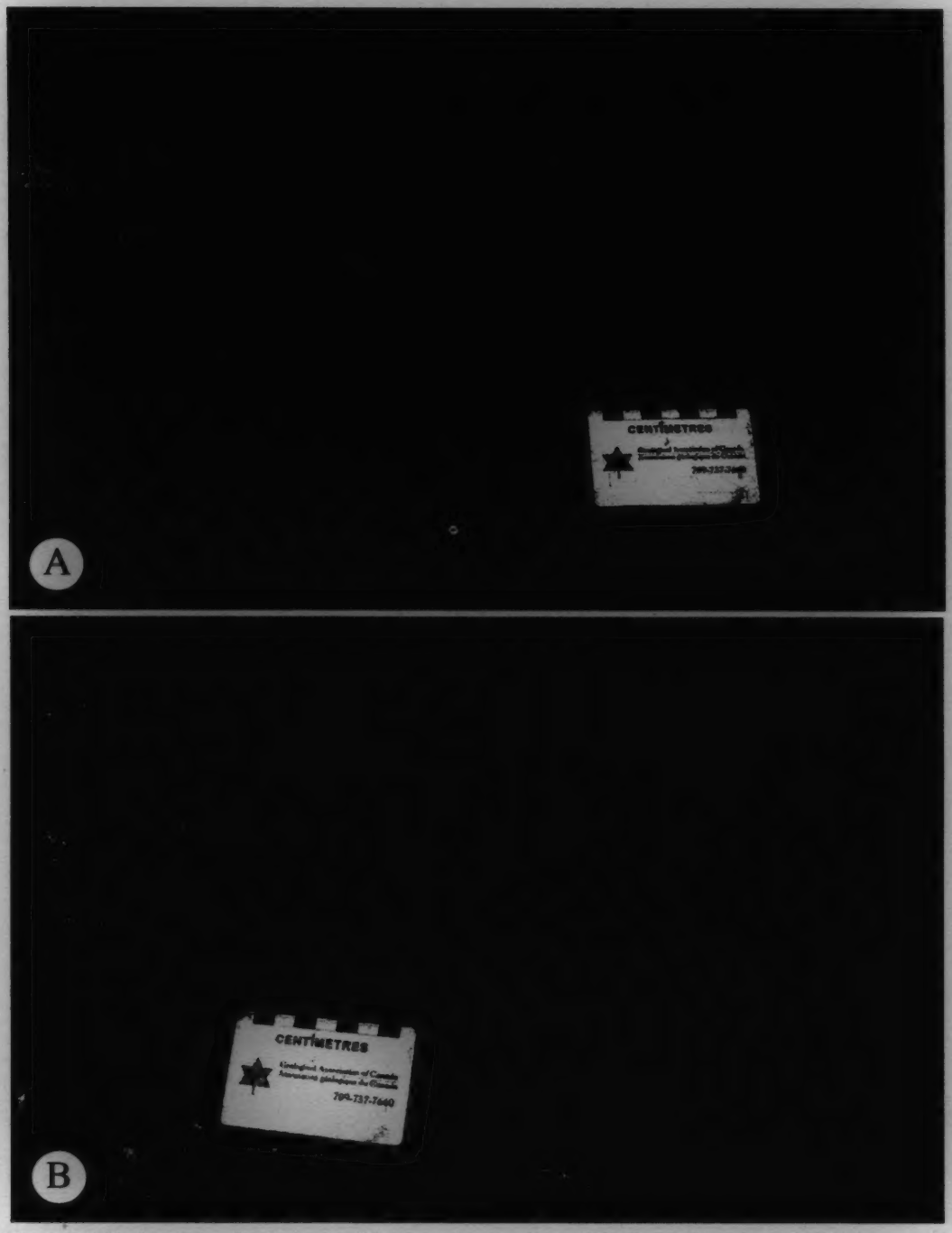

Figure 2-5. Facies D showing the variability in mud proportion within the sand/mud couplet. A. Average 10 cm couplet with ~10% mud. B. Average 10 cm couplets with ~50% mud. Note the presence of *Cylindrichnus* (*Cy*) and *Skolithos* (*Sk*).

Cylindrichnus and rare *Gyrolithes* are observed within the mud member. The bioturbation index ranges from II to IV.

Interpretation

Facies D is interpreted to accumulate in a similar environment as Facies C, on tidally influenced point bars within the upper estuary. This facies shows a higher degree of cyclicity than Facies B and C. This is manifest as thinner couplets and thicker mud members that are composed of numerable interlaminations of silt and mud. This increased cyclic nature is likely the result of slower sedimentation rates on portions of the point bar located up-dip of the channel thalweg. This cyclicity may also be related to an increase in the amount of fines that are input from the river.

The interpretation of the IHS couplet is subject to controversy as it is possible to have sand/mud or mud/sand being deposited depending on the 'ambient' depositional conditions. As sand is brought upstream via tidal currents or downstream via increased fluvial discharge, accumulation is thickest near the base of the point bar and thinnest near the top. This wedge shaped distribution of sand within the point bars of these successions is common. Where sand beds begin to thin and are not driven up near the tops of the point bar surfaces, aggradation of the point bar is mostly attributable to the accumulation of mud laminations. These accumulate after each seasonal shift as energy conditions return to normal.

The upper surfaces on point bars are in close proximity to the adjacent tidal flats and so the increased degree of burrowing and biodiversity within this facies reflects a decrease in overall energy on these surfaces. Only during periods where high fluvial discharge combines with spring tides and a backwater surge are bank-full stages reached within the channel (Thomas *et al.*, 1987). It follows then that infaunal organisms colonizing elevated portions of the point bar are subjected to fewer fluctuations in salinity thus facilitating the growth of denser trace fossil colonies.

Facies E- Mud-dominated inclined heterolithic stratification

Description

Facies E (Table 2-1) is characterized by gently dipping, interbedded, finely interlaminated mud and fine sand or silt, or homogenous mud. Mud proportions within each couplet exceed 50% (Figure 2-6). Typically the sedimentary structures are completely obliterated by biogenic reworking, but some vestigial planar laminations and double mud drapes within the mud member are locally preserved. Rare occurrences

of starved sand ripples are observed within the mud component. The tops of mud beds commonly exhibit a polygonal fracture pattern wherein individual polygons ranging in size from 1 to 3 cm across (Figure 2-7). The apertures of these fractures are generally sub-mm in width. The sandy constituent is generally massive appearing but rare current ripple-laminations are observed.

The bioturbation index is higher than observed in Facies C and D, ranging between III and V. Monospecific assemblages of *Gyrolithes* and *Cylindrichnus* are observed, and mixed *Gyrolithes* and *Cylindrichnus* are also observed. *Skolithos* and *Planolites* are more rarely observed (Figure 2-6). Trace fossils are diminutive compared to the sandier IHS deposits and overall, monospecific assemblages are dominant. However, biogenic reworking within many horizons is so intense that individual traces can be difficult to recognize and only a mottled fabric remains.

Interpretation

Facies E is interpreted to be deposited in shallow subtidal and intertidal zones. The lateral transition from upper point bar surfaces to the intertidal mudflat is gradational. These areas are coincident with decreased sedimentation rates and an overall reduction in energy conditions. The persistent stratigraphic occurrence of Facies E with underlying Facies D or C implies a close palaeoenvironmental relationship between all of these facies. It is suggested that this facies accumulated due to lateral accretion of the tidally-influenced point bar. Here, fluctuations in energy incurred by the upper surfaces of the point bar and intertidal areas are tidally derived. This is consistent with the presence of double-mud drapes, fine mud laminations and fine sand or silty sand laminae, resulting from small, repetitive fluctuations in energy conditions.

Although some mud within this facies may accumulate as a result of fines settling from suspension following fluvial discharge events, the bulk of the mud in this facies is interpreted to accumulate as a result of active sedimentation within the zone of the turbidity maximum by flocculation (Bechtel *et al.*, 1994). The sedimentary fabric and high-density burrow communities are similar to tidally-influenced point bar deposits at Willapa Bay, Washington in the upper estuary. Sandy point-bar deposits characterize the lower reaches of the estuary, and muddier point-bar deposits dominate the upper reaches (Gingras *et al.*, 1999). The majority of mud deposition occurs at slack water as the salt-wedge and turbid zone, situated between basinward flowing fresh water and landward moving marine water, reach their landward limit and are momentarily stationary.

The increase in the degree of biotubarion (B.I. IV or V) in this facies is interpreted to result from a decrease in overall energy and associated decrease in sedimentation

Figure 2-6. Facies E. A. Photo showing high mud fraction, interlaminated fabric, and high degree of bioturbation (B.I. of IV to V) characteristic of Facies E. B. Close up of A showing trace fossils present as well as undifferentiated bioturbation.

Figure 2-7. Photo showing mud fractures commonly found within Facies E. Fractures are commonly 1 to 3 cm in diameter.

rate. This signals the transition from deposition within the shallow subtidal to deposition within intertidal areas. Monospecific assemblages and diminutive sizes of burrows in this facies are still consistent with the brackish water model presented by Pemberton *et al.* (1982) and imply that the water reaching these upper surfaces is still brackish.

Mud fractures are interpreted to result from sub-aerial exposure of these upper point bar surfaces. This may occur during the course of a diurnal cycle between high tides. More likely, however, these fractures develop prior to spring tidal fluctuations when diurnal tidal ranges diminish, leaving the highest portions of the point bar sub-aerially exposed for the duration of the month.

Facies F- Mud intraclast breccia

Desciption

Facies F is characterized by fine-to medium-grained sand with common mud intraclasts (Table 2-1). The proportion of mud clasts is highly variable, comprising only a few percent in some instances and upwards of 70 % in other areas. Individual units may exhibit this variation within a short lateral distance (Figure 2-8). Clasts range in size from 0.3 cm to 2 cm in diameter and are typically subrounded or rounded. Where bedding is discernable, it is defined in part by the orientation of mud clasts, and by gently dipping low-angle cross-laminations (Figure 2-9a). Locally however, this facies appears as a massive brecciated unit. Facies G sharply overlies underlying ripple-bedded but generally grades upwards into overlying ripple-bedded sand.

Locally, the mud clasts consist of ripped up *Cylindrichnus* (Figure 2-9b). This is particularly evident where cross-sectional views of individual clasts reveal a mud-lined perimeter encompassing a fine-grained sand tube. Generally however, the mud clasts are homogenous grains with no discernable internal characteristics.

Interpretation

Facies F can be deposited in several ways (Stewart and MacCallum, 1978; Thomas *et al.*, 1987; Bechtel, 1996; Ranger and Gingras, 2005; Lettley, 2004): 1) as a result from downslope slippage of a point bars' inclined units; 2) as a result of the cutbank erosion of a migrating channel; and 3) from the reworking of previously deposited mud beds. In the first two scenarios the debris enters the thalweg of the channel. This debris is either preserved in place or is redistributed downstream in the traction load. The third interpretation is that this facies represents the remnants of a strong fluvial event that rips up mud beds that were deposited on the point bar. This debris is

Figure 2-8. Mud-clast breccia in outcrop. This example of Facies F shows short lateral extent as the proportion of mud clasts changes from >90% as seen on the left to < 10% on the right. Bedding is largely obscured on the left but is characterized by thin laminations of mud clasts, often 1 mud clast in thickness, on the right. The orientation of the this exposure is approximately perpendicular to the channel axis. Photographs from Type Section outcrop within Strip Log C at 21.6 m (Appendix 1).

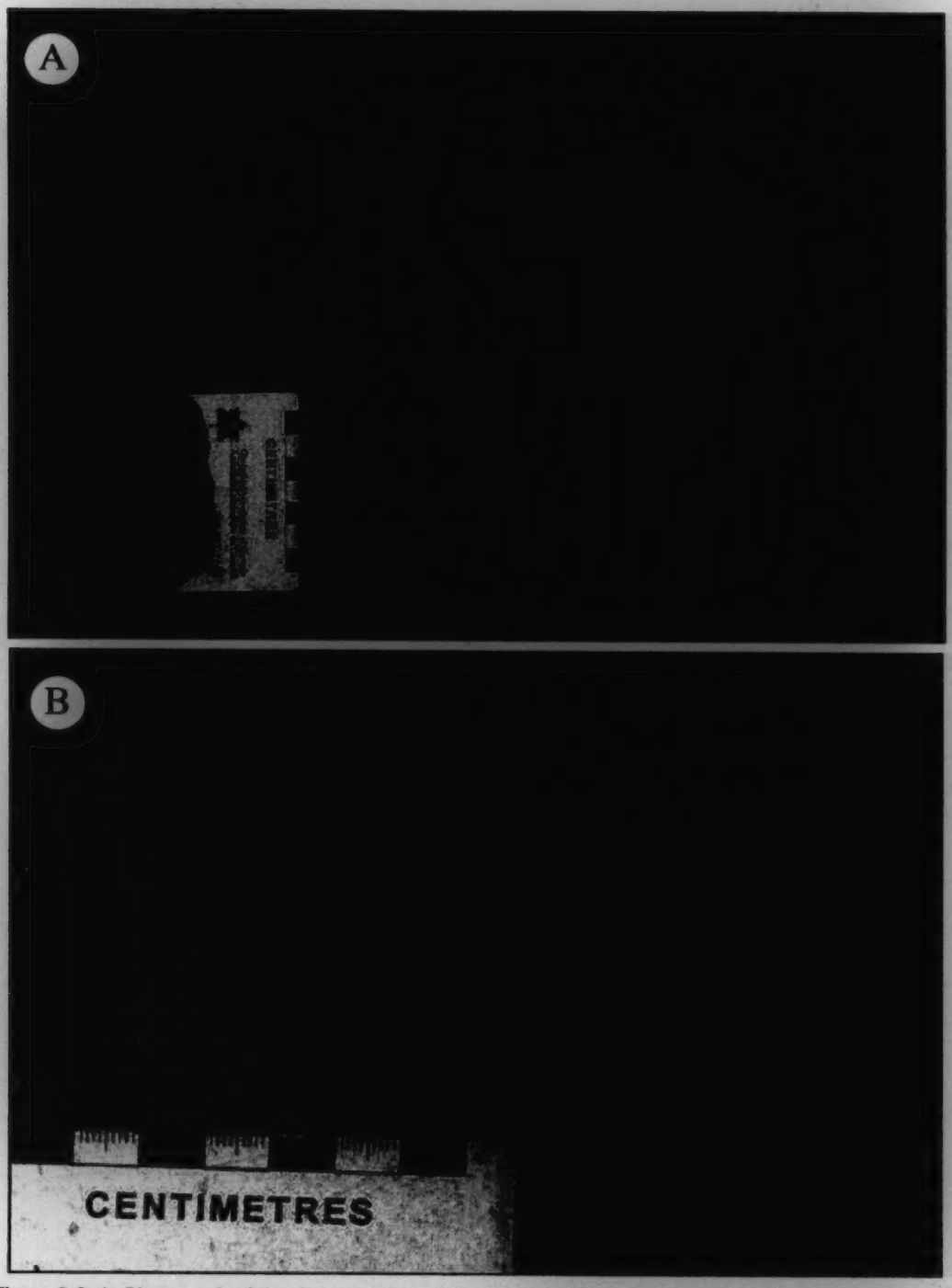

Figure 2-9. A. Photograph of the sharp transition from laminated fine sand to mud-clast breccia (Facies F). Arrows indicate low-angle cross laminations defined by orientated mud clasts. B. Locally, mud clasts consist of ripped up *Cylindrichnus* (arrows). These clasts show mud-lined perimeter and a central tube filled with sand.

then redistributed downstream as comparatively small, rounded-to sub-rounded clasts. Facies F is characterized by low percentages of mud clasts, clasts that are orientated along bedding planes, and rounded and disaggregated clasts. These characteristics do not preclude any of the above interpretations but do suggest, however, that if the clasts resulted from cutbank collapse and subsequent downstream transport, the transport distance would have been comparatively large (100's of meters). In this study, no angular clasts are observed and the clast sizes rarely exceed 2 cm, supporting this interpretation. High mud clast percentages, and sub-angular clasts support comparatively shorter transport distance, such as the occurrance of Facies F in Figure 2-8 (10's meters). Locally, mud-clast breccia is characterized by ripped up *Cylindrichnus* (Figure 2-9b) and supports the third interpretation where the colonized surface of the point bar was subjected to comparatively intense hydraulic energy conditions. Conditions most favorable for this occur when the velocity of high fluvial discharge events is increased by spring ebb tides.

FACIES ASSOCIATION 2

Facies Association 2 consists of transgressive lag deposits overlain by 2- and 3-dimensional outer estuarine subaqueous dunes where a normal succession includes thin coarse-grained sands that grade abruptly upwards into several meters of sub-meter to meter scale tabular and trough cross-bedded sand dunes. The outer estuarine deposits of Facies Association 2 are characterized by sedimentary structures indicative of flow-reversal, grain striping consistent with waning, diurnal tidal fluctuations, neap-spring sedimentary bundles, and an ichnological assemblage indicative of brackish and marine water.

Facies G- Large-scale cross-bedded sand

Description

Facies G is characterized by large-scale tabular and trough cross-bedded fine-to medium-grained sand (Table 2-1, Figure 2-10). Average thickness of the cross-bedded units is between 30 and 110 cm. Dune foresets dip dominantly towards the north at the Amphitheatre and Type Section outcrops. The bounding surfaces of the units are sharp and sub-planar and the foreset laminae maintain tangential contacts with these surfaces. A common attribute of the toesets is down-dip convergence of individual laminae onto the lower contact. Back-flow ripples are common along the toesets. Bedding and lamination is invariably defined by grain striping. Each bed set is composed of a series of fining

upward beds. Coarse-to medium-grained sand and, locally, pebble-size grains occur at the base of each bed. These grade upward into fine-grained sand (Figure 2-10c). Coarse-to fine-beds repetitively thicken upwards and then thin again within a bed set (Figure 2-11c). Less commonly these bed sets are composed of beds that have uniform grain sizes and grains of different lithologies that define the grain striping. Interbeds of mud are commonly found on top of the fine-grained sand.

Laminations of carbonaceous debris are usually constrained to the lower portions of the toesets of the cross-strata. These laminations are usually less than a millimeter thick. Imbricated mud clasts are also observed on the tops of beds (Figure 2-10a). These are confined to the lower portion of the toeset and occur as discrete horizons one mud-clast in thickness. Clasts average 0.5 cm in diameter. Convolute bedding is observed locally and displays upward deflection of laminae (Figure 2-2).

Biogenic structures within this facies are rare. Less than 5% Facies G possesses bioturbation. The tops of some cross-stratified beds are well burrowed with robust *Cylindricnus* (Figure 2-11c). Where present, these burrows are usually truncated by overlying sets of high-angle cross-beds. Fugichnia, or escape traces, are locally observed (Figure 2-11c). *Conichnus*, although very rare, are also observed within this facies.

Interpretation

Facies G is interpreted to be deposited within the outer estuary as 2-and 3-dimensional subtidal dunes (Ranger and Gingras, 2005). Dunes, similar in scale to those observed in the McMurray Formation, are also observed in Pleistocene outcrops in Willapa Bay, and are interpreted to be characteristic of subtidal, tidal channel deposits (Clifton, 1983). The morphology of the NE/SE dipping cross-beds indicates deposition stemming from a dominantly unidirectional current. The differential dip direction of this facies between these dunes is interpreted to be the result of ebb-or flood-orientated dunes. Side-scan sonar records of this phenomenom are observed in Willapa Bay and show bedforms orientated in both directions (Anima *et al.*, 1989).

Reactivation surfaces within this facies indicate changes in depositional current directions. The bedform dips in the direction of the dominant current, where the subordinate current modifies the upper surfaces of each foreset. The net result is a bedform with internal erosional sufaces that have a higher dip than the dune foresets (Ranger and Gingras, 2005). These are also observed in subtidal channel deposits in the Netherlands (de Mowbray and Visser, 1984). The repetitive nature of the graded beds within each bed set also suggests rhythmic variations in energy conditions. Internally, each laminae can be construed to result from a single pulse of energy in

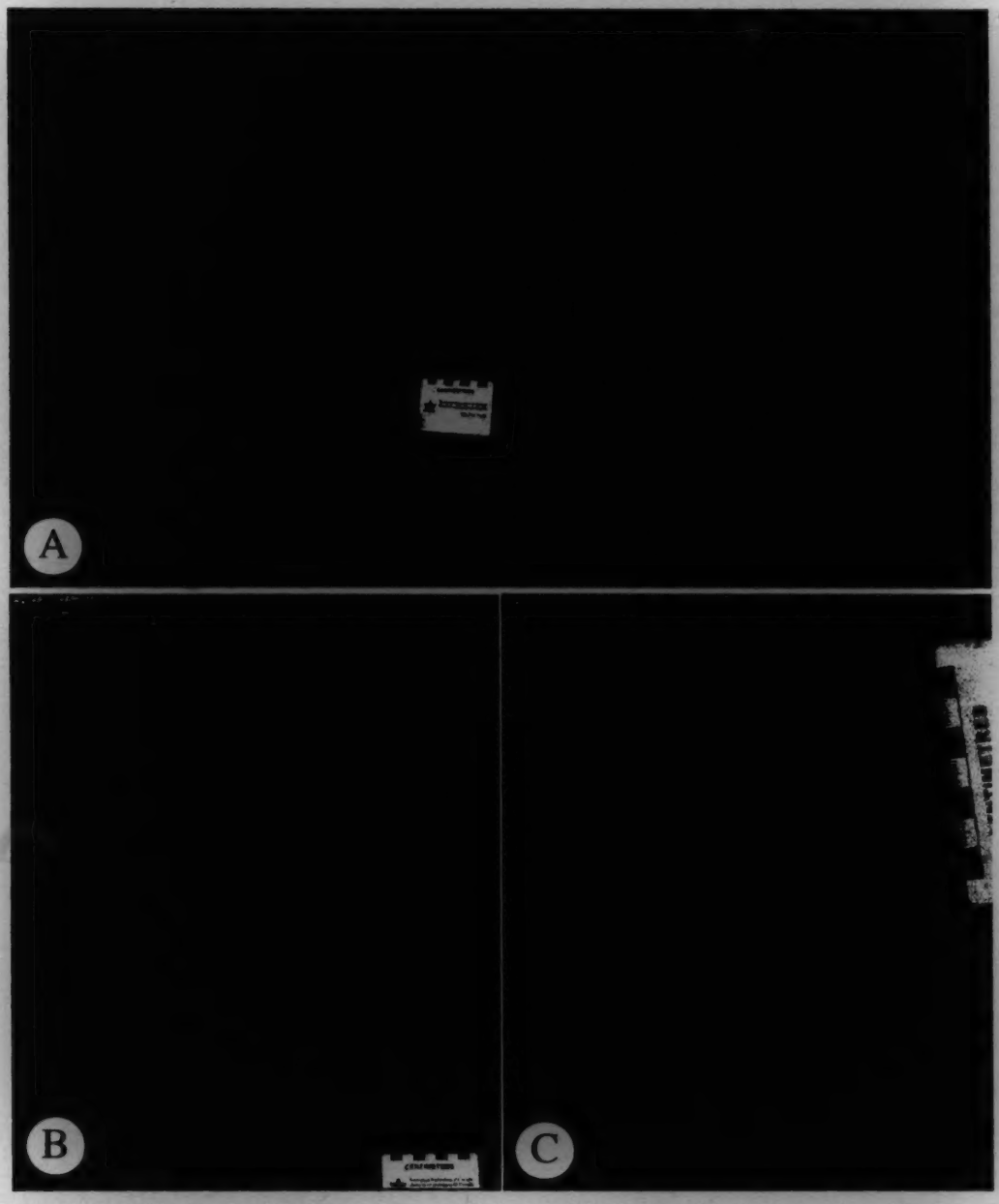

Figure 2-10. A. Photograph showing the average thickness of the large-scale tabular cross-stratification of Facies G. Also note the mud clasts (denoted by arrows) that average 0.5 cm in diamter. B. Trough-cross bedding of Facies G. C. Grain striping commonly observed in Facies G. Note the coarse sand that grades upwards into fine sand within each bed. Beds average 1 to 2 cm in thickness (sqaure bracket denoting single fining-upward unit).

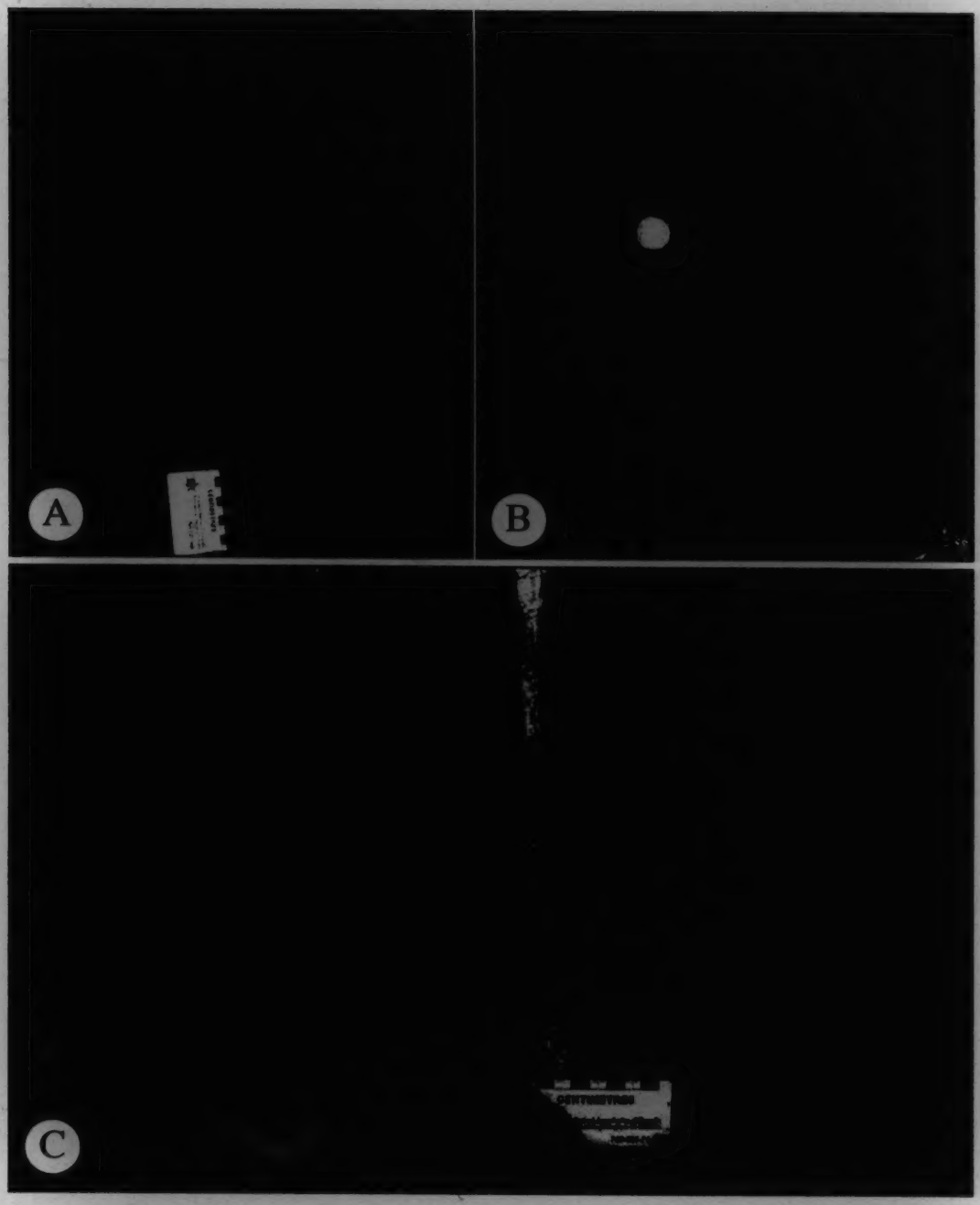

Figure 2-11. A. and B. Water escape structures within Facies G denoted by arrows show deflection of laminae upwards. C. Truncated cross-stratified bed set of Facies G with burrowed top. Escape traces (*Fu*) that sit stratigraphically below the *Cylindrichnus* horizon. Also note the square bracket bounding an interval in which grain-striped beds thin upwards.

which coarse- and medium-grained sediments settle out first, followed by the deposition of finer material; this is consistent with the energy fluctuations occurring throughout a single tidal cycle. Furthermore, crude patterns in bed thickness within bedsets emerge from these bedforms and can loosely be correlated to neap and spring bundles. The presence of marine trace fossils such as *Conichnus* and escape traces supports a subtidal interpretation and increased salinity levels.

Mud laminations draping the beds suggest that flow conditions periodically abated, allowing the settling of mud particles from suspension. Slack water between high and low tides offers one such means to facilitate the deposition of these muds. Alternatively, dune complexes may be experiencing periods of inactivity. The duration of time over which the muds accumulated is speculative at best. The carbonaceous debris intercalated with fine-grained sand maintains a platy nature and has the tendency to behave, hydraulically, more like sand grains within the water column.

Convolute bedding is interpreted to result largely from dewatering. As sediments begin to accumulate rapidly on top of sediment in which the pore space is saturated with water, the water must rise to maintain hydraulic equilibrium with the surface. Water than moves vertically through the sediment and deflects overlying lamination. Convolute bedding can also originate from high sedimentation rates. As sediment is carried up the stoss slope and begins to accumulate on the lee side, the steepness of the dune increases. The dune front becomes susceptible to slope failure, and coincident disturbances in bedding, as the angle of repose increases.

In short, Facies G is deposited as subtidal dunes within the outer estuary. These dunes are subjected to daily and monthly fluctuations in energy and current reversals, as well as periods of quiescence. These conditions favor the development of grain-striped bedding, thick bed sets, and laminated muds, respectively. Convolute bedding is associated with periods of higher sedimentation rates.

Facies H- Coarse-grained sand

Description

Facies H (Table 2-1) is a medium-to well-sorted, coarse-to medium-grained unit with normal graded bedding and low-angle cross-stratification and is very similar to Facies A. The beds in Facies A are thicker than in Facies H, where beds are approximately 3 to 5 cm thick and master bedding planes dip at angles between 5° and 15° (Figure 2-12). Rare coal fragments are observed at the base and also helps to differentiate this facies from Facies A. Otherwise, it is the association with overlying

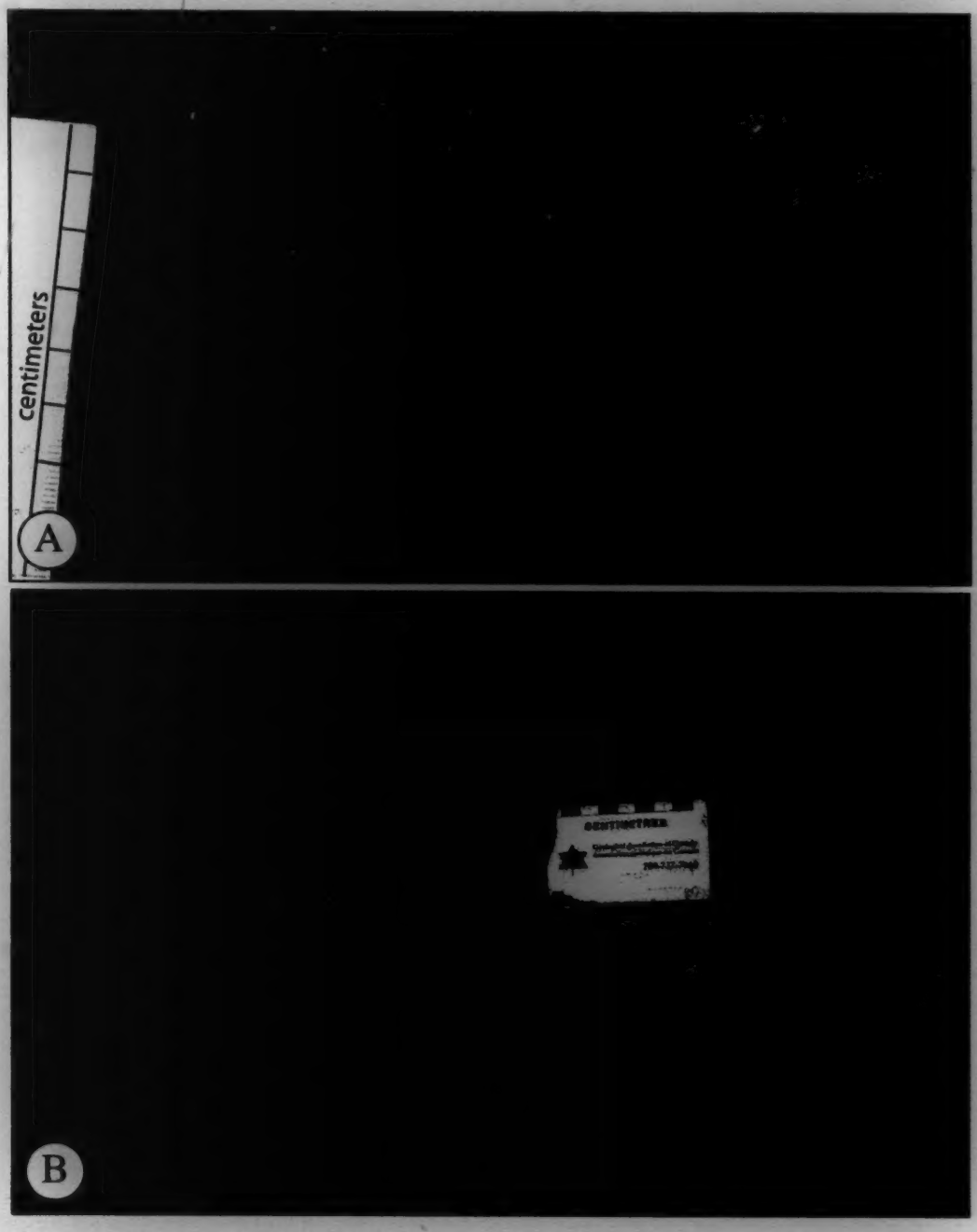

Figure 2-12. A. Low-angle, cross-bedded granular sand of Facies H. Sample from 34.6 m of Strip Log C (Appendix 1) at the Type Section outcrop. B. Contact of Facies H and underlying Facies E. Photo from same stratigraphic interval as A.

and underlying facies that warrant differentiation of Facies H from Facies A. This facies is observed cross-cutting underlying IHS units near the top of the Type Section outcrop (Figure 2-12b) and is overlain by Facies F, an association not observed at the Amphitheatre outcrop.

Interpretation

Although this facies has identical sedimentologic characteristics as Facies A, the interpretation is different. This facies erodes into underlying Facies D, E or C and grades upward into Facies G, which is interpreted to accumulate as subaqueous dunes in the outer estuary. Since the outer estuarine deposits of FA2 lie on inner and estuarine deposits of FA1, the basal lag represents a transgressive surface of erosion and, hence, is interpreted as a transgressive lag deposit. The depositional significance of this and other facies are discussed at length below.

FACIES ASSOCIATION AND FACIES SUCCESSION

The outcrops within the study area, although relatively small in scale, host highly variable sediment types that have been divided into facies. These facies have been grouped into facies associations to reduce the strata into manageable units used for stratigraphic interpretation. The section will interpret the facies associations as genetically related units, or as a series of genetic units deposited within a similar environment. References will be made to the lithostratigraphic implications of these facies associations with respect to the accepted nomenclature of the lower, middle, and upper McMurray Formation members used in previous studies.

Facies associations are recurring vertical successions of genetically related facies. These associations provide a stratigraphic framework within which individual facies interpetaions are given context. A facies association may have variable elements of individual facies within, due to local variability and heterogeneities that exist within the depositional environments, but provide a reliable means of applying Walther's Law.

Facies Association 1

Description

Facies Association 1 represents an imbricate coset of overall, fining-upward sets of IHS (Thomas *et al.*, 1987). Several vertical and lateral fining-upward grain size trends are recognized. These include: 1) coarse-to-fine couplets of IHS, a feature discussed at

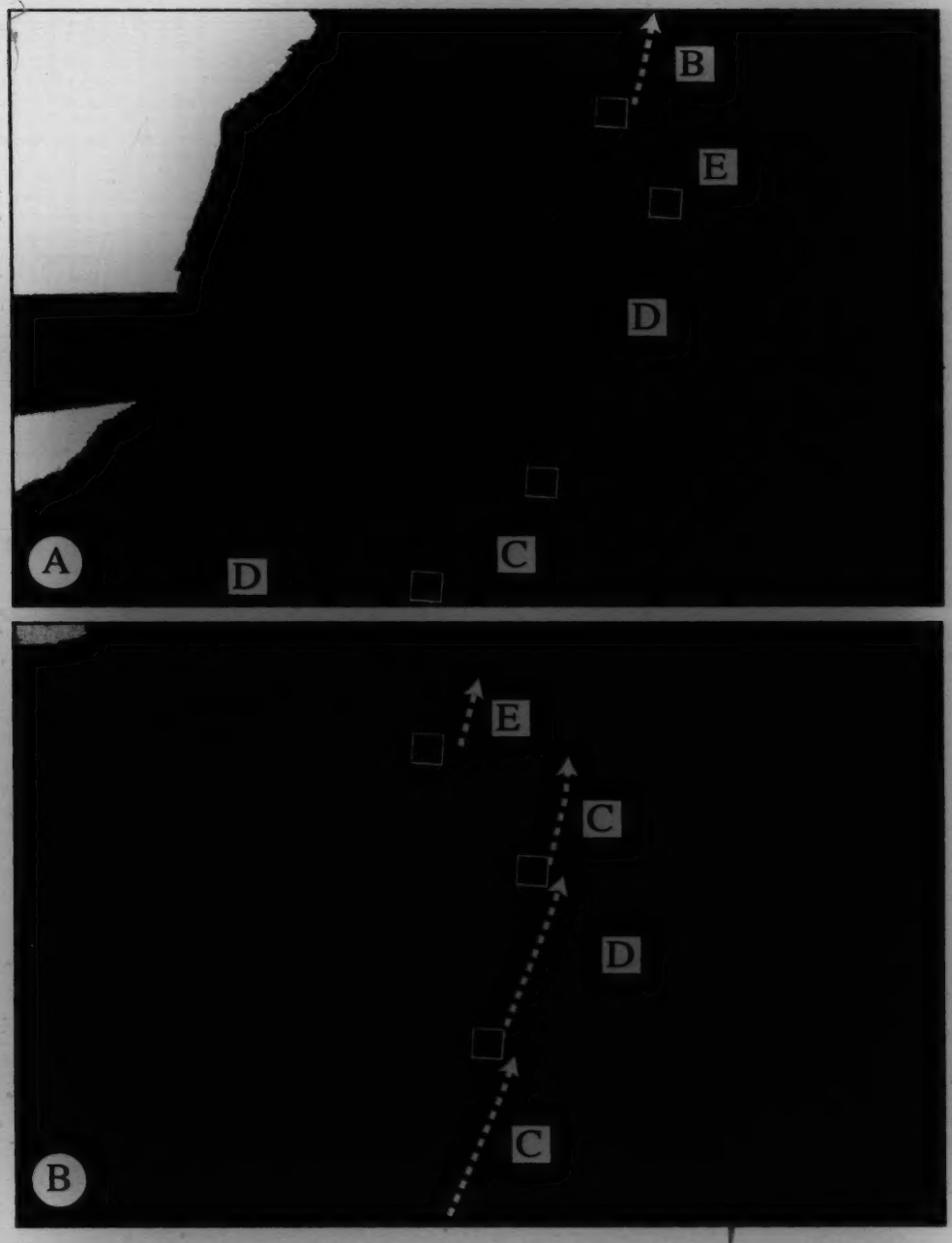

Figure 2-13. A. and B. Common facies relationships within Facies Association 1. Letters indicate facies and numbers indicate a heierarchy of most common (1) to least common (3) facies transitions. Most commonly, sandier IHS facies (Facies B and C) are overlain by progressively muddier IHS facies (Facies D or E) in a fining-upward succession (1). Also common is the periodic emplacement of sandier IHS intervals over mudder intervals (2). These transitions occur within a single genetic IHS unit. At the outcrop scale, the least common vertical relationship is that from muddy IHS (Facies E) to sand (Facies B) and sandy IHS (Facies C). These relationships usually demarcate the stratigraphic boundaries between genetically related IHS units in an IHS succession (3).

length within the description and interpretation sections select facies units; 2) upward-fining trends within each set of IHS; and 3) an upward-fining trend within the entire coset, across discontinuity surfaces.

Within the study area the most common vertical trend of facies observed is a fining upwards transition from the ripple-laminted sands of Facies B to the sand-dominated IHS of Facies C to the mud-dominated IHS of Facies D and E (Figure 2-13a). This trend is observed within each set of IHS. The transition from the sandy IHS of Facies C to the muddiest IHS of Facies E, and from sand (Facies B) to muddy IHS (Facies D) is also commonly observed. These fining upward trends result from a combination of more numerous and thicker mud beds, and thinner sand beds. Less frequently sandy IHS overlies the slightly muddier IHS Facies (D or E) (Figure 2-13b). Such transitions mark small-scale disconformities within sets of IHS.

Within the Athabasca outcrop section, the interval between 9 m and 15 m in Strip Log A (Appendix 1) preserves a repetitive thinning-upward trend in the thickness of sand beds, constituting several changes from the sandy IHS of Facies C to the muddy IHS of Facies D, followed by a single transition from the muddy IHS of Facies D to the muddiest IHS intervals of Facies E. Preserved at the base of two of these series (4 in total averaging between 1.0 m and 1.5 m) are sand beds with distinct ripple-laminations. In all other sand beds within this 6 m interval, ripple-laminations are not observed or have been subsequently destroyed by biogenic reworking. This trend is also observed in Strip Log C within the following intervals: 29.0 to 33.1 m, 24.3 m to 29.0 m, and 21.0 m to 24.3 m.

This facies association also shows an up-dip grain-size trend expressed as sand and sandy IHS (Facies B and C) that grades up-dip into muddy IHS (Facies D and E) (Figure 2-14). Down-dip, the muddiest IHS (Facies E) gradationally changes to the slightly less muddy IHS of Facies D and then to the sandy IHS of Facies C. Mud beds commonly bifurcate and merge, only to bifurcate again up- dip. This trend results is a preponderance of mud beds and muddy laminations up-dip (see Strip Log C). Sand beds, in general, thin up-dip and interdigitate with mud beds.

Between Strip Log A and C (Appendix 1), the surfaces demarcated by abrupt, vertical transitions from muddy IHS facies to sandy facies do not exhibit drastic changes in dip angle laterally. These surfaces are observed at 15.0 m and 22.3 m in Strip Log A, and 15.1 m and 24.3 m in Strip Log C. In other words, only minor truncations of underlying strata are apparent in 2-dimensions (Figure 2-14). Small gullies incised into the Type Section provide a few opportunities to view the third dimension of the Type Section outcrop. From these observation points, the section is observed to comprise amalgamated units averaging 6-9 m in thickness (Figure 2-15) bounded by surfaces of

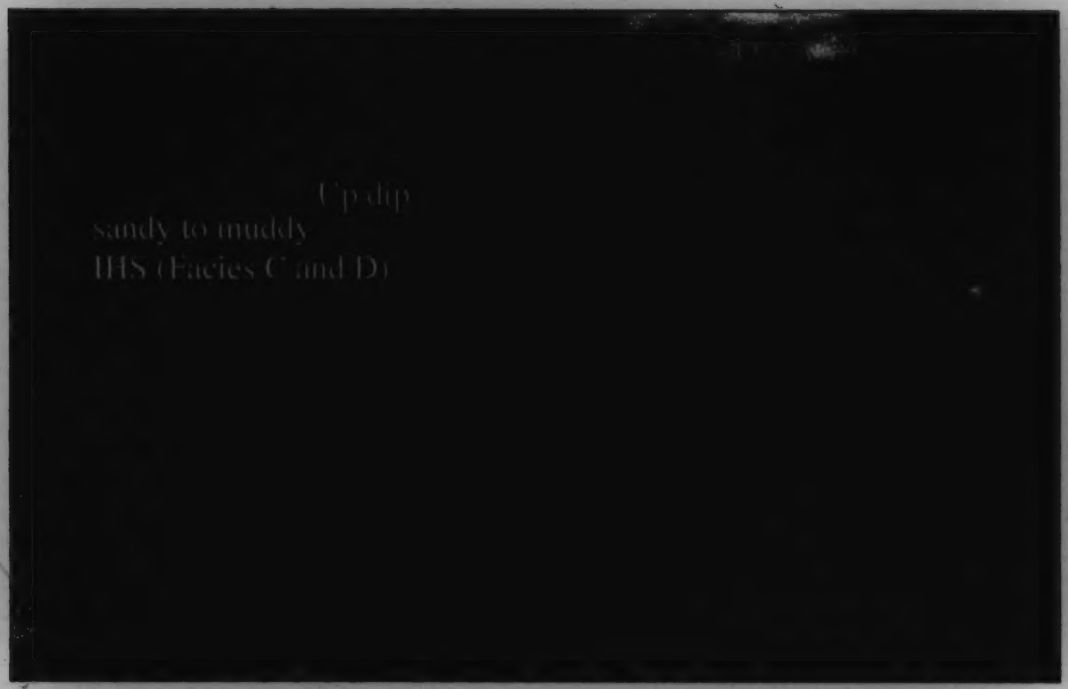

Figure 2-14. Type Section outcrop facing south/southeast. The up-dip transition from sandy and muddy IHS (Facies C and D) to the muddy IHS of Facies D and E. The dashed lines represent subtle truncations, or discontinuity surfaces, between sets of IHS. Solid lines outline truncated master bedding planes.

Figure 2-15. A. Cross-sectional view through the Athabasca outcrop section. View is looking south at east-west trending outcrop. B. Schematic overlay of amalgamated channel units. Note the relative uniform dip direction of each unit as well as onlapping upper channelized unit. Estimated 5 m scale bar is shown.

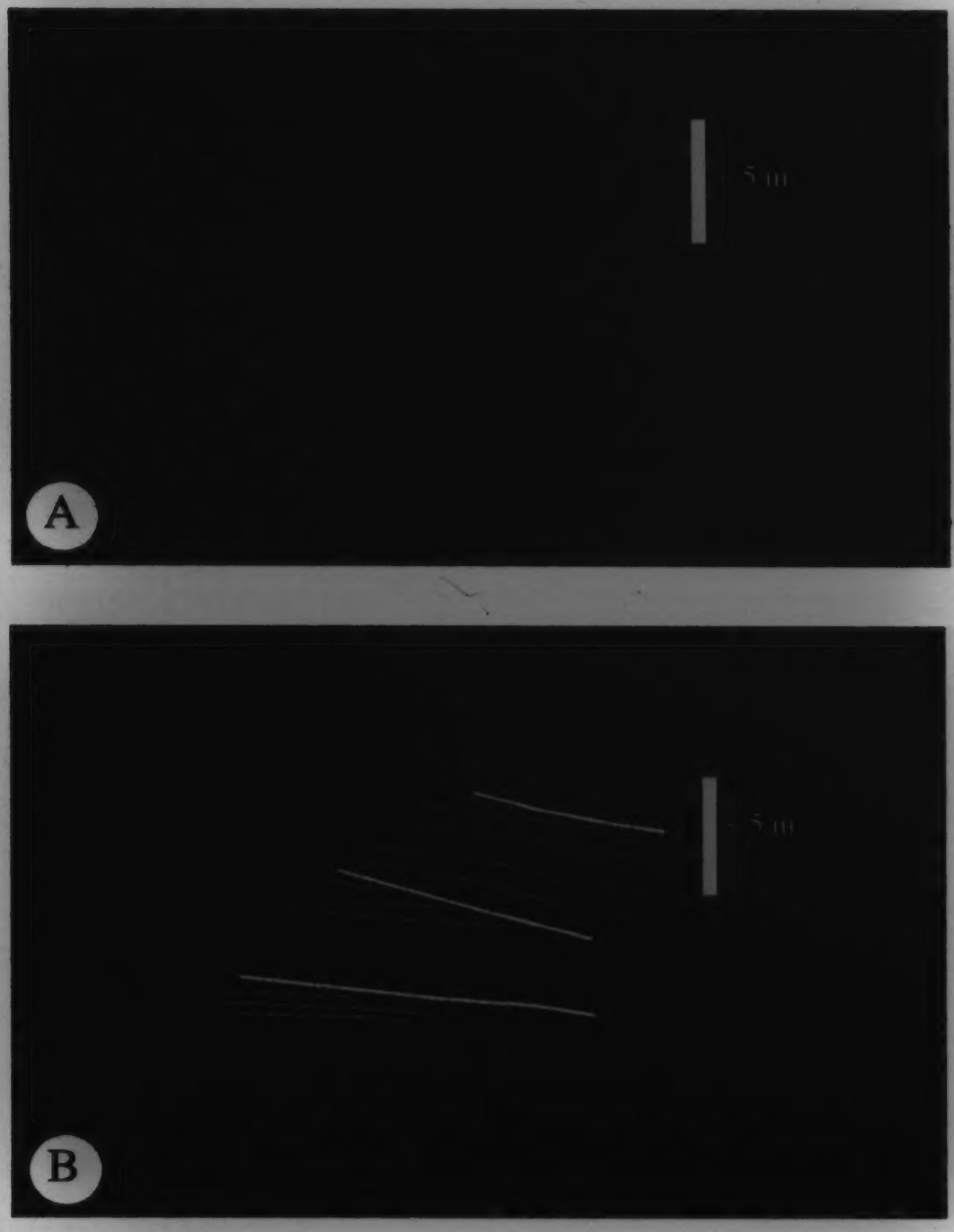

Figure 2-16. A. Christina River outcrop section. B. Schematic overlay of amalgamated channel units. Note the relative uniform dip direction of each unit. 5 m scale bar is estimated.

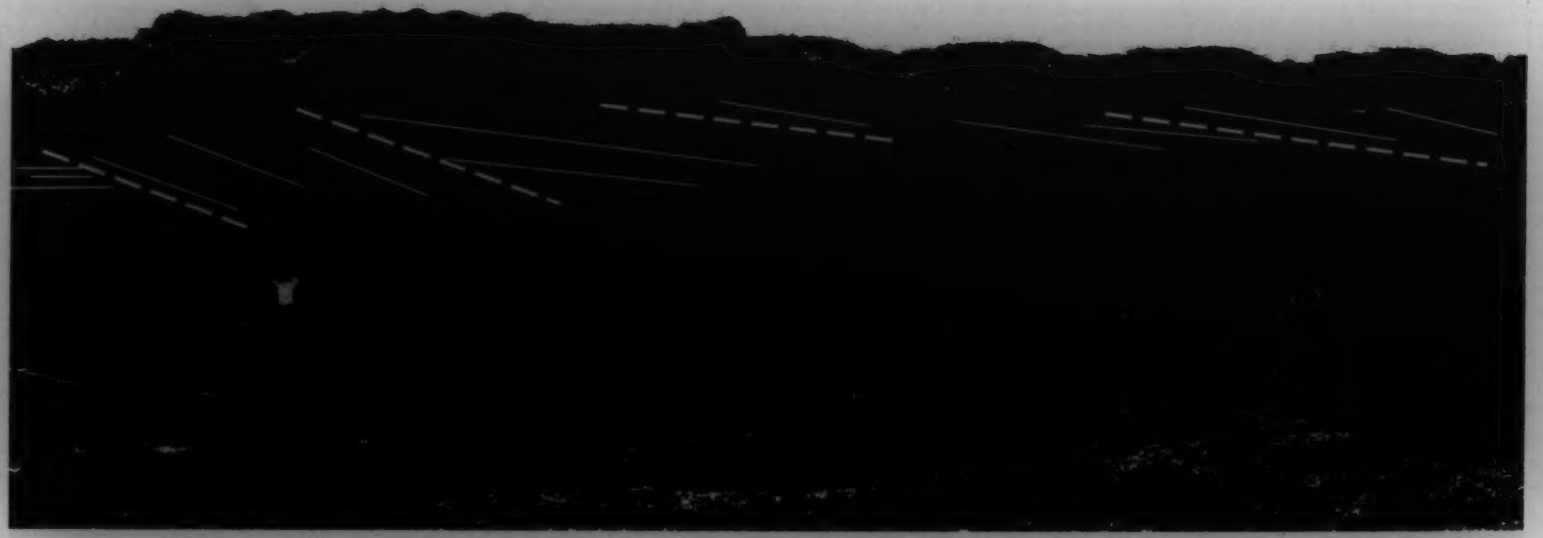

Figure 2-17. Syncrude Northmine exposure showing the stratigraphic boundaries between genetic IHS units (dashed lines). Solid lines outline the master bedding planes within each genetic unit. These represent stratigraphic boundaries between facies within Facies Association 1. Photograph compliments of Mike Ranger.

discontinuity. The bounding surfaces separating genetic units are subtle, and exhibit erosional truncations and onlapping surfaces with underlying strata. This trend is common within the McMurray Formation and is visible at outcrops along the Christina River (Figure 2-16) as well as within some exposures at Syncrude Northmine (Figure 2-17). A fining upward trend also persists through these surfaces of discontinuity. In general, sandy sets of IHS (Facies B and C) are present at the base of the succession and muddy IHS (Facies D and E) is dominant at the top of the succession.

Mud intraclast breccia (Facies F) is observed as discrete intervals within the ripple-laminated sands of Facies B. It can be observed sandwiched between two ripple-laminated sand units, or near the top or base of an interval of ripple-laminated sand.

Interpretation

This facies association is interpreted to represent amalgamated sets of laterally accreting and aggrading point bars in a tidally influenced, fluvial to estuarine setting. These are organized as imbricate cosets or laterally stacked, codirectional sets of IHS (Thomas *et al.*, 1987). Each channel unit possesses characteristics indicative of accretionary point bar settings, including gently inclined bedding, rhythmic changes in bed thickness and regularity of beds, and the presence of brackish-water trace fossil assemblages. These features are some of the most characteristic criteria for distinguishing tidally influenced, point-bar IHS (Thomas *et al.*, 1987).

The fining-upward facies trend visible within genetic IHS sets is interpreted to result from the lateral migration of the channel thalweg after initial channel incision. As the channel axis migrates laterally, the energy conditions become lower and mud deposition, mud-bed preservation, and bioturbation increases. This results in a vertical transition from sandy facies (Facies B or C) near the base to more muddy facies (Facies D or E) in the top portions of each channelized unit.

It was previously established that the sand-mud couplets typical of IHS are likely the result from seasonal adjustments of the turbidity maximum. Studies by Gingras *et al.* (2002) suggest that the biogenic fabrics found within bioturbated IHS imply depositional rates on the order of one year. The abrupt transition from comparatively muddy IHS (Facies D and E) to sandy IHS (Facies B and C) within and between genetic sets of IHS can be interpreted in several ways then, depending on whether the sand is delivered dominantly by tidal forces or fluvial forces. These include: 1) a higher order trend in continental discharge conditions, increasing and decreasing throughout several years; 2) variable growth stages on a single point bar, possibly initiated by upstream meander cut-offs and coinciding increase in hydraulic energy; or 3) small, punctuated changes in base

level caused by transgression.

Bechtel *et al.* (1994) attribute these trends in sand thickness to spring/neap fluctuations in the tidal cycle. This implies that each couplet is deposited during a single tidal cycle, however, and seems unlikely considering the time required for larval growth of infaunal organisms (Gingras *et al.*, 2002). Common to the channel environment is lateral accretion, aggradation and channel cut-off, which is somewhat equivalent to the channel abandonment within a fluvial regime. As one point bar suffers annihilation, the most proximal point bar will be subjected to changes in the flow conditions within the channel. The point bars furthest away suffer the least amount of change in hydraulic energy. This could also explain the periodic deposition of sandier IHS on top of muddier IHS within genetic IHS units.

In estuarine settings, sand is more prevalent within channels and on lower portions of the point-bar surfaces (Clifton, 1983). Up-dip, the point bars become muddier and are characterized by discontinuous mud beds, a feature observed within the Type Section outcrop. Possibly, where these mud beds pinch out down-dip is approximately equal to the mean low tide marker during its deposition. As lateral accretion progresses, sand-dominated IHS (Facies B and C) is overlain by mud-dominated IHS in the vertical succession.

The overall fining-upward trend between sets of IHS may be interpreted to result from deposition within an environment that was increasingly more proximal to the turbidity maximum. Because of the persistence of brackish-water trace fossils throughout much of the IHS units, the deposition is likely downstream of the turbidity maximum within the salt-water wedge. The deposits in Willipa Bay indicate that sandy IHS characterize the more distal bars, near the mouth, and muddy IHS dominate the inner estuary (Gingras *et al.*, 1999)

The interpretation of mud intraclast breccia (Facies F) suggests that the source of the mud is either from the collapse of the cutbank upstream, or from flood currents ripping mud from the point-bar surfaces and re-depositing it downstream as semi-rounded mud clasts. The presence of brecciated intervals within the host sand is simply a function of the relative timing of either cutbank collapse or fluvial discharge events capable of eroding burrowed point bar surfaces.

The abundant tidal indicators observed within these facies, namely the presence of a brackish-water trace fossil assemblage precludes its incorporation into the lower McMurray; the lower McMurray is traditionally associated with deposits of fluvial origin. This association is part of what is referred to as the middle McMurray, consistent with previous authors (Cuddy and Muwais, 1989; Bechtel *et al.*, 1994).

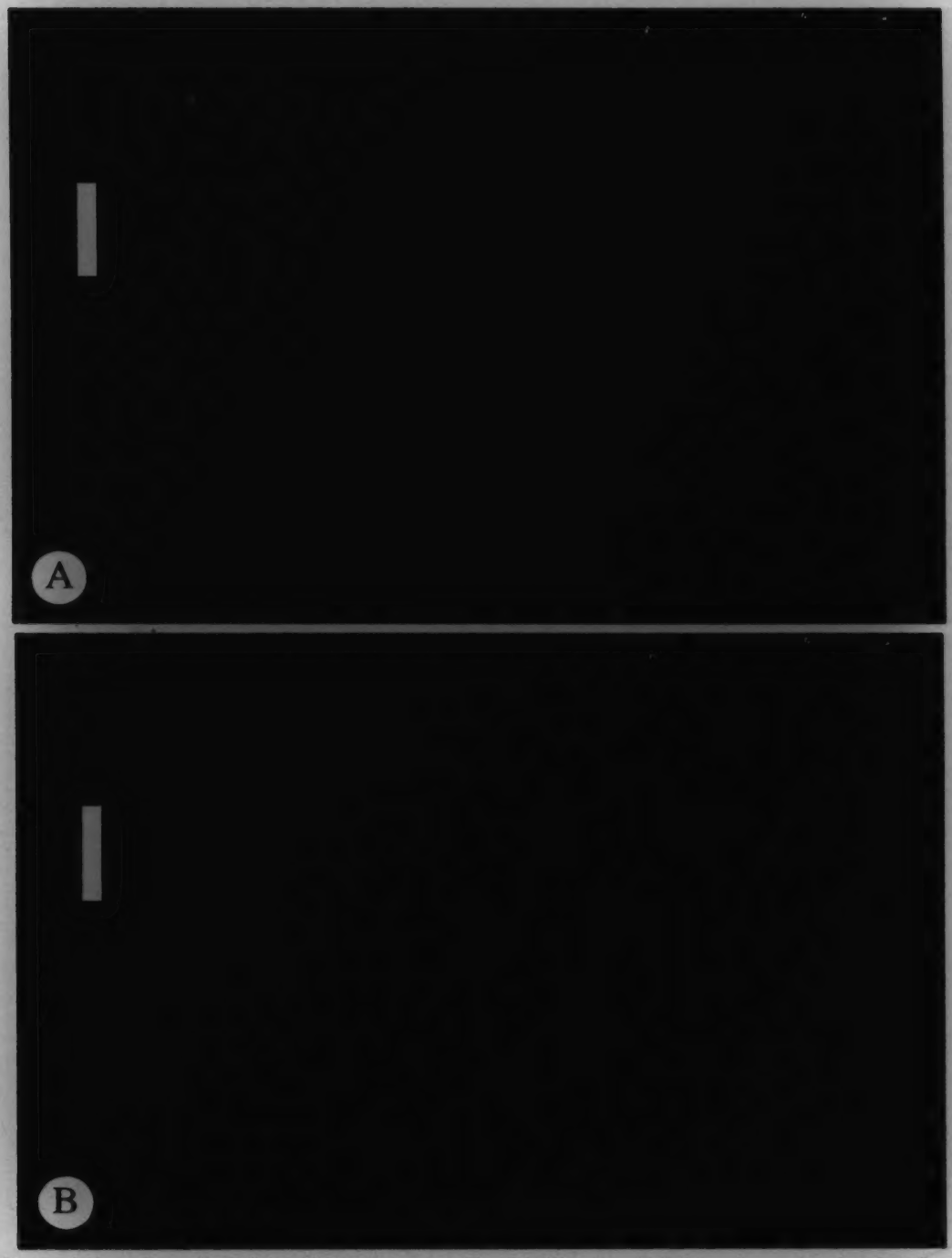

Figure 2-18. A. Overview of Amphitheatre outcrop, Fort MacKay area. B Schematic overlay showing the stacking of facies associations. The contact between the lower FA1 and overlying FA2 has been partly obscured by slumping and melting bitumen. The base of the upper FA 1 is demarcated by Facies A containing large coal fragments.

Facies Association 2

Description

Facies Association 2 (FA2) is characterized by an abrupt fining-upward trend from the coarse-grained, normally graded sands of Facies H, into the high-angle, cross-stratified, grain-striped beds of Facies G. Facies H is observed eroding into underlying facies of FA1 at 34.5 m in Strip Log C (Appendix 1) at the Type Section outcrop but is not observed at the Amphitheatre outcrop.

Interpretation

The facies within FA2 are deposited in an outer-estuarine subtidal channel setting (Ranger and Gingras, 2005). As previously noted, the tidal indicators, such as reactivation surfaces, backflow ripples, and neap/spring bundles, the scale of bedforms, and the trace fossil assemblage found within Facies G strongly suggest the deposition as subtidal dunes in the outer estuary as tidal shoals. In addition, bed foresets show different relative dip directions at both outcrops. Preserved at the Athabasca outcrop is a transgressive lag as outer-estuarine facies are deposited on inner and middle estuarine channel successions. Coarse-grained sands of Facies A are found near the base of the channel succession at the Type Section and represent the lag deposited at the base of a channel (FA1) just following initial incision. The repeated stacking of FA1 and FA2 (Figure 2-18) suggests multiple transgression events superimposing outer-estuarine strata onto older inner-to-middle-estuarine strata. Between transgressions, progradation of IHS of FA1 occurs over the outer estuarine dunes characteristic of FA2.

DISCUSSION

The successions of McMurray Formation under study were deposited as part of an estuarine valley-fill complex. The lower McMurray is not observed in this study. Outer-estuarine subtidal dunes are interpreted from the base of the Type Section outcrop based on flow reversal indicators and the presence of marine and brackish trace fossils (Clifton, 1983; Ranger and Gingras, 2005). The majority of the deposits fit within the middle McMurray category defined as a complex of estuarine channel successions with an element of fluvial input. As there is a drop in relative sea level, fluvial-to-estuarine facies prograde basinward over the outer estuarine dune complex. Upwards, this progradational unit is subjected to several depositional factors accounting for numerous fining upward trends. These trends occur on the couplet scale to the scale of the entire

succession of IHS. Factors attributed to influencing these include: lateral accretion of the point bars, rhythmic shift in tidal influence stemming from diurnal, monthly, and seasonal shifts in the tidal regime, and shifting of the turbidity maximum during fluvial flood season. The IHS within this portion record deposition on tidally influenced point bars in an upper-to-middle estuarine setting; deposition occurs more proximal to the turbidity maximum upwards. At least four genetically related channel units are observed within the Type Section outcrop, averaging 6 to 9 m thick. Each unit is rhythmically bedded and laminated, possesses a fining upward trend in grain size, and contains a brackish-water trace fossil assemblage consisting of *Cylindrichnus*, *Gyrolithes*, *Planolites*, and *Skolithos*, in order of decreasing abundance.

With respect to the regional stratigraphic model proposed by Ranger and Pemberton (1997), these sections were deposited within a valley incised into one of the stacked, fining upward shoreface successions that form the background sedimentary package of the McMurray Formation. It stands to reason that the deposits within an individual valley may preserve the estuarine expression of one of the transgressive events, more easily identified within the shoreface succession, and subsequent progradation of estuarine facies. This is observed within the Type Section as outer estuarine dunes are erosionally truncated by prograding channelized successions of IHS. The IHS units become increasingly muddy upwards, indicating deposition within the middle-to-upper estuary. The proceeding transgression causes a landward shift in facies resulting in outer estuarine dunes to overlay the IHS succession. In short, the progradational elements of FA2 over FA1, unique stacking of the IHS successions within the outcrop belt, supports the interpretation that the McMurray Formation outcrops within this study were deposited within a tide-dominated delta.

REFERENCES

Allen, J.R. 1970. Physical Processes of Sedimentation. Allen and Unwin, London

Allen, J.R. 1980. Sand waves: a model of origin and internal structure. Sedimentary Geology, v. 26, p. 281-328.

Allen, G. P. 1991. Sedimentary processes and facies in the Gironde estuary: a Recent model of macrotidal estuarine systems. *In*: Smith, G.D., Reinson, G.E., Zaitlin, B.A. (eds). Clastic Tidal Sedimentology: Canadian Society of Petroleum Geologists Memoir 16, p. 29-40.

Anima, R.J., Clifton, E.H. and Phillips, L.R. 1989. Comparison of modern and Pleistocene estuarine facies in Willapa Bay, Washington. *In:* G.E. Reinson (ed.), Modern and ancient examples of clastic tidal deposits, a core and peel workshop, Canadian Society of Petroleum Geologists, Second international research symposium on clastic tidal deposits, p. 1-19.

Bechtel, D.J. 1996. The stratigraphic succession and paleoenvironmental interpretation of the McMurray Formation, O.S.L.O. area, northeastern Alberta. Unpublished MSc. Thesis, University of Alberta, Edmonton. 153 pp.

Bechtel, D.J., Yuill, C.N., Ranger, M.J. and Pemberton, S.G. 1994. Ichnology of inclined heterolithic stratification of the McMurray Formation, northeastern Alberta. *In*: S.G. Pemberton, D.P. James, D.M. Wightman (eds.), Canadian Society of Petroleum Geologists Mannville Core Conference, Canadian Society of Petroleum Geologists, Exploration Update 1994, p. 351-368.

Clifton, E.H, and Gingras, M.G. 1999. Modern and Pleistocene Estuary and Valley-Fill Deposits, Willapa Bay, Washington: A Field Guide. 98 p.

Clifton, E.H. 1983. Discrimination between subtidal and intertidal facies in Pleistocene deposits, Willipa Bay, Washington. Journal of Sedimentary Petrology, v. 53, p. 352-369.

Cuddy, R.G. and Muwais, W.K. 1989. Channel-fills in the McMurray Formation: their recognition, delineation, and impact at the Syncrude Mine. Canadian Institute of Mining and Metallurgy Bulletin, 82, p. 67-74.

Gingras, M.K., Rasanen, M. and Ranzi, A. 2002. The significance of bioturbated inclined heterolithic stratification in the southern part of the Miocene Solimoes Formation, Rio Acre, Amazonia Brazil. Palaios, v. 17, p. 591-601.

Gingras, M.K., Pemberton, S.G. and Sauders, T. 1999. The ichnology of modern and Pleistocene brackish-water deposits at Willipa Bay, Washington: Variability in estuarine settings. Palaios, v. 14, p. 352-374.

Harris, C.E. 2003. Aspects of the Sedimentology, ichnology, stratigraphy, and reservoir character of the McMurray Formation, Northeast Alberta. Unpublished MSc. Thesis, University of Alberta, Edmonton. 209 pp.

Johnson, L.R. 1983. The transport mechanisms of clay and fine silt in the north Irish Sea. Marine Geology, v. 52, p.33-41.

Lettley, C. D. 2004. Elements for a genetic framework for inclined heterolithic strata of the McMurray Formation, northeastern Alberta. Unpublished M.Sc. Thesis, University of Alberta. 150 pp.

McKee, E.D. and Weir, G.W. 1953. Terminology for stratification and cross-stratification in sedimentary rocks. Bulletin of the Geological Society of America, v. 64, p. 381-390.

Meade, R.H. 1972. Transport and deposition of sediments in estuaries. Geological Society of America Memoir 133, p. 91-120.

de Mowbray, T. and Visser, M.J. 1984. Reactivation surfaces in subtidal channel deposits, Oosterschelde, southwestern Netherlands. Journal of Sedimentary Petrology, v. 54, p. 811-824.

Pemberton, S.G., Flach, P.D. and Mossop, G.D. 1982. Trace fossils from the Athabasca oil sands, Alberta, Canada. Science, v. 217, p. 825-827.

Postma, H. 1967. Sediment transport and sedimentation in the estuarine environment. *In*: G.H. Lauff (ed.), Estuaries, American Association for the Advancement of Science, Publication 83, Washington, DC, p. 158-179.

Ranger, M.J. and Gingras, M.K. 2005. Geology of the Athabasca Oil Sands: Field Guide and Overview, Canadian Society of Petroleum Geology Annual Convention. 132 pp.

Ranger, M.J. and Pemberton, S.G. 1997. Elements of a stratigraphic framework for the McMurray Formation in South Athabasca. *In*: S.G. Pemberton and D.P. James (eds.), Petroleum Geology of the Cretaceous Mannville Group, Western Canada, Canadian Society of Petroleum Geologists, Calgary, Memoir 18, p. 263-291.

Ranger, M.J. and Pemberton, S.G. 1992. The sedimentology and ichnology of estuarine point bars in the McMurray Formation of the Athabasca oil sands deposit, northeastern Alberta, Canada. *In*: S.G. Pemberton (ed.), Applications of Ichnology to Petroleum Exploration, Society of Economic Paleontologists and Mineralogists, Core Workshop No. 17, p. 401-421.

Rasanen, M.E., Linna, A.M. and Santos, C.R. 1995. Late Miocence Tidal Deposits in the Amazonian Foreland Basin. Science, v. 269, p. 386-390.

Smith, D.G. 1987. Meandering river point bar lithofacies models: Modern and ancient examples compared. *In*: F. Ethridge and R. Flores (eds.), Recent Developments in Fluvial Sedimentology, Society of Economic Paleontologists and Mineralogists, Special Publication 39, p. 83-91.

Smith, D.G. 1988a. Modern point bar deposits analogous to the Athabasca oil sands, Alberta, Canada. *In:* P.L. be Boer, A. van Gelder and S.D. Nio (eds.), Tide-influenced sedimentary environments and facies, D. Reidel Publishing Co., The Netherlands, p. 417-432.

Smith, D.G. 1988b. Tidal bundles and mud couplets in the McMurray Formation, northeastern Alberta, Canada. Bulletin of Canadian Petroleum Geology, v. 36, no. 2, p. 216-219.

Stewart, G.A. and MacCallum, G.T. 1978. Athabasca Oil Sands guide book. Canadian Society of Petroleum Geologists international conference: Facts about principles of world petroleum oil occurrence, Canadian Society of Petroleum Geologists, 33 pp.

Stone, M. and Droppo, I.G. 1994. Flocculation of fine-grianed suspended solids in river continuum. *In*: L.J. Olive, R.J. Loughran, and J.A. Kesby (eds.), Variability in Stream Erosion and Sediment Transport, International Association of Hydrological Sciences Publication, v. 224, p. 479-489.

Thill, A, Moustier, S., Garnier, J.M, Estournel, C., Naudin, J.J, and Bottero, J.Y. 2001. Evolution of particle size and concentration in the Rhone river mixing zone: influence of salt flocculation. Continental Shelf Research, v. 21, p. 2127-2140.

Thomas, R.G., Smith, D.G., Wood, J.M., Visser, J., Calverly-Range, E.A. and Koster, E.H. 1987. Inclined heterolithic stratification- terminology, description, interpretation, and significance. Sedimentary Geology, v. 53, p. 123-179.

Walker, R.G. 1992. Facies, facies models, and modern stratigraphic concepts. *In*: R.G. Walker and N.P. James (eds.), Facies Models: Response to Sea Level Change, Geological Association of Canada, p. 1-14.

Wightman, D.M, and Pemberton, S.G. 1997. The Lower Cretaceous (Aptian) McMurray Formation; an Overview of the Fort McMurray area, northeastern Alberta. *In*: S.G. Pemberton and D.P. James (eds.). Petroleum Geology of the Cretaceous Mannville Group. Western Canada, Canadian Society of Petroleum Geologists, Calgary, Memoir 18, p. 312-344.

CHAPTER 3:
THE MORPHOLOGICAL SIGNATURE OF ESTUARINE POINT BARS

INTRODUCTION

The dominant controls on the downstream geometry of a river channel include discharge, channel slope, channel (average) roughness, and sediment composition at channel boundaries (Huang and Warner, 1995). In addition to these controls, Knighton (1984) suggested that the discontinuous input of sediment and abrupt changes in hydraulic discharge and sediment transport at tributary junctions significantly impact downstream channel geometries. Gurnell (1997) assessed the influence of tidal controls, which generate discontinuous disturbances on river flows, impacting energy gradient and associated channel geometries.

Several authors have noted that morphological differences exist between channels that develop under wholly fluvial processes and those that develop under the influence of both fluvial-and tidal-forces (Ahnert, 1960; Coleman and Wright, 1978; Woodroffe *et al.*, 1989; Dalrymple *et al.*, 1992; Gurnell, 1997). These differences can be attributed, at least in part, to a combination of tidal and river-flood hydrodynamics. Dalrymple *et al.* (1992) also suggested that the relative length of estuarine zones, the valley shape, and the rate of sediment supplied compared to the rate of sea level rise may also impact the morphology of channels within the inner-, outer-, and middle-estuary zones. The focus of this chapter is to provide an inventory of the variety of morphological characteristics within riverine-estuarine environments and to sub-divide this realm into geomorphological zones that can be used to assist in the construction of 3-dimensional tidal point-bar models.

METHODOLOGY

The morphological channel trends between the outer/middle estuary transition zone and the inner estuary/fluvial transition zones along the main channels of several modern estuaries were examined using 1:100 000 and 1:50 000 satellite images from NASA, as well as published studies. Meander sinuosities, channel widths, meander amplitudes and wavelengths, and associated accretion-deposit thicknesses from numerous channel segments were tabulated from the following estuaries: 1) the South Alligator River, northern Australia; 2) the Ord River, northern Australia; 3) the King River, northern Australia; 4) the Willapa River, Washington, U.S.A.; 5) the Tillamook River, Oregon, U.S.A.; 6) the Digul River estuary, Indonesia; 7) the Salmon River estuary, Nova

Scotia, Canada; 8) the Fly River, Papua New Guinea; and 9) the Rio Tuira, Panama. These rivers were chosen to provide a range of relative tidal and fluvial input into each of the respective environments.

Sinuosity, the ratio between channel length and the valley length that the meander occupies, was measured at 10-12 channel segments along each of the nine rivers. The meander length is the distance along the channel between inflection points of adjacent channel meanders or bends. The wavelength, or the distance within which the channel changes course one full wavelength, as well as the amplitude of each of the meander segments, were also measured. These measurements are all schematically depicted in Figure 3-1. The channel width was measured at each segment but due to highly variable widths within individual bends, four measurements were taken along the bend and an average channel width was calculated. All of these measurements were tabulated and the profiles of each were constructed and plotted against the corresponding channel segment number. In addition, geomorphologic channel zones and associated accretion deposits were identified and discussed for each estuary.

This study was primarily concerned with identifying channel geomorphologies within the fluvial-tidal zone in a range of estuarine settings, but the processes responsible for the development of these channel forms within the estuarine environment were also addressed. In addition, the stratigraphic implications of the development and migration of the fluivial-tidal and tidal deposits during highstand conditions and transgression were discussed for comparison with the deposits of the McMurray Formation and to help characterize the 3-dimensional architecture of IHS reservoirs.

CHARACTERIZATION OF CHANNEL MORPHOLOGY THROUGH THE ESTUARY: PREVIOUS WORK

Historically, the estuary has been subdivided in several ways. Dalrymple *et al.* (1992) suggest a tripartite classification scheme based primariliy on the dominant processes within each zone. The outer estuary is marine-dominated, the inner estuary is river-dominated, and the central zone is of mixed or null energy. A similar classification scheme of the Gironde estuary refers to the estuary inlet, the estuarine funnel, and upper estuary channels (Allen, 1991). The subdivision of the estuary on the basis of morphological channel classes or zones has also been employed (Wright *et al.*, 1973; Coleman and Wright, 1978; Woodroffe *et al.*, 1989; Dalrymple *et al.* 1992).

Ahnert (1960) first addressed planimetric channel morphologies within the fluvial-marine environment in the Chesapeake Bay area and used the term estuarine meanders to

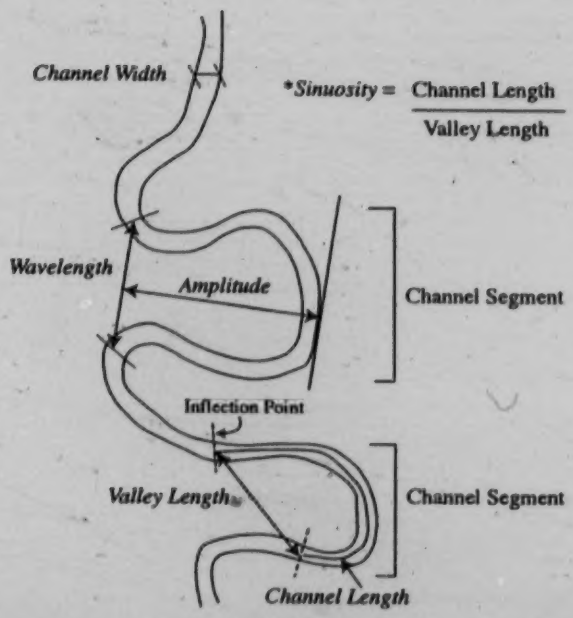

Figure 3-1. Schematic showing the manner in which measurements were collected from Landsat images of the estuaries within the study. All of the measurements that are recorded in Appendix 2 are italicized above.

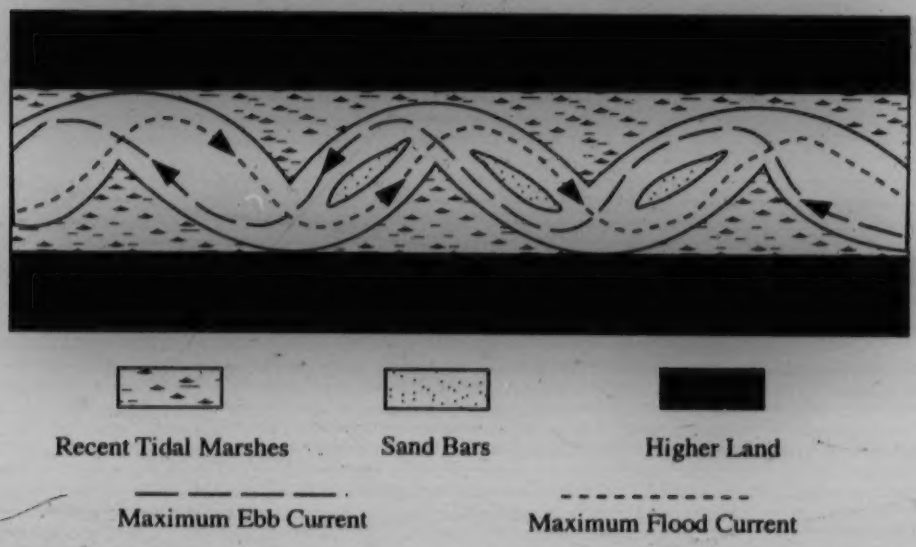

Figure 3-2. Schematic showing the proposed development of estuarine meanders. The cuspate form of pointbars is due to differntial erosive power and flow directions of the flood and ebb tides (modified from Ahnert, 1960).

describe those meanders that are periodically affected by tidal reversals. These meanders were described as a series of oblong pools connected by narrow channels (Figure 3-2). Within these meanders, accretion deposits comprise shore-detached, or partially detached sand or gravel bars. Similar channel meanders were documented from several other coastal environments in eastern Panama and Columbia using radar imagery (Lewis and MacDonald, 1970). These types of meanders are typically situated within the middle estuary, where ebb and flood tides are of comparable strength (Ahnert, 1960).

The Ord River estuary in northern Australia was characterized by two channel morphologies, a sinuous, narrow channel with a low width/depth ratio and a broad, funnel-shaped lower river course with high width/depth ratios (Wright *et al.*, 1973). In addition, the tight-meander zone was suggested to be indicative of most funnel-shaped estuaries (Coleman and Wright, 1978). Specific channel morphologies were characterized from the South Alligator River between the mouth of the estuary and the upper limit of tidal influence. These include the estuarine funnel, the sinuous zone, the cuspate zone, and the upstream tidal channels (Woodroffe *et al.*, 1989). The cuspate channels are consistent with those meanders described by Ahnert (1960), where channel width diminishes at the meander corners and increases between the bends. A similar progression was observed on the Salmon River, located within the tide-dominated Cobequid Bay estuary, referred to as a 'straight-meandering-straight' morphology (Dalrymple *et al.*, 1992; Figure 3-3). Dalrymple *et al.* (1992) propose that outer straight reach experiences net sediment transport landward because tidal processes dominate river processes. The inner straight reach experiences net sediment transport downstream due to long-term dominance of river flow over tidal flow. Both straight reaches host alternate, bank-attached bars and some mid-channel bars. The transition zone is characterized by the convergence of river-dominated and tide-dominated processes. This convergence is thought to give way to the development of tight channel meanders and symmetrical bars (Dalrymple *et al.*, 1992).

OVERVIEW OF THE DATA SET

The results of sinuosity, wavelength-to-amplitude and channel-width calculations are presented in Appendix 2. The profiles of each of the three parameters for the nine study areas are displayed in Figure 3-4, 3-5, and 3-6.

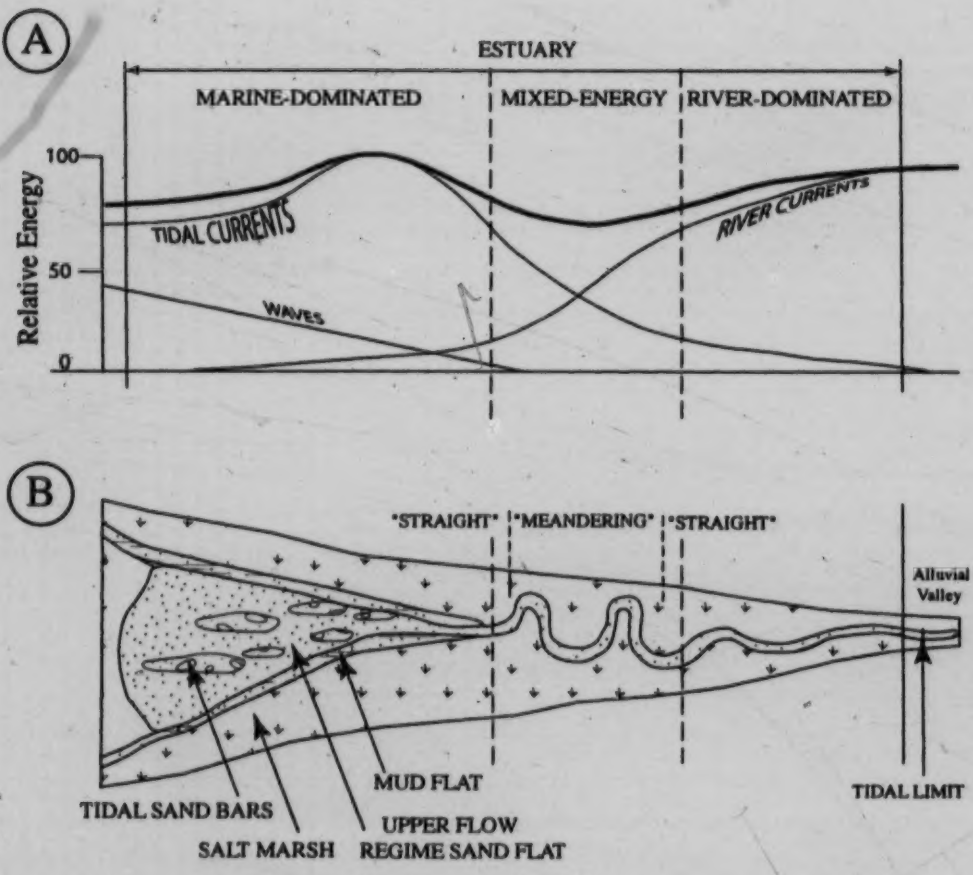

Figure 3-3. A. Schematic tripartate estuarine zonation within a typical tide-dominated estuary showing: the outer, marine-dominated zone; central, mixed-energy zone; and inner, river-dominated zone. These are plotted against total energy within the estuary. B. Schematic classes of channel morphology and the "straight-meandering-straight" channel morphology model with respect to energy classification scheme (after Dalrymple *et al.*, 1992).

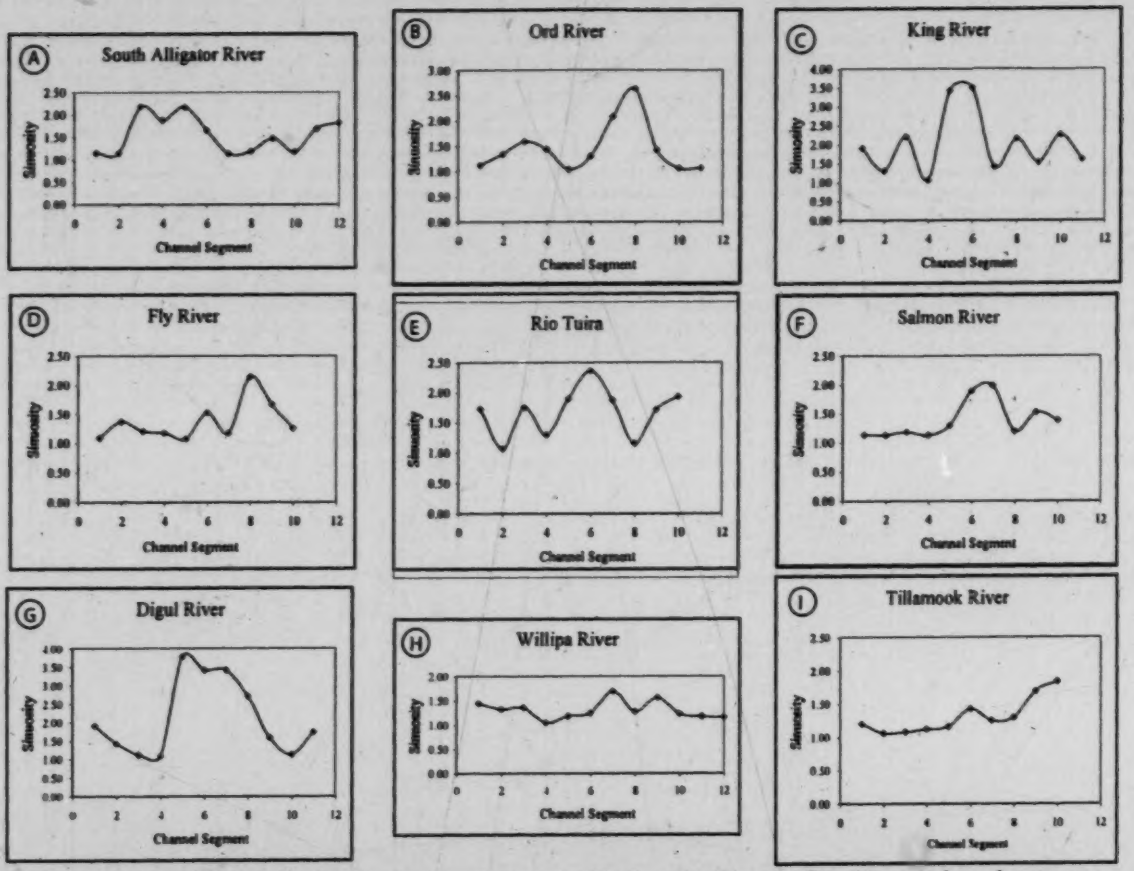

Figure 3-4. A-I. Sinuosity profiles for the nine estuaries examined in the study. These profiles represent channel segments spanning the estuary from the mouth (left side of the profile) towards the upper limit of tidal influence (right side of profile).

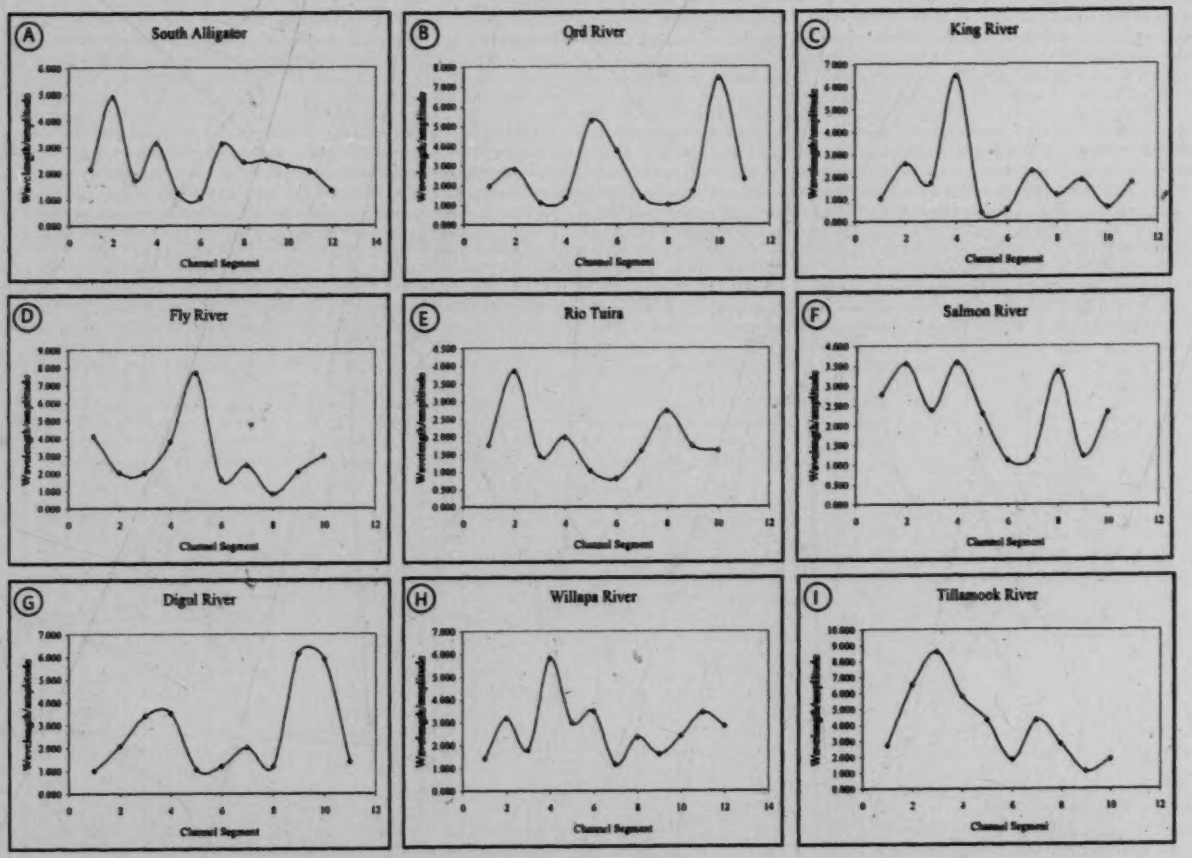

Figure 3-5. A-I. Wavelength-to-amplitude profiles for the nine estuaries examined in the study. These profiles represent channel segments spanning the estuary from the mouth (left side of the profile) towards the upper limit of tidal influence (right side of profile).

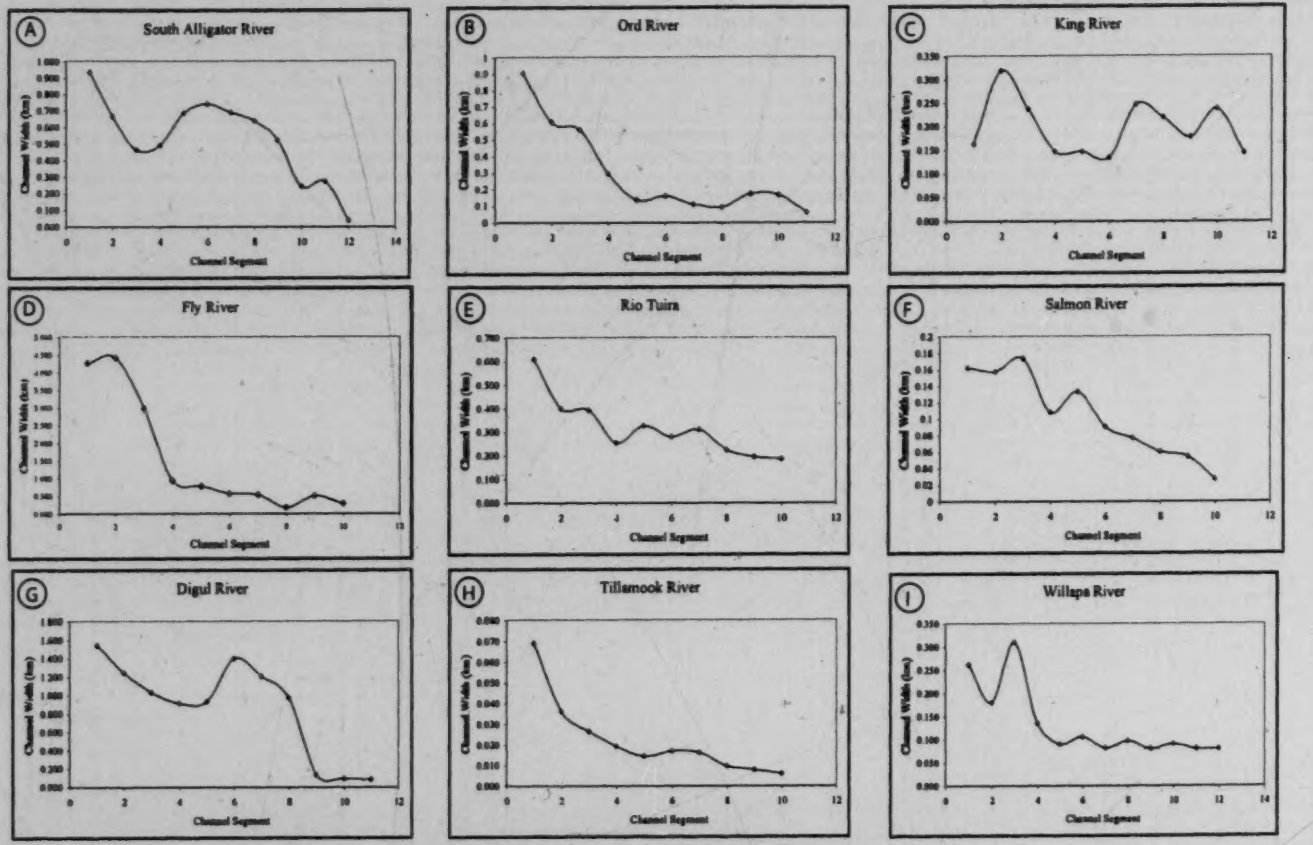

Figure 3-6. A-I. Channel width profiles of the nine estuaries under study. Each profile measures the average width of channel segments from the estuary mouth (left side of the profile) towards the upper limit of tidal influence (right side of the profile).

South Alligator River, northern Australia

The South Alligator River (Figure 3-7a), located in the Northern Territory of Australia, is a macrotidal, tide-dominated estuary with an average spring-tide range of 5 to 6 m that extends some 100 km upstream (Woodroffe *et al.*, 1989). The drainage basin of the South Alligator River has a catchment area of about 9000 km^2 with an annual precipitation of 1300 to 1400 mm that falls predominantly during the wet season from December to April. During the dry season the estuary is saline to the upper limit of tidal influence but the fluvial discharge during the wet season positions the salt wedge within 20 to 40 km of the mouth (Woodroffe *et al.*, 1989). Woodroffe *et al.* (1989) estimated average river flows between 400 and 700 m^3/s based on comparisons to the nearby Daly River.

Measured sinuosity values (Appendix 2, Figure 3-4a) from the estuary mouth to the upper limits of tidal influence along the South Alligator River show a distinct trend concordant with the 'straight-meandering-straight' trend within tide-dominated estuaries discussed by Dalrymple *et al.* (1992). Figure 3-4a shows three distinct sinuosity zones separated by a sinuosity magnitude of approximately 1.7. The outer, low-sinuosity (< 1.7) zone is much shorter than the inner low-sinuosity zone. The inner portion has increasing sinuosity values towards the upper tidal limit into the fluvially dominated reaches of the river. The wavelength-to-amplitude (Figure 3-5a) ratio profile reflects the changes in sinuosity along the river; changes in slope along the wavelength-to-amplitude profile consistently oppose changes in sinuosity. Abandoned channel meanders, although rare, are visible in the meandering zone and, in general, have undergone translation and rotation landward (Figure 3-7b). The channel width profile (Figure 3-6a) consistently decreases upstream to the river mouth and increases abruptly above the meander belt. The channel width is typically variable around each bend and between bends above the meander belt but remains more uniform within the meander belt.

Three channel shape-classes, refined from Woodroffe *et al.* (1989), are recognized along the South Alligator River (Figure 3-7c):

1) Estuarine-funnel zone: a funnel-shaped segment, approximately 1 km wide, with a large bend at approximately the halfway point. Channel width decreases rapidly within this reach and sinuosity values are less than 1.7. The insides of channel bends are angular to sub-rounded. Channel width increases between channel bends and decreases at the bends. These characteristics are similar to the 'cuspate' channel forms that are referred to by Woodroffe *et al.* (1989); the term cuspate is adopted hereafter. Rare abandoned cutoffs are observed in this zone (Figure 3-7b).

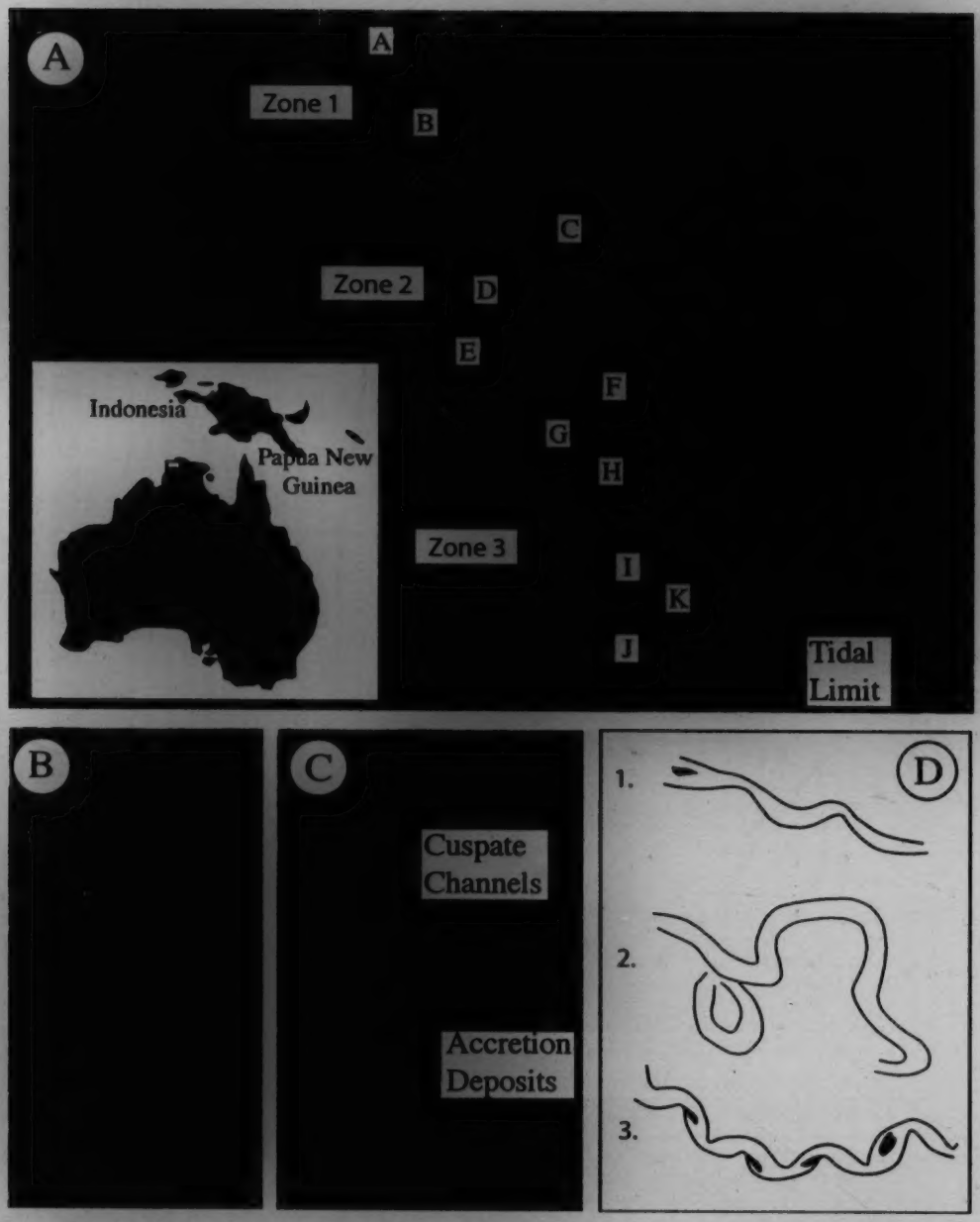

Figure 3-7. A. Location map of the South Alligator River, northern Australia (see inset). Letters indicate the channel segments from which measurments were collected. B. Image showing the rare cutoffs. C. Image showing visible accretion deposits and cuspate channel forms from the lower portion of Figure A. D. Schematic depicting the three shape zones identified from the South Alligator River (see A for location within the estuary). (NASA).

2) Sinuous-meander zone: these are channel meanders that closely resemble fluvial meanders. Sinuosity values are high (> 1.7), and the insides of channel bends remain rounded. Accretion deposit accumulation is thought to be analogous to those found in fluvial meanders as point bars.
3) Cuspate-meander zone: this zone is characterized by channel meanders that become wider between bends and narrow at the bends. These are analogous to the estuarine meanders defined by Ahnert (1960) where the insides of channel bends are pointed. Bank-attached or mid-channel bars characterize the accretion deposits within this zone (Figure 3-7c). The rare paleochannels found within this zone are the result of channel avulsion rather than channel migration (Woodroffe *et al.*, 1989).

Ord River, northern Australia

The Ord River is a macrotidal estuary that adjoins the Gulf of Cambridge in northern Australia (Figure 3-8a). The entrance of the Gulf experiences tidal ranges between 3.8 m and 5.15 m. Tidal amplification in the Ord River causes areas approximately 85 km upstream to experience an average spring tide of 6.6 m (Wright *et al.*, 1975; Coleman and Wright, 1978). Water depths of the Ord River range from 7 m at the mouth to 1.5 m approximately 42 km upstream of the mouth (Wright *et al.*, 1973). The Ord River system drains a catchment area of approximately 7800 km^2, which suffers an average rainfall of 510 mm. Fluvial discharge rates range from 0.07 m^3/s in September to 730 m^3/s in January (Coleman and Wright, 1978).

Measured sinuosity values (Appendix 2, Figure 3-4b) from the estuary mouth to the upper limits of tidal influence, show a distinct 'straight-meandering-straight' trend. The wavelength-to-amplitude profile (Figure 3-5b) maintains a discordant relationship with the sinuosity profile; increases in sinuosity values are consistent with decreases in wavelength-to-amplitude ratios. Abundant abandoned-channel meanders are present in the inner reaches. Channel width consistently decreases landward. However, there is a small increase in channel width coincident with the transition from the uppermost reach of the meandering belt to the upper straight segment (Figure 3-6b). Channel width is variable around meanders.

The morphological channel zones identified from the Ord River (Figure 3-8c) include:

1) The estuarine funnel zone: a funnel-shaped segment with a large bend near the transition from zone 1 to zone 2. Channel width decreases gradually within this reach and sinuosity values are less than 1.7. The insides of channel bends

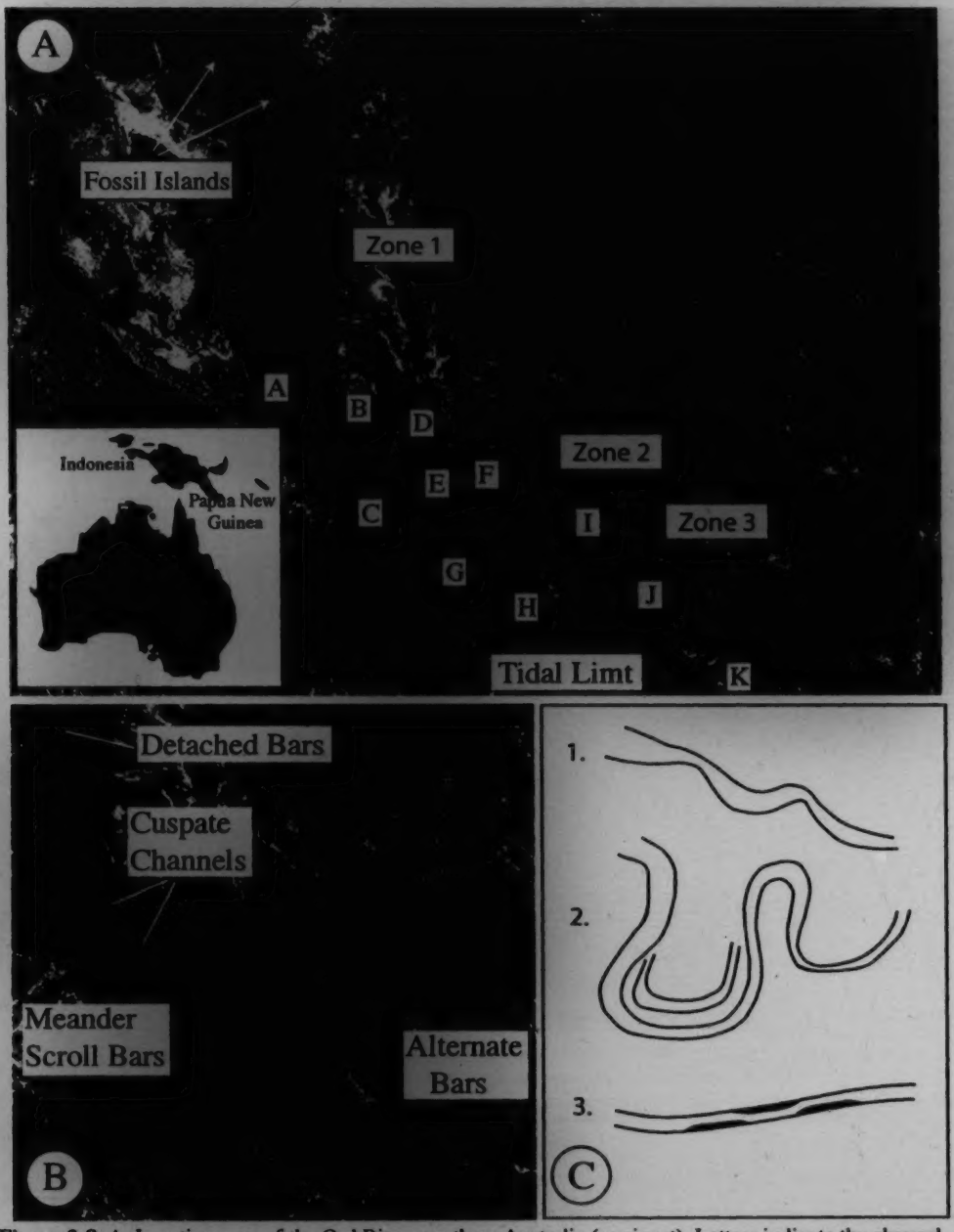

Figure 3-8. A. Location map of the Ord River, northern Australia (see inset). Letters indicate the channel segments from which measurments were collected. The mouth of the Ord River is located approximately 20 km north of the image. B. Image showing large meander scrolls, rare cuspate channel forms, and detached bars. C. Schematic depicting the three morphological zones identified. See A. for their relative location within the estuary. (NASA).

are sub-rounded to pointed and, in general, channels are cuspate in nature. Flood-orientated megaripples with heights of 30 cm to 1 m are observed within this reach, downstream of Fossil Islands (Wright *et al.*, 1973).

2) The meander zone: a sinuous (>1.7) reach with abundant meander scroll bars (Figure 3-8b). Channel width within this reach remains fairly uniform with a gradual decrease towards the limit of tidal incursion. Accretion deposits are reported to average 12 m in thickness with rare occurrences of 25 m thick deposits in deep scour pools (Coleman and Wright, 1978). The insides of channel bends are rounded.
3) The inner straight zone: characterized by a low (<1.7) sinuosity channel with laterally attached and partially detached alternate bars (Figure 3-8b). Channel width, estimated at low water as evidenced by emergent bars, remains uniform within this zone.

King River, northern Australia

The King River (Figure 3-9a), located in the Gulf of Cambridge in the Northern Territory of Australia, is a large (30 km long) tide-dominated channel with little fluvial input. The channel has a depth of 10 m at the mouth and approximately 5 m at the upper reaches of tidal influence. Tidal amplitude is constant along the length of the river, unlike that of the Ord River (Coleman and Wright, 1978).

The course of the King River is highly sinuous, with an average sinuosity of 2.03 (Appendix 2, Figure 3-4c). The sinuosity profile is symmetrical with a similar number of channel segments seaward and landward of the high sinuosity class. Despite the highly sinuous course, abandoned meanders are not visible on the satellite images of the King River and were not reported by Coleman and Wright (1978). In general, as sinuosity values decrease the wavelength-to-amplitude ratios increase (Figure 3-5c). The channel width averages 180 m (Coleman and Wright, 1978) and the profile (Figure 3-6c) displays a slight increase in width at the upper limit of the high-sinuosity class segment.

Three morphological zones are identified from the King River (Figure 3-9c):

1) The outer straight zone: characterized by comparatively low (1.6) average channel sinuosity. The insides of channel bends are rounded and no accretion deposits are discernable from available images (Figure 3-9b).
2) The meander zone: this zone, characterized by higher sinuosity values than zones 1 and 3, is similar to that of the other estuaries studied despite the lack of river influence. Sinuosities are high (> 2.1), but few meander scars are present long the King River (Wright *et al.*, 1975).

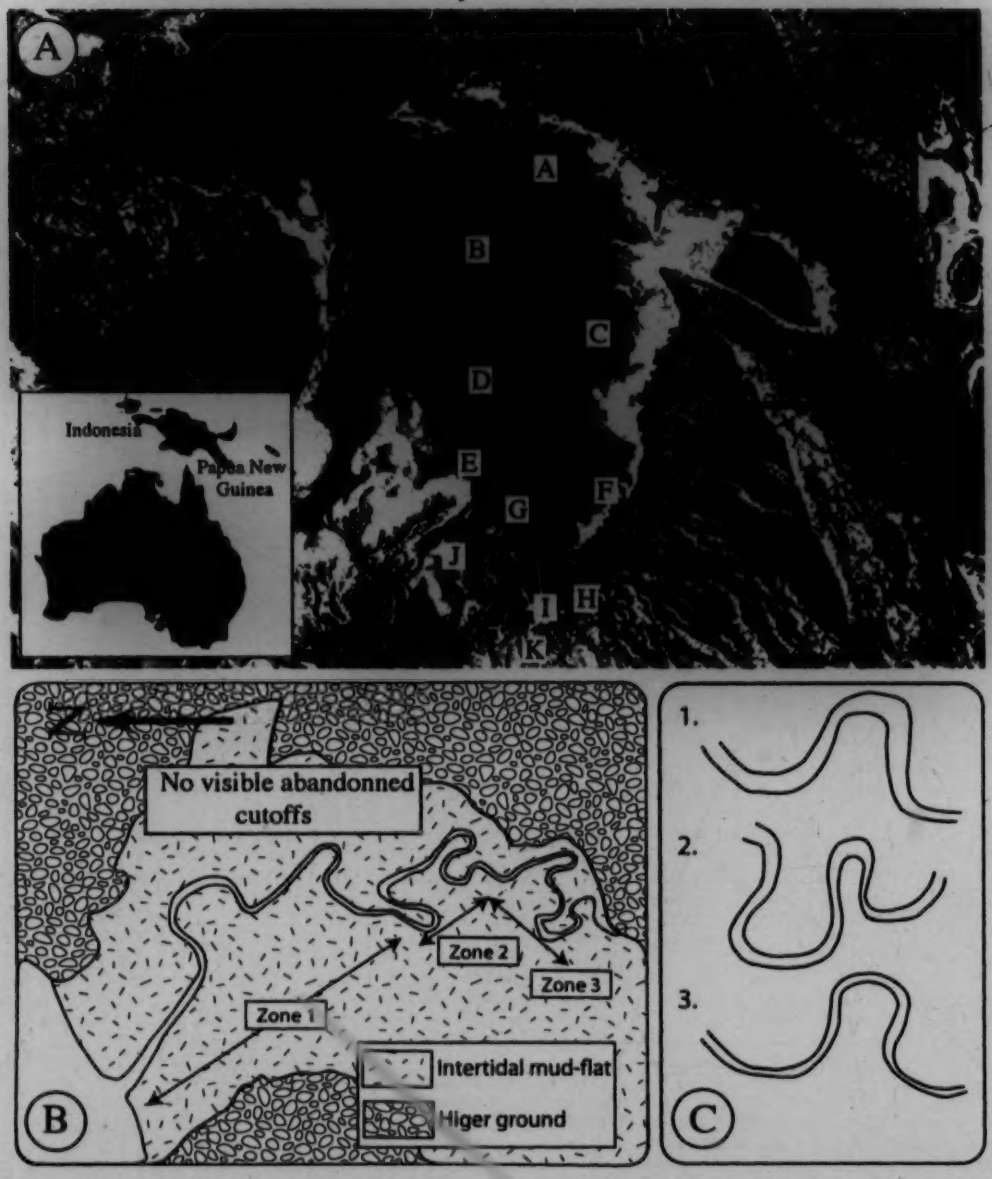

Figure 3-9. A. Location map of the King River, northern Australia (see inset). Letters indicate the channel segments from which measurments were collected. B. Schematic diagram depicting the King River. Note the absence of abandoned cut-offs despite the high degree of sinuosity. C.Schematic depicting the three morphological zones identified. See B. for their relative position within the estuary. (NASA).

3) The inner meander zone: characterized by higher sinuosities (average 1.8) than in the inner straight fluvial zones of the Ord and South Alligator rivers. The insides of all channel bends are rounded.

Fly River, Papua New Guinea

The Fly River is a large fluvial-dominated river that empties into the Gulf of Papua, located in southeast New Guinea (Figure 3-10). The Fly River and adjoining tributaries cover a catchment area of approximately 76000 km^2 and discharge between 3000 m^3/s and 7000 m^3/s of water into the Gulf of Papua (OK Tedi Mining Limited, unpublished data). As a result of mining, sediment inflow, the majority of which moves as suspended load into the estuary, is estimated to be 120 X 10^6 tons $year^{-1}$ (Wolanski *et al.*, 1995). The salt-water intrusion is limited to ~100 km from the mouth of the delta (Alongi *et al.*, 1992). Thus, for the purposes of this study, the Fly River represents a fluvially dominated end member and the majority of channel segments measured are situated in the fluvially-dominated environment.

Within the Fly River, the sinuosity values average a comparatively low 1.36 (Appendix 2). In general, sinuosity values (Figure 3-4d) increase upstream. Wavelength-to-amplitude ratios (Figure 3-5d) directly reflect changes in sinuosity values; increases in this ratio are accompanied by decreases in sinuosity values. The channel width (Figure 3-6d) of the Fly River decreases linearly landward and shows significant variability within the lower reaches.

The three morphological channel zones identified from the Fly River (Figure 3-10d) are:

1) Estuarine funnel: A funnel-shaped zone that displays an abrupt decrease in channel width upstream. Locally, channel bends exhibit a decrease in width, and abundant cuspate-shaped intervals are visible, characterized by alternating pointed channel banks (Figure 3-10c). Accretion deposits appear to be largely bank-detached, longitudinal bars that occupy the downstream portion of minor bends. Several of these bars are identified near the upper limit of this zone.
2) Bifurcating channel zone: this zone is characterized by channel meanders that were created by two open and active channels. Sinuosity values are difficult to discern because of this feature but values average less than 1.5. No abandoned cutoffs are visible and the insides of channel bends are dominantly rounded. Scroll bars are rare and are confined to upstream locations within this zone (Figure 3-10b).

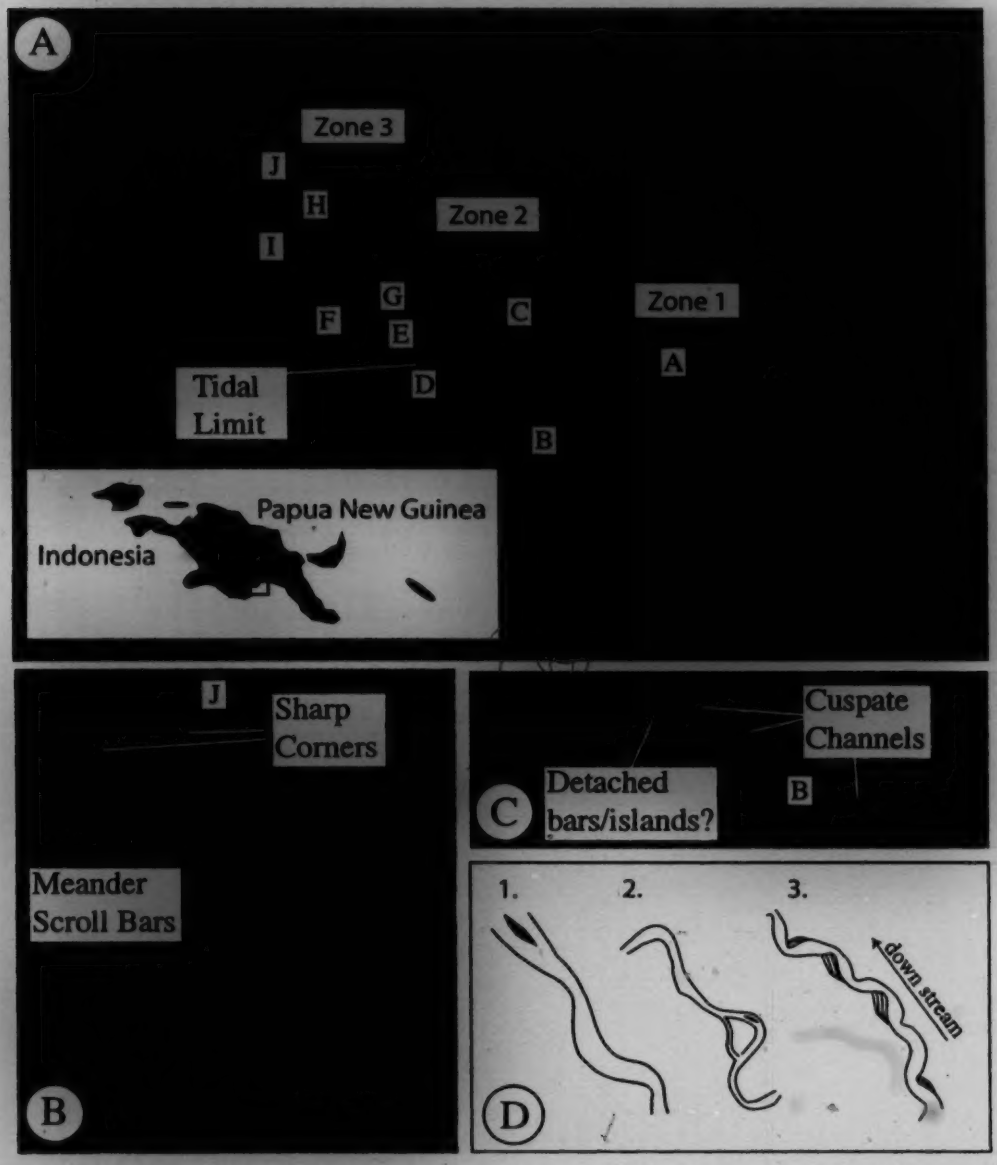

Figure 3-10. A. Location map of the Fly River, Papua New Guinea (see inset). Letters indicate the channel segments from which measurments were collected. B. Figure showing distribution of meander scroll bars and cuspate channels. C. Figure showing abundance of cuspate channel forms and detached bars near the mouth of the Fly River. D. Schematic depicting the three morphological channel zones identified from the Fly River. (NASA).

3) Meandering channel zone: characterized by comparatively high sinuosity (> 1.5) bends that preserve abundant meander scroll bars. Valley width is relatively narrow and may inhibit the channel from developing a more sinuous course. These meanders are consistent with the confined meanders described by Knighton (1984). Scroll bars preferentially migrate towards the estuary mouth and oblique to the valley axis. These bars maintain low curvature radii and the insides of channel bends are quite sharp (Figure 3-10b). Channel classes 2 and 3 are situated within the fluvial environment.

Rio Tuira, Panama

The Rio Tuira, located in eastern Panama (Figure 3-11a), is a tide-dominated estuary that drains into the Gulf of Panama. The course of the Rio Tuira exhibits a straight-meandering-straight sinuosity profile similar to other tide-dominated estuaries/ deltas examined within this study (Appendix 2, Figure 3-4e). The meander zone and inner straight zone occupy a comparatively shorter portion of the valley compared to the long, outer straight zone. Changes in the wavelength-to-amplitude ratio (Figure 3-5e) consistently oppose changes in sinuosity. Channel width decreases linearly from the river mouth to the upper limit of tidal influence (Figure 3-6e).

Three morphological channel zones are identified from the Rio Tuira (Figure 3-11c) and include:

1) Estuarine funnel/lower straight zone: a funnel-shaped segment characterized by sinuosity vales less than 1.7. Channel bends are cuspate and a large bend occurs near the upper limit of this class (Figure 3-11b). This particular bend hosts a large rounded island or bar with active channels open on either side. Accretion deposits are more visible within the upper reaches of this zone and are characterized by bank-detached and partially attached longitudinal bars.
2) The meander zone: this zone is characterized by a relatively uniform channel width and sinuosity values greater than 1.7. The insides of bends are rounded and accretion deposits occur as point bars (Figure 3-11b). No abandoned cutoffs or large scroll bars are observed within this zone.
3) Upper straight zone: this zone is characterized by estuarine meanders (cuspate) with sinuosities less than 1.7. Accretion deposits are longitudinal and may occur as fully or partially bank-attached, or detached. Comparison of modern satellite images and those obtained by Lewis and Macdonald (1970) reveals that limited (< ~200 m) migration and growth of these bars had occurred. Most bars have undergone little growth in the downstream direction. The bar upstream of channel

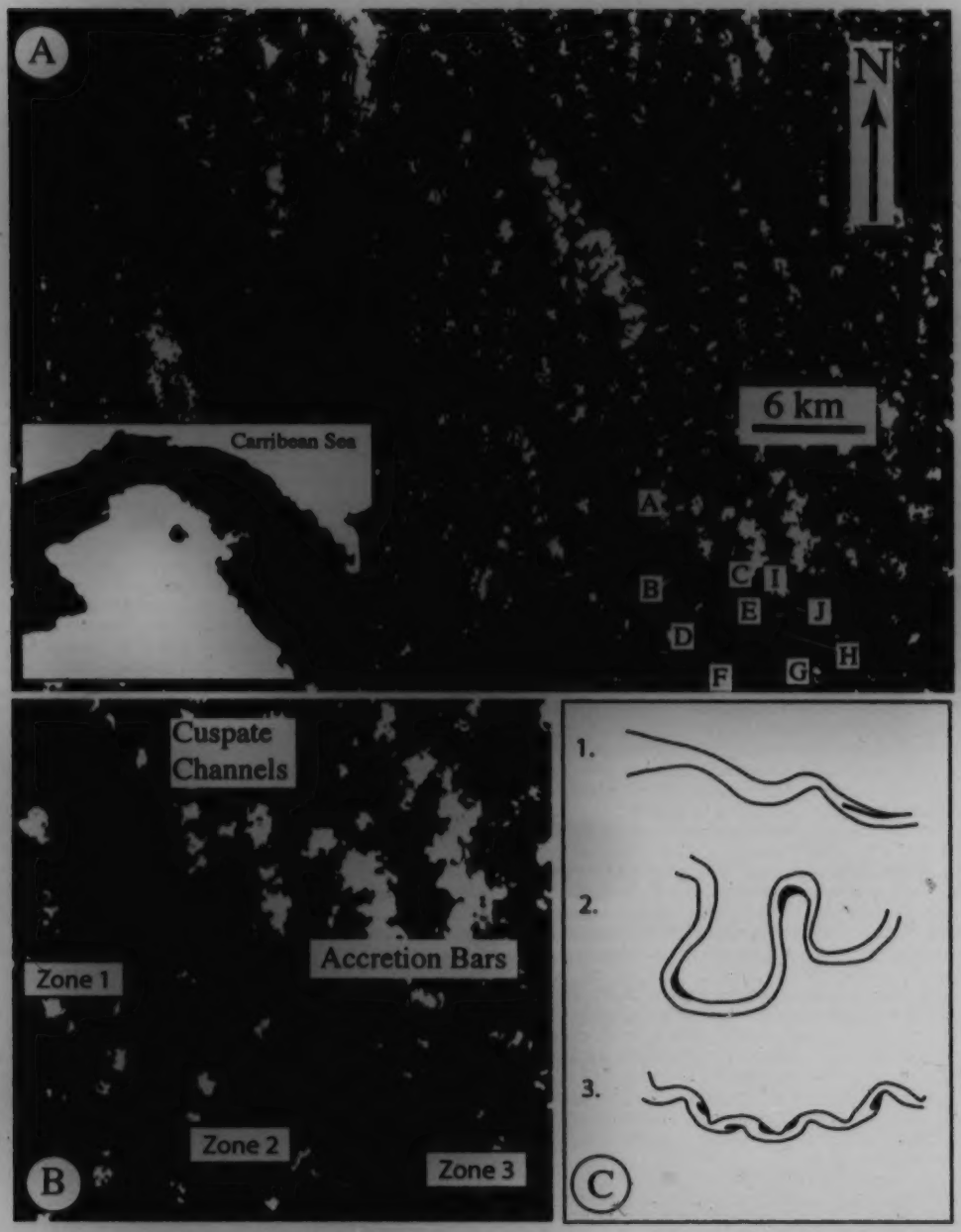

Figure 3-11. A. Location map of the Rio Tuira, Panama (see inset). Letters indicate the channel segments from which measurments were collected. B. Figure showing distribution of accretion deposits and cuspate channel forms relative to the high-sinuosity channel class. C. Schematic depicting the three morphological zones identified from the Rio Tuira. See B. for their relative position within the estuary. (NASA).

segment F, for example, maintains the same shape, is attached to the same position on the bank, and is only marginally longer.

Salmon River, Nova Scotia, Canada

The Salmon River (Figure 3-12) is a tide-dominated river that empties into Cobequid Bay, a subsidiary bay within the hypertidal Bay of Fundy, eastern Canada. Previous studies have identified a 'straight-meandering-straight' profile along the Salmon River from the estuarine mouth to the upper limit of tidal influence (Dalrymple *et al.*, 1992). The sinuosity measurements and profile (Appendix I; Figure 3-4f) support this morphological trend. In general, the meandering zone attains sinuosity values greater than 1.5, while the channels in the straight zones are characterized by sinuosities less than 1.5. The wavelength-to-amplitude ratio (Figure 3-5f) reflects these changes in sinuosity; major increases in this ratio are opposed by decreases in sinuosity. Channel width consistently decreases towards the upper limit of tidal influence (Figure 3-6f).

The three types of morphological zones identified from the Salmon River (Figure 3-12c) include:

1) Lower straight zone: this class is characterized by channel meanders with small sinuosity values (<1.6). The insides of bends are rounded and abundant alternate bars flank the banks of the channel. Long reaches of the river therefore appear to possess low sinuosity values at high water but these reaches host a relatively low-sinuosity channel that meanders in between the alternate bars (Figure 3-12b).
2) Meander zone: this class occurs over a small (<2 km) longitudinal valley distance and is characterized by channel bends that have sinuosity values greater than 1.6. The insides of bends are rounded and sediment accretion occurs as point bars. Channel width increases at the bends and, overall, remains more uniform than that of channels within the first class.
3) Upper straight channel zone: characterized by channel meanders with comparatively low sinuosity values (<1.6) and alternate bars attached to the banks (Dalrymple *et al.*, 1992).

Digul River, Indonesia

The Digul River estuary is located along the west coast of Indonesia (Figure 3-13a). It flows approximately 500 km from the Sterren Mountains and empties into the Arafura Sea. The sinuosity profile from the data collected displays a large high-sinuosity segment between channel segments D and H, which occupies a valley length of approximately 30 km. Abundant meander scroll bars are observed within

Figure 3-12. A. Location map of the Salmon River estuary, eastern Canada. B. Figure showing distribution of accretion deposits relative to the high-sinuosity channel class. Letters indicate the channel segments from which measurments were collected. C. Schematic depicting the three morphological channel zones identified from the Salmon River. (NASA).

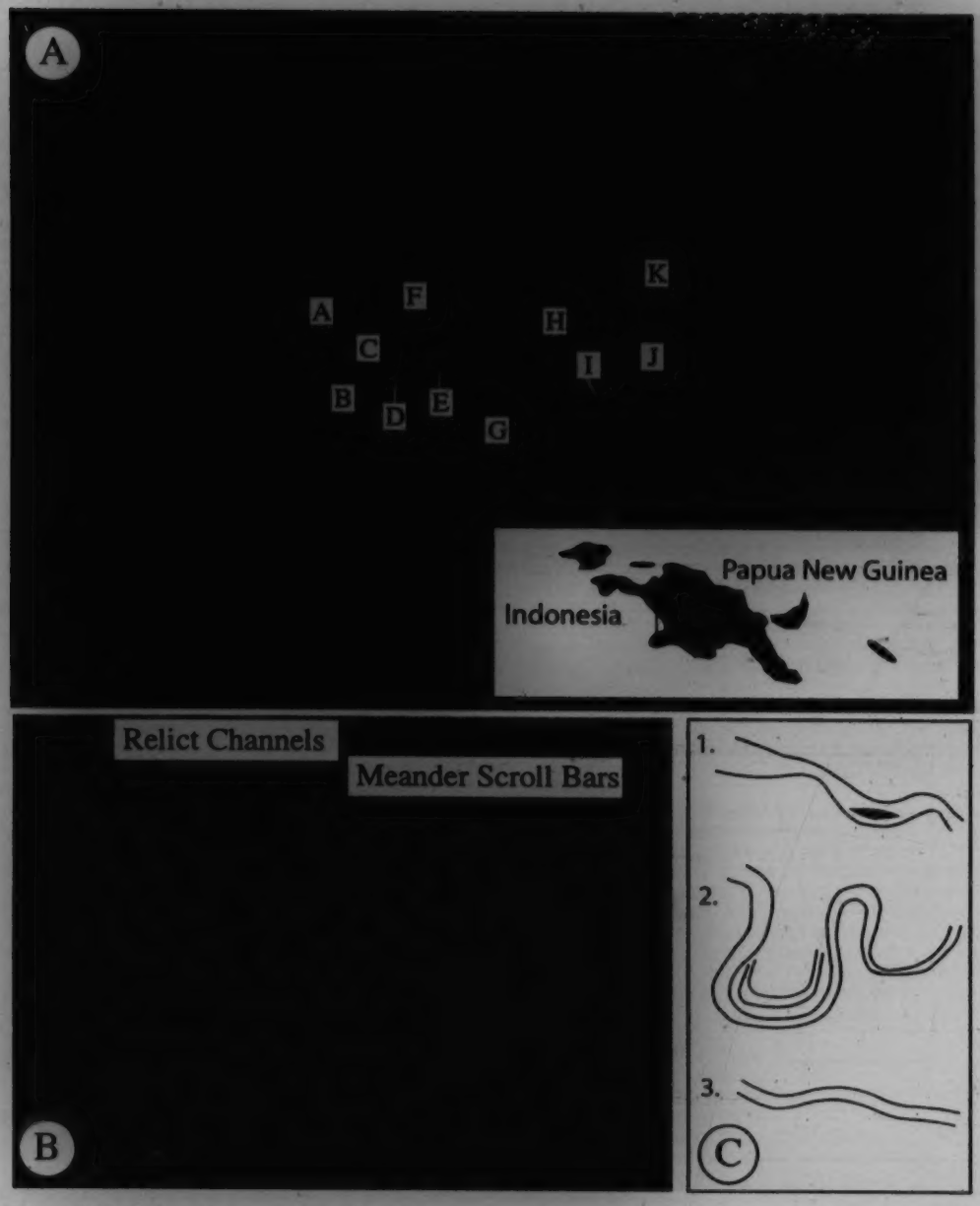

Figure 3-13. A. Location map of the Digul River estuary, Indonesia. Letters indicate the channel segments from which measurments were collected. B. Figure showing large meander scroll bars and abundant relict channels. C. Schematic depicting the three morphological channel zones identified from the Digul River. (NASA).

this zone which are bounded by low-sinuosity (< 1.8) channel segments upstream and downstream towards the mouth of the estuary. Increases in the wavelength-to-amplitude measurements are generally accompanied by a decrease in sinuosity (Figure 3-4g). The channel width of the Digul River decreases dramatically upstream from the mouth of the estuary (Figure 3-6g). Locally, however, channel width is highly variable, particularly along portions of the high-sinuosity channel segments.

Three morphological channel zones are identified within the Digul River (Figure 3-13c):

1) Estuarine funnel/lower straight zone: A funnel-shaped portion of the river with large, longitudinal, bank-detached tidal shoals accumulating proximal to minor channel bends. Upstream within the funnel zone, channel width begins to decrease rapidly. Channel bends typically maintain low-sinuosity (<1.8) values and cuspate forms. This portion of the estuarine and river valley, adjacent to the active channel, is host to abundant relict channels, most of which are remnants of straight and low-sinuosity channels.
2) Meander zone: this class is characterized by highly sinuous (>1.8) channel bends with large (approximately 5 km in length) meander scroll bars (Figure 3-13b). Channel width is highly variable within this class and displays a series of minor bends, or second order meanders. These bends, or kinks, have sharp insides of bends that appear to be asymmetrical in both the landward and seaward directions. This class occupies a relatively large portion of the valley, approximately 32 km in length.
3) Upper straight zone: this zone is characterized by low-sinuosity (<1.8) channels within a reach affected dominantly by fluvial processes. Accretion deposits are difficult to discern with available imagery.

Willapa River, Washington, U.S.A.

The Willapa River (Figure 3-14a) is a mesotidally-influenced river (tidal regime between 2 and 4 m) that drains into Willipa Bay, southwest Washington State, U.S.A. Willipa Bay is a wave-dominated estuary protected from the Pacific Ocean by a barrier spit. The channel is approximately 7 m deep at bankfull stages (Smith, 1988) and has an average width of approximately 160 m.

Measurements of channel sinuosity (Appendix 2) average 1.3, the lowest values in this study. The profile (Figure 3-4h), which is similar to that of several other profiles, shows a distinct tripartite zonation of sinuosity values with a high-sinuosity zone occurring between channel two low-sinuosity classes. These are separated from

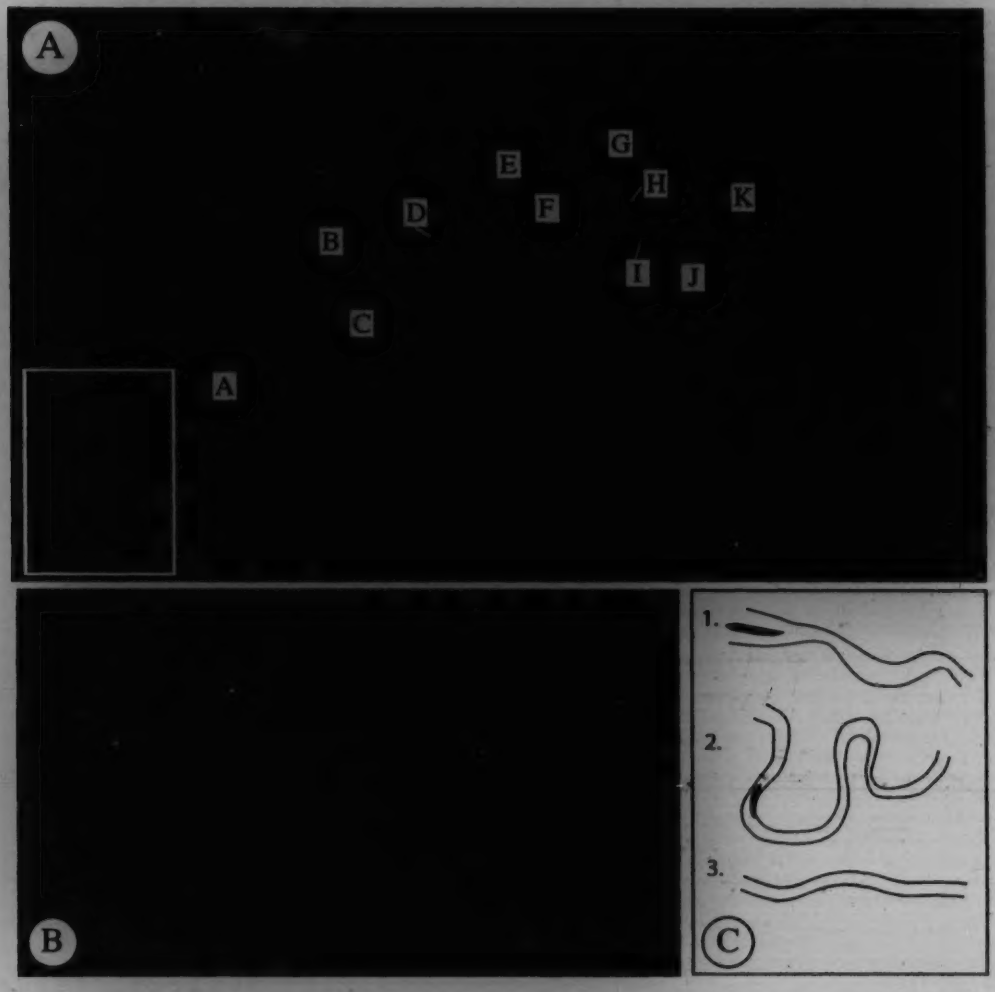

Figure 3-14. A. Location map of the Willipa River estuary, Washington, U.S.A. Letters indicate the channel segments from which measurments were collected. B. Figure showing cuspate channel forms and areas of IHS deposition (denoted by arrow). C. Schematic depicting the three morphological zones identified from the Willipa River. (NASA).

each other by a sinuosity of approximately 1.9. The wavelength-to-amplitude profile (Figure 3-5h) displays a direct relationship to the sinuosity profile; almost every decrease in sinuosity is met with a increase in wavelength-to-amplitude value. Channel width measurements (Figure 3-6h) within the middle, high-sinuosity class, show a minimal decrease between channel segments 8 and 10. More drastic decreases in channel width occur from the mouth of the estuary to this zone, and from the upper limit of this zone to the most upstream channel segment.

Three morphological zones are observed along the Willipa River (Fig. 3-14c) and include:

1) Lower straight zone: characterized by a low sinuosity (<1.9) channel that displays distinct cuspate channel architectures (Figure 3-14b). The landward extent of observed cuspate channel segments is within the upper limit of intertidal areas. Accretion deposits are not discernable from available imagery.
2) Meander zone: a high-sinuosity (>1.9) class with meanders similar to those within meander fluvial environments in which the insides of bends are well rounded. Accretion deposits are reported to occur as tidally-influenced, laterally accreted point bars that exhibit inclined heterolithic stratification (Smith, 1988) along the insides of meander bends. No distinct meander scrolls are observed within this class despite the presence of laterally accreting point bars along reaches with high sinuosity values.
3) Upper straight zone: a low-sinuosity (<1.9) class that persists to the upper limit of tidal influence. The insides of channel bends remain well rounded but accretion deposits are not visible on satellite images and are not reported.

Tillamook River, Oregon, U.S.A.

The Tillamook River (Figure 3-15a) drains into Tillamook Bay along the northeast coast of Oregon State, U.S.A. It has a small catchment area where fluvial input occurs as an ephemeral stream with virtually no input during the dry season. The Tillamook River at its upper limit is approximately 10 m wide. Bathymetry maps indicate that the depth at the mouth of the Tillamook River is approximately 7 m and approximately 3 m near the upper limit of tidal influence.

The sinuosity profile (Figure 3-4i) of the Tillamook River displays an overall increase to the most upstream channel segment examined with only a minor peak at segment 6. From available imagery, this trend extends approximately 450 m upstream before a less sinuous channel course is observed. At this point channel width is too small to measure with any degree of accuracy and as such, measured channel segments were

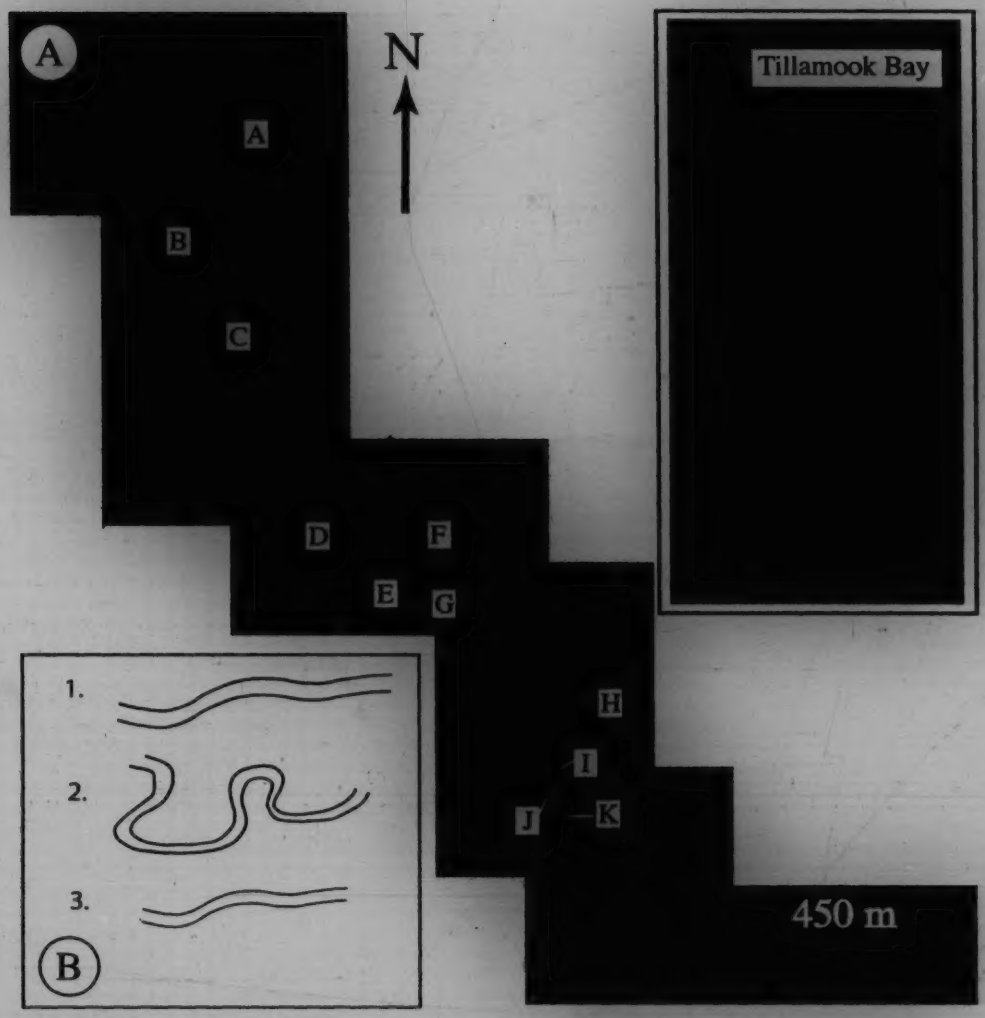

Figure 3-15. A. Location map of the Tillamook River, Oregon, U.S.A. Letters indicate the channel segments from which measurments were collected. B. Schematic depicting the three morphological zones identified from the Tillamook River. (NASA).

selected along portions of the river with an appreciable width. The meandering segment has sinuosity values greater than approximately 1.8 and occurs between segment 10 and the upper limit of the study. Channel width averages 22 m and the profile (Figure 3-6i) shows a steady decrease upstream. Channel width remains fairly uniform around and at channel bends and no meander scrolls are visible. Channel classes therefore represent simple forms and are distinguished from each other by sinuosity alone.

Three morphological zones that characterize the Tillamook River (Fig 3-15c), including:

1) Lower straight zone: this zone is characterized by channels with sinuosity values less than 1.8 and rounded insides of bends.
2) A meander zone, of which only the lowest channels bends are included in this study, with sinuosity values greater than 1.8.
3) An upper low-sinuosity channel zone that is otherwise not represented within this study. No abandoned cutoffs are observed within any reaches of the Tillamook and the styles of accretion deposits are difficult to discern with available imagery.

DISCUSSION

Estuarine Processes

This study examines the morphological characteristics of several tidally influenced channels, each developed within environments hosting variable tidal, fluvial, and topographic conditions. Some characteristics are common to almost all case studies as all of the channels are subjected to similar, but variable, estuarine processes. A brief discussion of tidal amplification, the asymmetry of ebb- and flood-tide components, and maximum tidal velocities is warranted as all of these processes influence the channel morphology and the size and shape of accretion deposits.

As the tide enters a bay along the pitch, the width-to-depth ratio increases and forces tides to increase landward. This process is known as tidal amplification. Landward, frictional forces overcome the effects of tidal amplification and the flood tides begin to diminish to the upstream tidal limit. Within the main channel of an estuarine system, this phenomenon initiates an asymmetry of the tidal cycle. Flood tides tend to maintain their highest velocities at mean water level between low and high tide. Conversely, ebb tides attain maximum strength between high and low tides. As a result, different localities within any particular channel are exposed to variable strengths and durations of flood and ebb tides. For example, Coleman and Wright (1978) document flood tides that persist for

only 2.5 hours some 42 km upstream of the mouth of the Ord river, northern Australia. The ebbing tide, in contrast, requires approximately 9.5 hours.

Estuarine meanders are best developed at locations where the strength of flood and ebb tides at mean water level is comparable (Ahnert, 1960). Both currents are also subject to centrifugal forces along the insides of down-current edges of the channel, the area where the channel attains its maximum erosive capabilities. Sedimentation occurs in areas farthest away from the lines of highest velocity, namely between the crossing points of ebb and flood currents (Ahnert, 1960). Accumulation of sediment in the areas subjected to phase shifting may occur as: partially bank-attached, flood-orientated deposits; partially bank-attached, ebb-orientated deposits; or as deposits fully detached from the channel bank when divergence of the ebb and flood tides is significant enough.

Channel Morphology

Despite the variability between the estuaries examined above, including tidal range, relative dominance of wave and tidal processes, and amount of fluvial discharge, all of these systems can be subdivided into three morphological zones. These characteristically display a straight-meandering-straight morphology, analogous to that described by Dalrymple *et al.* (1992), from the mouth of the river to the upper limit of tidal influence. Although the magnitude of sinuosity that subdivides the channels into high and low-sinuosity classes varies marginally between estuaries, the low-sinuosity classes generally maintain sinuosity values less than approximately 1.7. The magnitude of sinuosity in the high-sinuosity classes ranges from 1.7 up to 3.5. The King and Digul rivers have the most sinuous courses.

Several sedimentary deposits characterize the outer straight zone, including tidal sand bars, confined to the funnel portion of the estuary, partially or completely detached bars, and bank-attached bars. The tidal sand bars can range in size from 100's of meters in length, such as in the Rio Tuira, to several kilometers in length, such as in the Fly, Ord, and Digul rivers. They are linear features in tide-dominated systems and are orientated parallel to the channel axis. Flood-or ebb-orientated sedimentary structures may dominate the shoals depending on the position of the bars with respect to the dominant flood-and ebb-channels (Wright *et al.*, 1975). The other deposits, concentrated within the transition zone from outer estuary to the middle estuary, also maintain sinuosity values less than 1.7. These deposits can be 100's of meters in length and are orientated parallel to the channel. The width of these deposits is generally small, presumably kept in check by the adjacent active channel. Some accretionary bars are approximately 60 m in width

(Salmon River, Figure 3-12) to approximately 100 m such as within the Rio Tuira (Figure 3-11).

Deposits within the sinuous channel class include point-bar deposits that closely resemble fluvial pointbars. Within this study the sinuosity values of pointbars exceed 1.7 but the width can be highly variable. In the Digul River the width of a meander-belt deposit can reach approximately 5 km. Conversely, point bars along the Willapa River occur on the scale of 10's of meters. This may be largely controlled by the width of the meander belt and, hence, the lateral distance within which a channel is permitted to migrate. Despite the high degrees of sinuosity within many of the case studies examined, relatively few abandoned cutoffs are observed. This may be constrained by the valley width or may be due to low migration rates of these sinuous channels. Meander scroll bars are the result of fluvially-dominated conditions, such as those developed within the Digul and Ord rivers. The combination of ebb runoff and strong fluvial currents results in preferential erosion on the cutbank. Flood tides may not be strong enough to reduce the degree of erosion and lateral migration of the channel. Some meander zones that develop in tide-dominated environments lack scroll bars. The King River, for example, despite having the largest sinuosity values obtained, has no observed or documented meander cutoffs (Coleman and Wright, 1978). Tidal mud flats likely minimize erosion along the channel cutbank and prevent the channel from notable migration.

The thickness of these deposits is largely unknown from available data but studies of the Ord River indicate that the bars in this transition zone and in the highly sinuous channel segments may average 12 m in thickness (Coleman and Wright, 1978). Accretion deposits with thicknesses in excess of 20 m, such as those described from the McMurray Formation (Mossop and Flach, 1983) and the Kootenai Formation (Hopkins, 1985) remain very rare. Conversely, 12 m thick deposits are common in extreme tidal ranges, and within meander-belt deposits with an average lateral width of 10 km (Coleman and Wright, 1978).

The relative valley length occupied by each shape class is also quite variable. For example, along the Tillamook River the high-sinuosity shape class occupies only a very small proportion of the total valley length (approximately 450 m of the total 4 km of valley length examined). Conversely, the high-sinuosity channel class along the Digul River estuary occupies a valley length almost 25 km long within the 50 km examined.

Channel Width Variation

Channel width variation along the rivers examined shows some consistencies between depositional systems. The cuspate channel form of Woodroffe *et al.* (1989),

analogous to the estuarine meanders discussed by Ahnert (1960), are prevalent in many of the systems examined but not in the same geographic position with respect to the mouth of the estuary. They are present in both the upper and outer low-sinuosity reaches of the Rio Tuira, within the outer reaches of the Fly, Ord, and Willipa rivers, and within the inner reaches of the South Alligator River. The Digul River bears no prominent cuspate channels but the secondary meanders along the highly sinuous reach maintain sharp inner boundaries and exhibit slight swelling of channel width between these bends. No such channel form is observed along the Tillamook, Salmon, and King rivers. One notable influence that is lacking within these three systems and is prominent in the others is significant volumes of fluvial discharge, or at least in comparison to the volume of water within the tidal prism. The Ord River, for example, maintains an average riverine discharge of 163 m^3, which is only a small fraction of water compared to the volume within the tidal prism, estimated at 1.02×10^9 m^3 at the mouth of the Ord River (Wright *et al.*, 1975). This is a significantly higher proportion of freshwater input than the King River receives. There is almost negligible fluvial input here, as well as the Tillamook River. The Salmon River has slightly more freshwater input throughout the year but must compete with the extreme volumes of water transported in the tidal prism of the Cobequid Bay under supratidal conditions.

Estuarine meanders form in segments of the river where flood and ebb tides are out of phase with each other or where an appreciable difference exists between the velocity of flood-orientated currents and ebb-orientated currents (Figure 3-2). Flood-tide currents erode opposing banks to those of the ebb-tide currents thus generating angular, pointed channel bends. This may explain why cuspate channels are observed both upstream and downstream of the highly sinuous channel segments. Seaward of this class, ebb currents maintain appreciably greater velocities than those recorded near the landward limit of tidal influence owing to the greater amount of time for ebb current to gain momentum. Landward of the high-sinuosity class, increased fluvial input may offset the flood currents enough to form these cuspate forms.

Underlying Sediment Composition

Sediment composition no doubt plays some role in the erosion trends of channel incision. For example, sandy sediments that are present within an overall muddy system will be preferentially exhumed. Also, where mud concentrates on a point bar in the highly sinuous channel zone is the area expected to host IHS deposits (Smith, 1988; Dalrymple *et al.*, 1992). Smith (1988) reported that mean grain size becomes finer upstream and up-section along the Willapa River. If this trend in grain size persists in other localities

(i.e. where the upstream side of point bars are likely to accumulate more mud) then the upstream side is also more likely to be armored from incising channels from above. In other words, preferential incision may take place on the downstream side of underlying channel successions. If intitiation of these overlying channels occurs on the down-dip side, there should be a preservational bias of dip-direction between stacked channels.

Stratigraphic Implications

Several authors have examined the stratigraphic relationships that evolve from estuary initiation to estuary filling with respect to morphological differences in channel types (Allen, 1991; Dalrymple *et al.*, 1992; Woodroffe *et al.*, 1989). Conceptually, initial incision of the paleovalley at lowstand conditions results in the base of the paleovalley being demarcated by fluvial deposits. Following the end of lowstand conditions, the estuary will be subjected to transgression causing translation of the estuary and the estuarine sub-environments landward. In tide-dominated settings, these sub-environments include tidal sand bars, outer-straight tidal-dominated meanders, tidal meanders, and inner-straight tidal-fluvial channels. As transgression continues and the estuary begins to fill, progradation of these sub-environments may persist causing tidal sand bars to erosionally overlay fluvial sediments. Low-sinuosity accretion deposits, formed in the outer-to-middle estuary transition zone, will directly overlay these sand bars during-regression. Superimposed on these will be high-sinuosity accretion deposits formed as pointbars. These transgressive-regressive sequences are well documented from the Gironde estuary (Allen, 1991). Dalrymple *et al.* (1992) suggested that IHS deposits are more likely to develop in this zone as it represents a pronounced zone of mixing of tidal and fluvial sediments.

Both the transgressive and progradational successions may be preserved but the fluvial-estuarine facies have higher preservational potential seaward of the landward limit of shoreline highstand. This is due to the removal of fluvial-estuarine facies during transgression of the shoreline, represented as a ravinement surface. The filling stages and progradation of estuarine facies are shown in Figure 3-16.

McMurray Formation Paleochannels

The first attempts of paleochannel reconstruction of the channel units in the McMurray Formation were completed on the Type Section along the banks of the Athabasca River (Mossop and Flach, 1983; Flach and Mossop, 1985). Here, a 25 m thick point bar was interpreted with a channel sinuosity of 1.6 and an estimated channel width, based largely on accretion deposit thickness, of 250 m. Dip meter log data was also used

to interpret channelized successions of the McMurray Formation. Cuddy and Muwais (1989) and Muwais and Smith (1990) interpreted amalgamated channel units, reaching cumulative thicknesses of 25 to 30 m from the McMurray Formation. Each genetic unit ranged in thickness from 6 to 12 m and was distinguished from underlying units by abrupt changes dip-meter azimuth or dip magnitude.

Two varieties of channel forms were reported based on vertical trends in dip meter values. These include laterally accreting and vertically accreting channels. Muwais and Smith (1990) suggest that the dip angles in laterally accreting channels increase upwards but vertically accreted channels, conversely, are characterized by decreasing dip angles upwards (Figure 3-17). In addition, several types of stacking patterns were reported. In some instances three laterally accreted channel units were superimposed, and in other cases amalgamated successions were characterized by a lower, laterally accreted channel at the base and one or more vertically accreting channels above. Vertically accreting channels were not reported underlying the laterally accreted units. The vertically accreting channels were interpreted to represent the vertical accretion of fine-grained sediments such as in those channels described by Schumm (1960).

The McMurray Type Section, as discussed in Chapter 2, hosts very uniform dipping channel deposits invoking the interpretation that it represents a large, single point bar. However, a cross-sectional view of the Type Section within a small gulley entering the Athabasca River, revealed bounding surfaces separating discrete genetic units 6-10 m thick (Figure 2-15). Several erosional truncations were apparent as well as surfaces where separate channel units onlap underlying strata. Other outcrop sections around the Fort McMurray area host uniformly dipping stacked channel deposits similar to those along the Type Section. These include a Christina River outcrop section (Figure 2-16) and an outcrop within the Northmine site at Syncrude (Figure 2-17).

Of the nine estuaries examined in this study, the deposits that are most analogous to the McMurray Formation outcrops are those from the Digul River and the Ord River, both of which are tide-dominated deltaic depositional systems. The middle estuary hosts high sinuosity point bars with large meander scroll bars. Internal disconformities within the Type Section outcrop of the McMurray Formation are interpreted to represent growth stages of a single pointbar, much like the meander scroll bars within the high-sinuosity channel zone of the Ord and the Digul Rivers (Figure 3-8b, 3-13b). Migration and rotation of the channel seaward produces genetic units that truncate units below. Newly developed scroll bars would also show onlapping relationships with the channelized units below. Both of these features are observed within the Type Section outcrop. Commonly the dip angle between individual genetic units diminishes upward. This is observed

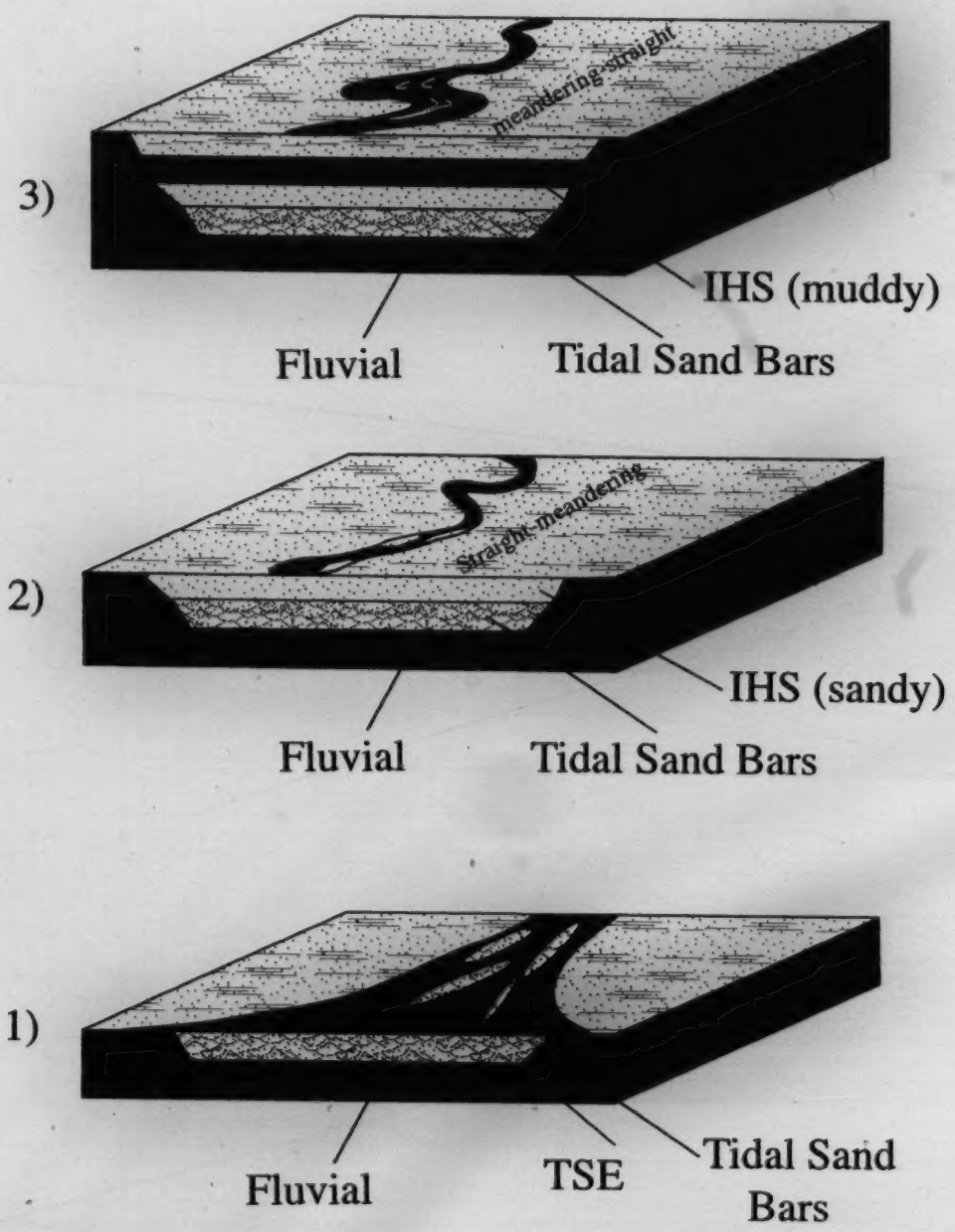

Figure 3-16. Schematic representation of the development of variable stacked channels during progradation. 1. Deposition of tidal sand bars within the outer estuary (lower McMurray equivalent). 2. Deposition of sandy, low-sinuosity bars within the outer-to-middle estuarine transition. 3. Deposition of sandy-to-muddy IHS point bars as the high sinuosity class progrades over the seaward low sinuosity class.

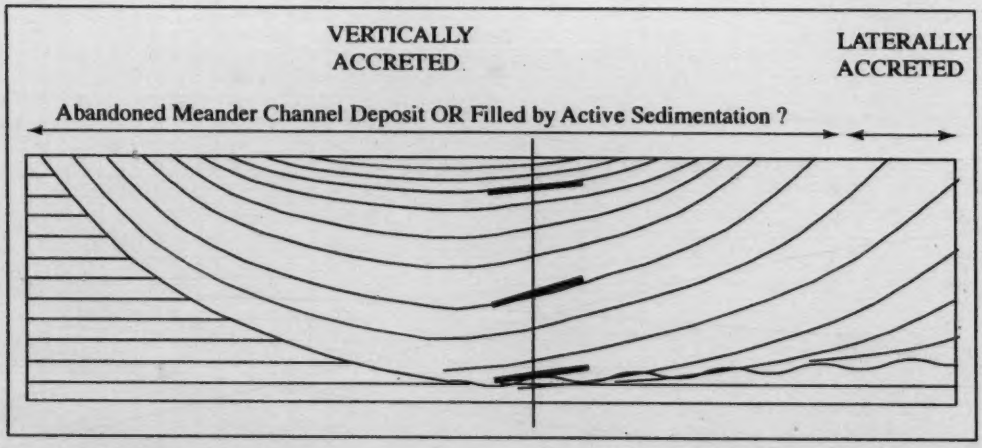

Figure 3-17. Schematic illustration showing how a dip angle profile can increase upwards during lateral accretion (lowermost fill), as well decrease upwards within a vertical accretion fill (uppermost fill) (modified from Muwais and Smith, 1990).

within the Northmine site at Syncrude (Figure 2-17) and within outcrops along the Christina River (Figure 2-16).

SUMMARY

The nine estuaries examined within this study comply with the straight-meandering-straight model coined by Dalrymple *et al.* (1992). Distinct accretion deposits occur within the outer, middle, and inner estuary zones. These include tidal shoals and detached sand bars within the funnel and transition zone to the middle estuary, point bars within the middle estuary, and low sinuosity bank-attached and partially detached bars within the upper estuary. Meander scroll bars are notably absent in high sinuosity zones that are dominated by tidal energy; this is achieved when fluvial input is negligible or when the tidal prism is orders of magnitude larger than existing fluvial input. Jones *et al.* (1993) recognize high sinuosity channels in the zone of interaction of fluvial and tidal processes corroborating this generalization. Lateral migration is also reduced when the host sediment is mud-dominated such as in the King River.

The Type Section of the McMurray Formation hosts a uniformly dipping succession of stacked genetic units of IHS. These have previously been interpreted to develop as meander scroll bars within a high sinuosity channel (Flach and Mossop, 1985). Subtle truncations of 6 to 10 m thick genetic units of IHS are interpreted to be the result of periodic growth stages of a channel within the meandering channel zone of

a tide-dominated estuary. This succession progrades over large-scale planar tabular bars hosting abundant tidal indicators such as sigmoidal bedding, grain striping, and brackish water traces fossils. These are deposited as outer estuarine tidal shoals.

REFERENCES

Ahnert, F. 1960. Estuarine meanders in the Chesapeake Bay area. Geographical Review, v. 50, p. 390-401.

Allen, G. P. 1991. Sedimentary processes and facies in the Gironde estuary: a Recent model of macrotidal estuarine systems. *In*: Smith, G.D., Reinson, G.E., Zaitlin, B.A. (eds). Clastic Tidal Sedimentology: Canadian Society of Petroleum Geologists Memoir 16, p. 29-40.

Alongi, D.M., Christofferson, P., Tirendi, F., and Robertson, A.I. 1992. The influence of freshwater and material transport on sedimentary facies and benthic processes within the Fly Delta and adjacent Gulf of Papua (Papua New Guinea). Continental Shelf Research, v. 12, no. 2/3, p. 287-326.

Coleman, J.M., and Wright, L.D. 1978. Sedimentaion in an arid macrotidal alluvial river system: Ord River, western Autralia. Journal of Geology, v. 86, p. 621-642.

Cuddy, R.G. and Muwais, W.K. 1989. Channel-fills in the McMurray Formation: their recognition, delineation, and impact at the Syncrude Mine. Canadian Institute of Mining and Metallurgy Bulletin, 82, p. 67-74.

Dalrymple, R.W., Zaitlin, B.A., and Boyd, R. 1992. Estuarine facies models: Conceptual basis and stratigraphic implications. Journal of Sedimentary Petrology, v. 62, p. 1130-1146.

Flach, P.D and Mossop, G.D. 1985. Depositional environments of Lower Cretaceous McMurray Formation, Athabasca oil sands, Alberta. American Association of Petroleum Geologists Bulletin, v. 69, no. 8, p. 1195-1207.

Gurnell, A.M. 1997. Adjustments of river channel geometry associated with hydraulic discontinuities across the fluvial-tidal transition of a regulated river. Earth Surface Processes and Landforms, v. 22, p. 967-985.

Hopkins, J.C. 1985. Channel-fill deposits formed by aggradation in deeply scoured, superimposed distributaries of the lower Kootenai Formation (Cretaceous). Journal of Sedimentary Petrology, v. 55, p. 42-52.

Huang, H.Q., and Warner, R.F. 1995. The multivariate controls of hydraulic geometry: a casual investigation in terms of boundary shear distribution. Earth Surface Processes and Landforms, v. 20, p. 115-130.

Jones, B.G., Martin, G.R., and Senapati, N. 1993. Riverine-tidal interactions in the monsoonal Gilbert River fandelta, northern Australia. Sedimentary Geology, v. 83, p. 319-337.

Knighton, D. 1984. Fluvial Forms and Processes. Edward Arnold, London. 218 p.

Lewis, A.J., and MacDonald, H.C. 1970. Significance of estuarine meanders identified from radar imagery of eastern Panama and northwestern Columbia. Modern Geology, v. 1, p. 187-196.

Mossop, G.D. and Flach, P.D. 1983. Deep channel sedimentation in the Lower Cretaceous McMurray Formation, Athabasca, Alberta. Sedimentology, v. 30, p. 493-509.

Muwais, W., and Smith, D.G. 1990. Types of channel-fills interpreted from dipmeter logs in the McMurray Formation, northeast Alberta. Bulletin of Canadian Petroleum Geology, v. 38, p.53-63.

NASA, Nasa's Earth Science Enterprise Scientific Data Purchase Program, produced by Earth Satellite Corporation, https://zulu.ssc.nasa.gov/mrsid/. 2004.

OK Tedi Mining Limited: http://www.oktedi.com/community/flyRiverSystem.php. 2004.

Schumm, S.A., 1960. The effect of sediment type on the shape and stratification of some modern fluvial deposits. American Journal of Science, v. 258, p. 177-184.

Smith, D.G. 1988. Modern point bar deposits analogous to the Athabasca oil sands, Alberta, Canada. *In:* Tide-influenced sedimentary environments and facies. P.L. de Boer, A. van Gelder, and S.D. Nio (eds.). D. Reidel Publishing Co., The Netherlands, p. 417-432.

Wolanski, E., King, B., and Galloway, D. 1995. Dynamics of the Turbidity Maximum in the Fly River Estuary, Papua New Guinea. Estuarine, Coastal, and Shelf Science, v. 40, p. 321-337.

Woodroffe, C.D., Chappell, J., Thom, B.G., and Wallensky, E., 1989. Depositional model of a macrotidal estuary and floodplain, South Alligator River, northern Autralia. Sedimentology, v. 36, p. 737-756.

Wright, L.D., Coleman, J.M., and Thom, B.G., 1973. Processes of channel development in a high-tide range environment: Cambridge Gulf-Ord River delta, western Australia. Journal of Geology, v. 81, p. 15-41.

Wright, L.D., Coleman, J.M., and Thom, B.G., 1975. Sediment transport and deposition in a macrotidal river channel: Ord River, western Australia. *In*: Estuarine Research, v. II, p. 309-321, New York, Academic Press.

CHAPTER 4.
SUMMARY AND CONCLUSIONS

1. A progradational relationship between facies associations is observed at the Type Section and the Fort Mackay outcrops. This includes the erosional truncation of outer estuarine dunes of Facies G by middle estuarine IHS facies successions (Facies A to F).
2. Internal disconformities within the succession of IHS deposits at the Type Section outcrop are interpreted as growth stages that developed within a single channel deposit. Upward-decreasing dip angles of genetic IHS units and the tendency of IHS successions to fine upwards across these disconformities (within several outcrop successions) support this interpretation.
3. Three geomorphologic zones were identified that characterize channel types within modern, tidally-influenced settings. These include an outer straight zone, a middle meandering zone, and an inner straight zone. Other noteworthy observations include the following:
    a) Tidally-influenced reaches maintain lower sinuosity values than their fluvial counterparts.
    b) Point bar length in tidally-influenced reaches can locally exceed 150 m.
    c) Only rare channel abandonments, or oxbow lakes, are observed within tidally influenced channel reaches.
    d) Large meander scroll bars are observed in systems with comparatively high fluvial input, such as the Ord River and Digul River systems.

Appendix 1. Legend for outcrop descriptions and outcrop strip log data

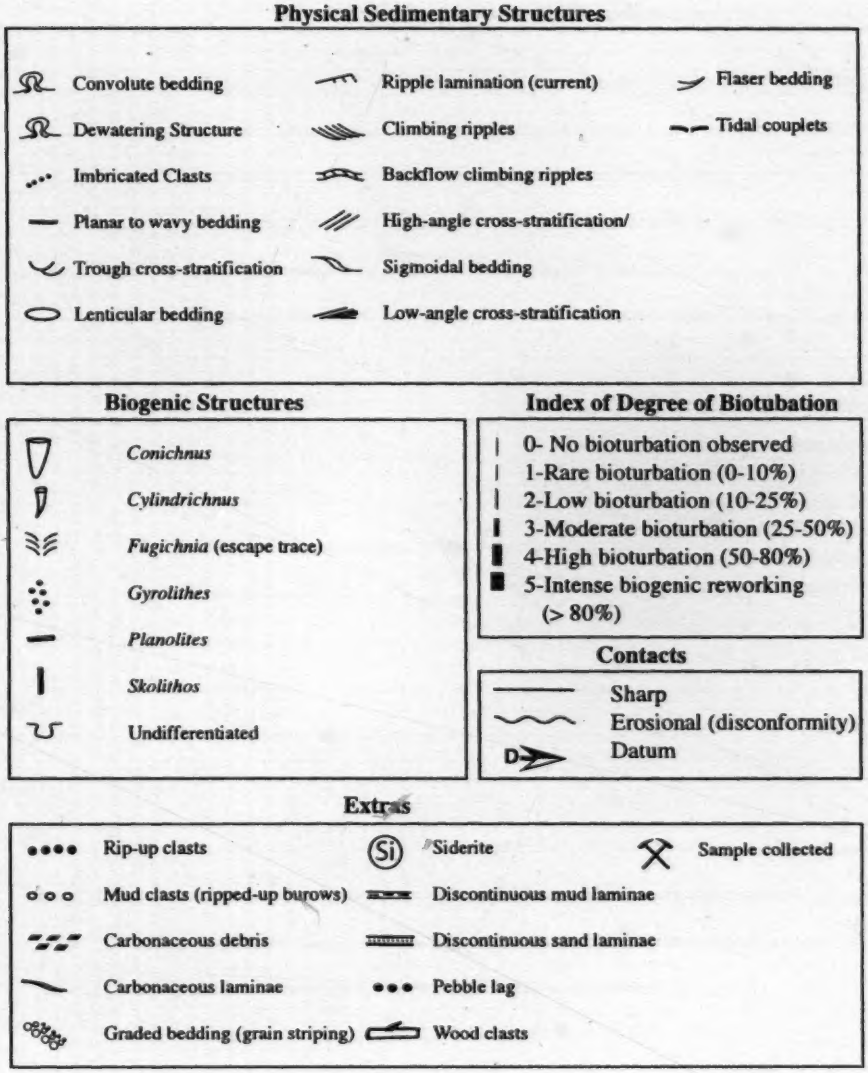

1. Strip Log A from the Amphitheatre outcrop near Fort McKay, Alberta.

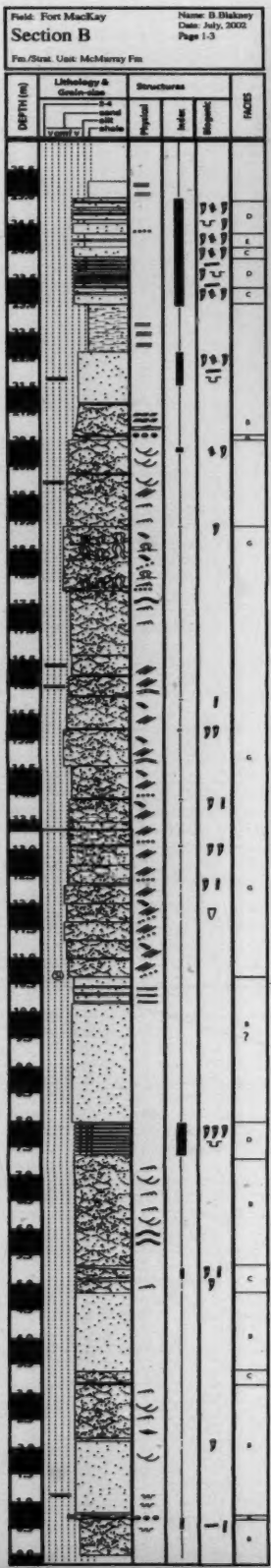

2. Strip Log B from the Amphitheatre outcrop near Fort McKay, Alberta.

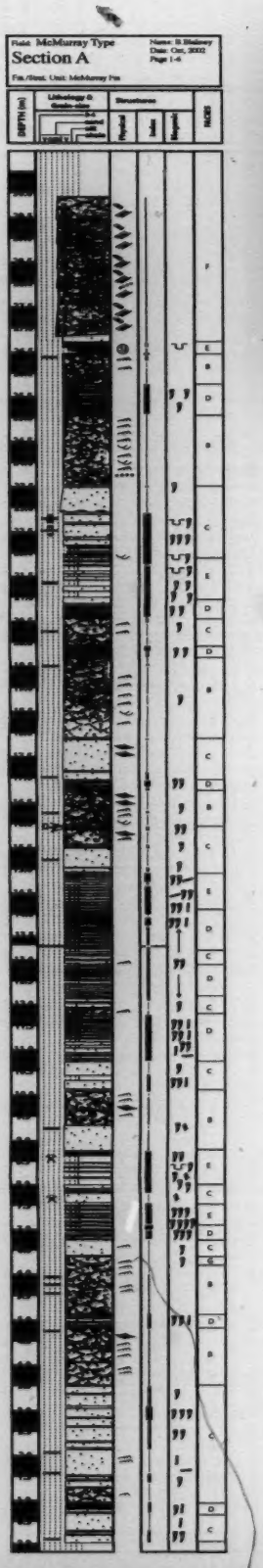

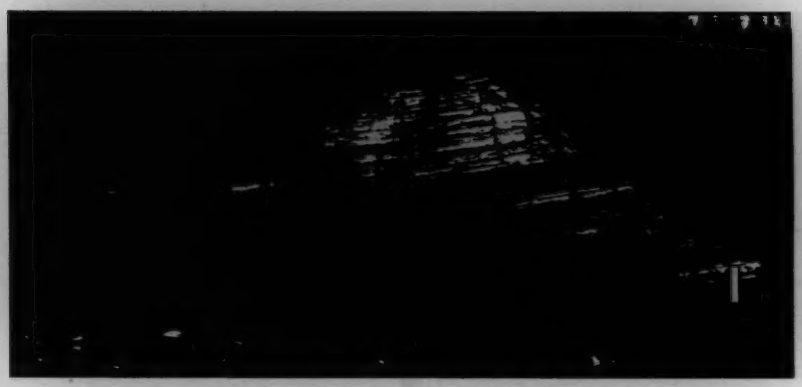

3. Strip Log A from the Type Section outcrop near Fort McMurray, Alberta.

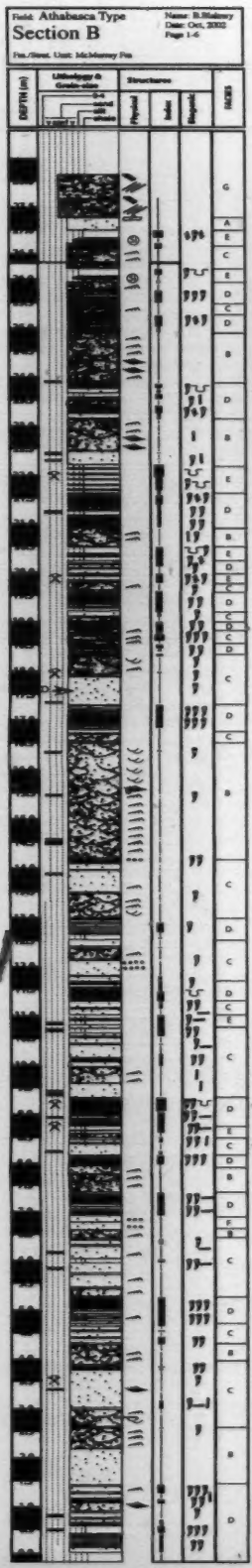

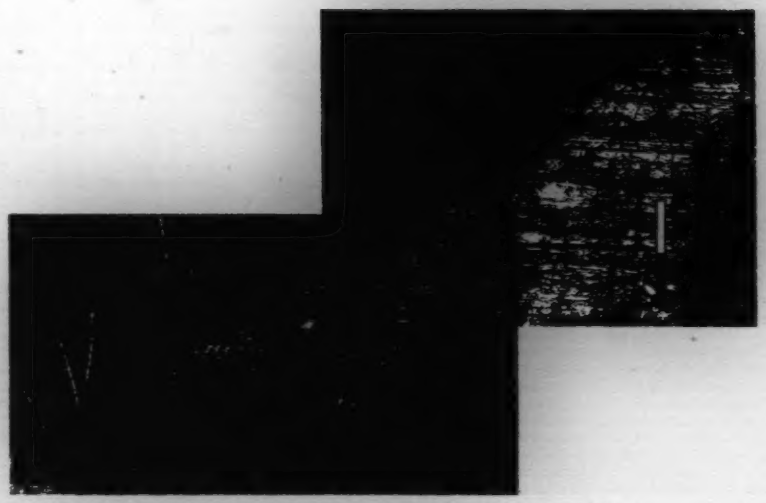

4. Strip Log B from the Type Section outcrop near Fort McMurray, Alberta.

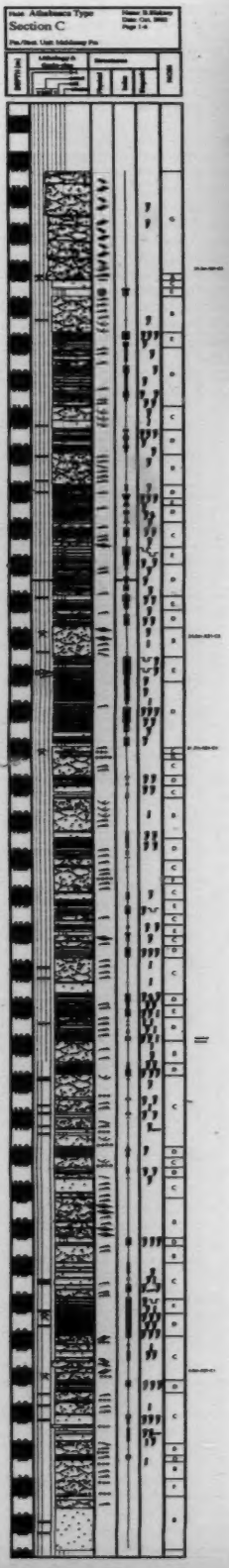

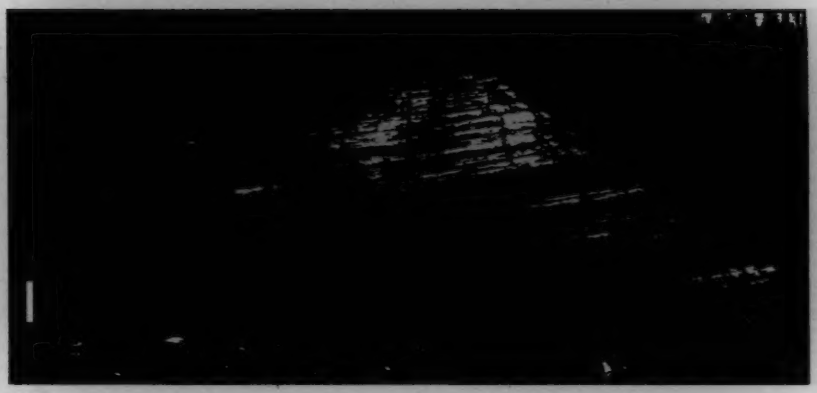

5. Strip Log C from the Type Section outcrop near Fort McMurray, Alberta.

Appendix 2. Sinuosity, wavelength, amplitude, and channel-width calculations of modern estuarine environments

Location	Channel Width	Amplitude	Wavelength	Wave/Amp.	Sinuosity
	km	km	km		
King River, northern Australia					
A)	0.163	2.100	2.113	1.006	1.90
B)	0.319	1.688	4.350	2.578	1.30
C)	0.238	1.238	2.125	1.717	2.20
D)	0.147	0.463	3.000	6.486	1.06
E)	0.147	1.988	0.800	0.403	3.42
F)	0.134	1.625	0.850	0.523	3.49
G)	0.247	0.625	1.413	2.260	1.41
H)	0.219	1.000	1.188	1.188	2.15
I)	0.178	0.788	1.450	1.841	1.54
J)	0.238	1.250	0.788	0.630	2.25
k)	0.144	0.900	1.563	1.736	1.61
				average	
Ord River, northern Australia					
A)	0.905	1.688	3.278	1.942	1.12
B)	0.605	1.125	3.156	2.804	1.33
C)	0.561	2.299	2.544	1.106	1.58
D)	0.294	1.223	1.663	1.360	1.43
E)	0.135	0.563	2.960	5.261	1.03
F)	0.159	1.370	5.113	3.732	1.30
G)	0.110	4.379	6.067	1.385	2.07
H)	0.092	4.403	4.403	1.000	2.63
I)	0.171	3.156	5.333	1.690	1.42
J)	0.165	1.223	9.010	7.440	1.06
k)	0.061	1.981	4.550	2.296	1.06
				average	

South Alligator River, northern Australia					
A)	0.933	2.899	6.196	2.138	1.14
B)	0.664	1.775	8.659	4.878	1.14
C)	0.462	2.210	3.804	1.721	2.18
D)	0.489	1.739	5.435	3.125	1.88
E)	0.684	2.391	2.899	1.212	2.18
F)	0.738	2.572	2.681	1.042	1.65
G)	0.688	1.178	3.659	3.108	1.13
H)	0.639	1.268	3.062	2.414	1.18
I)	0.521	1.214	3.025	2.493	1.47
J)	0.240	1.449	3.279	2.263	1.18
k)	0.272	1.178	2.428	2.062	1.69
L)	0.036	1.051	1.377	1.310	1.82
				average	
Rio Tuira, Columbia					
A)	0.608	2.197	3.870	1.762	1.72
B)	0.401	1.386	5.341	3.854	1.06
C)	0.393	1.876	2.721	1.450	1.74
D)	0.254	1.487	2.941	1.977	1.29
E)	0.325	1.707	1.741	1.020	1.89
F)	0.279	1.538	1.217	0.791	2.36
G)	0.309	0.879	1.403	1.596	1.87
H)	0.225	0.423	1.149	2.720	1.15
I)	0.194	0.693	1.200	1.732	1.71
J)	0.186	0.879	1.403	1.596	1.93
				average	

Digul River Estuary, Papua-New Guinea					
A)	1.543	0.848	0.841	0.991	1.90
B)	1.247	0.462	0.955	2.066	1.42
C)	1.032	0.242	0.826	3.406	1.11
D)	0.912	0.220	0.773	3.517	1.08
E)	0.931	0.947	0.992	1.048	3.77
F)	1.399	0.833	0.985	1.182	3.42
G)	1.208	1.288	2.591	2.012	3.42
H)	0.970	1.220	1.432	1.174	2.70
I)	0.129	0.174	1.068	6.130	1.57
J)	0.091	0.311	1.826	5.878	1.12
K)	0.081	1.114	1.553	1.395	1.73
				average	
Fly River Estuary, Papua-New Guinea					
A)	4.264	12.930	53.026	4.101	1.08
B)	4.419	18.638	37.758	2.026	1.36
C)	2.975	16.781	33.838	2.016	1.20
D)	0.928	4.195	15.887	3.787	1.17
E)	0.774	1.513	11.623	7.682	1.07
F)	0.567	8.941	14.237	1.592	1.52
G)	0.533	4.814	11.692	2.429	1.17
H)	0.172	5.089	4.058	0.797	2.14
I)	0.499	5.571	11.554	2.074	1.66
J)	0.275	4.470	13.343	2.985	1.25
				average	
Salmon River, Cobequid Bay, Canada					
A)	0.162	0.396	1.098	2.773	1.13
B)	0.158	0.279	0.990	3.548	1.12
C)	0.173	0.450	1.071	2.380	1.17
D)	0.108	0.252	0.900	3.571	1.12
E)	0.133	0.369	0.846	2.293	1.29

F)	0.090	0.639	0.711	1.113	1.88
G)	0.077	0.639	0.774	1.211	1.98
H)	0.060	0.18	0.603	3.350	1.19
I)	0.054	0.351	0.432	1.231	1.52
J)	0.027	0.441	1.026	2.327	1.38
				average	
Wave-Dominated Estuary					
Willipa River, Washington					
A)	0.261	2.147	3.041	1.416	1.44
B)	0.180	0.783	2.480	3.168	1.32
C)	0.310	0.824	1.482	1.798	1.35
D)	0.135	0.409	2.369	5.797	1.04
E)	0.090	0.353	1.053	2.980	1.18
F)	0.106	0.416	1.448	3.483	1.25
G)	0.081	0.355	0.866	1.147	1.69
H)	0.097	0.423	0.997	2.361	1.27
I)	~0.100	0.423	0.679	1.607	1.56
J)	~0.090	0.526	1.261	2.395	1.22
K)	~0.080	0.388	1.330	3.429	1.17
L)	~0.081	0.339	0.963	2.837	1.15
				average	
Tillamook River, Tillamook Bay, Oregon					
A)	0.069	0.343	0.934	2.720	1.20
B)	0.036	0.164	1.065	6.510	1.05
C)	0.026	0.116	0.991	8.583	1.07
D)	0.019	0.093	0.539	5.793	1.11
E)	0.014	0.135	0.581	4.310	1.15
F)	0.017	0.170	0.308	1.811	1.42
G)	0.016	0.080	0.347	4.320	1.24
H)	0.001	0.186	0.520	2.793	1.30
I)	0.008	0.132	0.141	1.074	1.69
J)	0.006	0.078	0.143	1.850	1.83
				average	